

AN INVESTIGATION OF THE UPPER MANTLE P-VELOCITY MODELS
USING SYNTHETIC SEISMOGRAMS

by

Yoichi Harita

B.S., University of California at Berkeley
(1967)

submitted in partial fulfillment of the
requirements for the degree of Master of
Science

at the
Massachusetts Institute of Technology
May 1968

Signature of Author.
Department of Geology and Geophysics, May, 1968

Certified by
Thesis Supervisor

Accepted by
Chairman, Departmental Committee on Graduate Students

WITHDRAWN
MASS. INST. TECH.
AUG 1 1969
M.I.T. LIBRARIES

AN INVESTIGATION OF THE UPPER MANTLE P-VELOCITY MODELS
USING SYNTHETIC SEISMOGRAMS

by

Yoichi Harita

Submitted to the Department of Geology and Geophysics,
Massachusetts Institute of Technology, May 1968, in
partial fulfillment of the requirements for the degree
of Master of Science

Abstract

A computer program written on the basis of the Cagniard-de Hoop's method to calculate the response from flat layered media to a unit impulse source was used to examine the upper mantle P-velocity structure of the earth, in the southern part of the United States.

Two existing models relevant to our locality were examined and found unsatisfactory on the basis of the synthetic seismogram they generated.

Several P-velocity models were constructed and examined. A model which gives correct arrival times and satisfactory synthetic seismograms has been found. This model includes a low-velocity zone similar to that of other models. A new feature of this model is a rapid increase in velocity near a depth of 500 km.

Thesis Supervisor: M. Nafi Toksoz
Title: Associate Professor of Geophysics

Table of Contents

	<u>Page</u>
Abstract	ii
Table of Contents	iii
List of Figures	iv
List of Tables	vii
Acknowledgements	viii
Notation	ix
I. INTRODUCTION	1
II. THEORY	
1. Response from an Infinite Medium	4
2. Response from a Two-layered Medium	7
3. High Frequency Approximation	9
4. A Multi-layered Case	10
5. Generalized Transmission Coefficient	12
6. First Motion Approximation	13
7. Directivity Function	17
8. Spherical Layer Approximation	18
9. Transfer Function	20
III. METHOD OF COMPUTATION	23
IV. DISCUSSION AND RESULTS	33
V. CONCLUSION	66
References	68
Appendix: Program Listing	

List of Figures

<u>Figure</u>		<u>Page</u>
2.1	Pressure near $t = t_0$ (Reflection Time)	14
2.2	Theoretical Response from a Nearly Linear gradient	21
3.1	Ray Configurations for Two-layered Cases	25
3.2	Ray Configurations for Four-layered Cases	27
4.1	P-velocity Models of the Upper Mantle -Nulli and Johnson	34
4.2	Transfer Function	35
4.3	Modified Transfer Function	35
4.4	Exact Response	35
4.5	Approximate Response	35
4.6	Approximate Synthetic Response	37
4.7	Exact Synthetic Response	37
4.8	Bilby Event - Range 1039 km	38
4.9	Bilby Event - Range 1426 km	39
4.10	Bilby Event - Range 1831 km	40
4.11	Bilby Event - Range 2274 km	41
4.12	Bilby Event - Range 3376 km	42
4.13	Theoretical Response - Nuttli - 1039 km	44
4.14	Synthetic Seismogram - Nuttli - 1039 km	45
4.15	Synthetic Response - Nuttli - 1426 km	47

List of Figures - continued

<u>Figure</u>		<u>Page</u>
4.16	Synthetic Response - Nuttli - 1831 km	47
4.17	Synthetic Response - Nuttli - 2274 km	48
4.18	Synthetic Response - Nuttli - 3376 km	48
4.19	Synthetic Response - Johnson - 1039 km	50
4.20	Synthetic Response - Johnson - 1426 km	50
4.21	Synthetic Response - Johnson - 2274 km	51
4.22	Models I, II and III	52
4.23	Synthetic Response - Model I - 2274 km	53
4.24	Theoretical Response - Model I - 2274 km	53
4.25	Synthetic Response - Model II - 2274 km	55
4.26	Theoretical Response - Model II - 2274 km	55
4.27	Synthetic Response - Model III - 2274 km	56
4.28	Theoretical Response - Model III - 2274 km	56
4.29	Models IV and V	58
4.30	Synthetic Response - Model IV - 2274 km	59
4.31	Theoretical Response - Model IV - 2274 km	59
4.32	Synthetic Response - Model V - 2274 km	60
4.33	Theoretical Response - Model V - 2274 km	60
4.34	Synthetic Response - Model V' - 2274 km	61
4.35	Theoretical Response - Model V' - 2274 km	61
4.36	Model V - Reduced Time vs. Range	62

List of Figures - continued

<u>Figure</u>		<u>Page</u>
4.37	Synthetic Seismogram - Model V - 1831 km	63
4.38	Theoretical Response - Model V - 1831 km	63
4.39	Synthetic Seismogram - Model V - 3376 km	64
4.40	Theoretical Response - Model V - 3376 km	64

List of Tables

<u>Table</u>		<u>Page</u>
4.1	Bilby Event (1963)	36
4.2	First Arrival Times and Magnitudes for the Nuttli's Model	46
4.3	First Arrivals and Amplitudes for the Johnson's Model	49
4.4.	Model V P-velocity	65

Acknowledgements

I am greatly indebted to Dr. Donald Helmberger, who gave me a patient guidance. I also should like to express my cordial gratitude to Professor M. Nafi Toksoz, my thesis supervisor, for making this thesis possible, and to Mr. John Fairborn for his program to compute travel times. The computation was done in the M.I.T. IBM 360-40/65 system and in the M.I.T. IBM CTSS system.

This work was supported by the Advanced Research Projects Agency (and monitored by the Air Force Office of Scientific Research) under Contract No. AF 49(638)-1632 at the Massachusetts Institute of Technology.

Notation

- c_i : P-Velocity in the i th layer
 d_i : Density in the i th layer
 δ : d_i/d_{i+1}
 $f(p)$: Integrated Transmission-Reflection Coefficient
 h : Vertical Distance to the Source from the Station
 H : Step Function
 K_0 : Modified Bessel Function of the Second Kind,
of Order 0
 L : dp/dt
 p : $\sin(i_c)/c_i$, where i_c is the Angle of Incident
 p_0 : Critical p at Reflection
 P : Pressure
 r, x : Horizontal Distance between the Source and the Station
 $R(p)$: Reflection Coefficient
 k_i : $-\frac{1}{2} \rho_i / (\mu_j - \mu_i)$
 k_r : $k_i + k_j$
 R : $\sqrt{r^2 + z^2}$
 s_i : Shear Velocity in the i th layer
 t, τ : Time
 t_c : Refraction Time
 t_0 : Reflection Time
 $T(p)$: Transmission Coefficient
 η_i : $\sqrt{1/c_i^2 - p^2}$
 η_i' : $\sqrt{1/s_i^2 - p^2}$
 z : Depth
 μ, λ : Lamé Parameters
 ρ : Density

I. INTRODUCTION

The best known property of the interior of the earth is the seismic velocity profile as a function of depth. Any theory of the earth's structure must, therefore, satisfactorily predict this velocity profile as closely as possible. The usual method of determining velocity is to use the Wiechert-Herglotz equation [See Bullen (1965)] which involves the integration of the $dt/d\Delta$ curve obtained experimentally from the travel time-distance information. The method cannot use the valuable information such as wave shape of the seismogram or varying amplitude with time in a seismogram and with the distance from the source. Also the method fails to determine a low velocity structure which is believed to exist at the depth of 100 km. Moreover, obtaining travel time and $dt/d\Delta$ curve requires a great deal of data - many stations - in order to approximate a smooth $dt/d\Delta$ curve.

In spite of these difficulties, numerous attempts have been made in the past to determine the velocity structure, and there are widely varying models [See, for example, Julian and Anderson (1968)] which give approximately correct arrival times. Of course, the variety may be due to the lateral heterogeneity of the earth. However, since Cagniard developed the revolutionary technique for computing the response from flat layered media, followed by de Hoop's (1960) modification, a more sophisticated method to determine the velocity structure has become possible.

In this thesis, the technique developed by those mentioned above and by others [Strick (1959) and Helm-

berger (1965 & 1967)] is discussed and applied to the spherical earth. The validity of the spherical approximation has not yet been confirmed. However, this technique is known to work to the travel time computation, and the relatively small curvature of the earth in the upper mantle should not cause significant errors in computing transmission coefficients and reflection coefficients. The advantage of this new method are that it generates synthetic seismograms and that it enables us to examine the models from many more standpoints - the first and the following arrivals, amplitudes and wave forms.

The Cagniard-de Hoop technique and the theory for the synthetic seismogram computations are presented in Chapter II. The entire chapter is a summary of Dr. Donald Helberger's contributions and included in this thesis for the sake of completeness in presentation.

In Chapter III, the computer program, originally written by Dr. Helberger, modified and improved in the course of the research for this thesis by him and by the author, is described.

Chapter IV presents the result of this study - the P-velocity structure along an east-west profile in the southern United States. To determine the velocity structure, first we examine two existing models proposed for this region. One model is by Dowling and Nuttli (1964), based on the travel time data from the underground nuclear explosion BILBY (1963), which we use in our investigation. The other model is by Johnson (1967), and was obtained, using the $dt/d\Delta$ data from the Tonto Forest Seismological Observatory in Arizona. After the exam-

ination of these models, we construct some new models. in so doing, we use a conventional method for computing travel times for a given model. [See Bullen (1965)] Then, we compute the synthetic seismograms and compare them with the records from the BILBY event. The criteria for comparison are the travel times of various P-arrivals, amplitudes and the wave forms of P-wave arrivals.

II. THEORY

In this chapter we present the theory which is the basis of the technique of computing the synthetic seismograms. Also shown in this chapter are several approximations we make in our computation.

1. Response from an Infinite Medium

For an infinite fluid with a unit pulse source at $r = 0$, $z = 0$, the Laplace-transformed pressure is:

$$\bar{P}(r, z, s) = -\frac{i}{\pi} C_0 \int_0^\infty K_0(s\rho r) e^{-s\eta_1 |z|} \frac{\rho}{\eta_1} d\rho. \quad (1)$$

Due to the symmetry of the integrand with respect to the real p axis, (1) can be rewritten as:

$$\bar{P}(r, z, s) = \frac{2}{\pi} \int_0^{i\infty} K_0(s\rho r) e^{-s\eta_1 |z|} \frac{\rho}{\eta_1} d\rho. \quad (2)$$

C_0 is a constant with dimensions of pressure times length and assumed unity from here on. Back-transforming (2), we obtain:

$$\underline{P}(r, z, t) = \frac{2}{\pi} \int_0^{i\infty} \frac{\rho}{\eta_1} \frac{H(t - \rho r - \eta_1 |z|)}{\sqrt{(t - \eta_1 |z|)^2 - \rho^2 r^2}} d\rho, \quad (3)$$

where $H(t)$ is a step function. Since the argument of a step function must be real, we must have the path such that:

$$\tau = \rho r + \eta_1 |z| \quad (4)$$

is real and positive. Due to de Hoop's modification of Cagniard's method (1960), we solve (4) for p to obtain:

$$p = \frac{r}{R^2} \tau + i \frac{|z|}{R^2} \sqrt{\tau^2 - \frac{R^2}{c_1^2}} \quad (5)$$

In order that $\tau^2 - \frac{R^2}{c_1^2}$ be positive, we must have $\frac{R}{c_1} < \tau < \infty$. And this is the path of the contour Γ . Now, (3) is equivalent to:

$$P(r, z, t) = \frac{2}{\pi} \int_{\Gamma} \frac{f}{\eta_1} \frac{H(t - \tau r - \eta_1 |z|)}{\sqrt{(t - \tau)(t - \tau + 2pr)}} \frac{dp}{d\tau} d\tau, \quad (6)$$

and differentiating (5), we get:

$$\frac{dp}{d\tau} = \frac{i\eta_1}{\sqrt{\tau^2 - \frac{R^2}{c_1^2}}} \quad (7)$$

For $p < \frac{r}{Rc_1}$, the integrand of (6) is real, and we rewrite (6) as:

$$P(r, z, t) = \frac{2}{\pi} \operatorname{Re} \int_{t_0}^t f(\tau) \frac{d\tau}{\sqrt{(t - \tau)(t - \tau + 2pr)(\tau^2 - \frac{R^2}{c_1^2})}} \quad (8)$$

Since $H(t - \tau) = 0$ for $t < \tau$, and for $\tau < \frac{R}{c_1}$ the denominator of the integrand in (8) becomes complex. We define the reflection time $t_0 \equiv R/c_1$ and simplify (8). Let

$$\theta \equiv \arcsin \sqrt{\frac{t - \tau}{t - t_0}} \quad (9)$$

and with the transformation, (8) becomes:

$$P(r, z, t) = \frac{4}{\pi} \operatorname{Re} \int_0^{\frac{\pi}{2}} F(\theta) d\theta \quad (10)$$

where

$$F(\theta) = \frac{p(\theta)}{\sqrt{(\tau(\theta) + t_0) \cdot (t - \tau(\theta) + 2p(\theta)r)}}$$

$$p(\theta) = \frac{r}{R^2} \left\{ (t - (t - t_0) \sin^2 \theta) \right\} + i \frac{|z|}{R} \sqrt{\left\{ t - (t - t_0) \sin^2 \theta \right\}^2 - t_0}$$

$$\tau(\theta) = \tau - (t - t_0) \sin^2 \theta$$

In order to perform the integration (10), we must find $F(\theta)$ numerically for each t . This costly procedure can be avoided by the following approach. Define

$$p_R \equiv \text{Re}(p)$$

$$p_I \equiv \text{Im}(p)$$

$$p_0 \equiv \frac{r}{Rc_1}$$

We choose a set of p_R 's starting at p_0 and increasing on some small interval δ , to $p_t \equiv p_R(t)$. We find, for each p_R , p_I such that $\text{Im}(\tau)$ is zero. To clarify the situation, the limits are:

$$p_0 < p_R < p_t$$

$$t_0 < \tau < t$$

$$0 < \theta < \pi$$

As $t \rightarrow t_0$, $p \rightarrow r/Rc_1 = p_0$ (The First Motion Approximation).

And also

$$\tau(\theta) \Rightarrow t_0 = \frac{R}{c_1},$$

$$F(\theta) \Rightarrow \frac{r}{Rc_1} \frac{1}{\sqrt{2t_0 \frac{2r^2}{Rc_1}}} = \frac{1}{2R},$$

and

$$P(r, z, t) \Rightarrow \frac{1}{R} H(t - t_0) \quad [\text{Dix (1953)}] \quad (11)$$

This is the exact solution to (10).

2. Response from a Two-layered Medium

For a problem involving two-layered media, let suffixes 1 and 2 denote the upper and the lower layers, respectively. We have, for the equivalence of (6),

$$P(r, z, t) = \frac{2}{\pi} \int_0^{\infty} \frac{\rho}{\eta_1} \frac{R(\rho) H(t - \tau)}{\sqrt{(t - \tau)(t - \tau + 2\rho r)}} \frac{d\rho}{d\tau} d\tau \quad (12)$$

Note the quantity $R(\rho)$ in the integrand, which is:

$$R(\rho) = \frac{\eta_1 \{ (1 - 2s_2^2 \rho^2)^2 + 2s_2^4 \rho^2 \eta_2 \eta_1' \} - \delta \eta_2}{\eta_1 \{ (1 - 2s_2^2 \rho^2)^2 + 4s_2^4 \rho^2 \eta_2 \eta_1' \} + \delta \eta_2} \quad (13)$$

and

$$\tau = \rho r + (z + h) \eta_1$$

$$R = \sqrt{r^2 + (z + h)^2}$$

Assuming $c_1 < s_2 < c_2$, p leaves the real axis at $p = p_0$ and $1/s_2 < p_0 < 1/c_1$. We can obtain the S-refracted time, the reflected time (t_0) and the P-refracted time (t_c) by substituting $p = 1/s_2$, p_0 , $1/c_2$ into (13), respectively. For example, let $p = 1/c_2$ and from (13) we get:

$$t_c = \frac{r}{c_2} + (z + h) \sqrt{\frac{1}{c_1^2} - \frac{1}{c_2^2}}$$

When we perform the numerical integration (12), we break P into two parts - from t_c to t_0 where p is real, and from t_0 onward where p is complex. Thus, (12) can be rewritten as:

$$P(r, z, t) = P_1(r, z, t) + P_2(r, z, t), \quad (14)$$

where

$$P_1(r, z, t) = \frac{2}{\pi} \int_{t_c}^{t_0} \frac{p}{\eta} \frac{R(p)}{\sqrt{(t-z)(t-z+2pr)}} \frac{dp}{dz} dz$$

and

$$P_2(r, z, t) = \frac{2}{\pi} \int_{t_0}^t \frac{p}{\eta} \frac{R(p)}{\sqrt{(t-z)(t-z+2pr)}} \frac{dp}{dz} dz$$

By letting

$$\theta \equiv \arcsin \sqrt{\frac{z}{t}}, \quad (15)$$

we change variables in (14) to

$$P_1(r, z, t) = \frac{4}{\pi} \int_{\theta_0}^{\pi/2} F(\theta) d\theta, \quad (16)$$

where

$$F(\theta) = \int_{t_0}^t \left\{ R(p) \frac{p}{\eta} \frac{dp}{dz} \right\} \frac{\sqrt{z}}{\sqrt{z-z+2pr}}$$

$$\theta \equiv \arcsin \sqrt{\frac{t_0}{t}}$$

The integration can be carried out by trapezoidal rule. Thus, $P_1(r, z, t)$ can be numerically evaluated, and $P_2(r, z, t)$ is evaluated by the same method described in (10).

The pressure response to a delta function source is:

$$P(r, z, t) = \frac{2}{\pi} \frac{\partial}{\partial t} \int_0^t R(\rho) \frac{\rho}{\eta} \frac{d\rho}{d\tau} \frac{d\tau}{\sqrt{(t-\tau)(t-\tau+2\rho r)}} \quad (17)$$

3. High Frequency Approximation

When we deal with sources of high frequency or of a short duration, the following approximation holds:

$$t - \tau + 2\rho r \approx 2\rho r \quad (18)$$

From (17) we get by substituting (18):

$$P(r, z, t) = \frac{2}{\pi} \frac{\partial}{\partial t} \left(\frac{1}{\sqrt{t}} * \int_0^t R(\rho) \frac{\sqrt{\rho}}{\eta} \frac{d\rho}{d\tau} \frac{1}{\sqrt{2r}} \right) \quad (19)$$

Define

$$\psi(t) \equiv \int_0^t R(\rho) \frac{\sqrt{\rho}}{\eta} \frac{d\rho}{d\tau} \frac{1}{\sqrt{2r}}$$

Thus (19) can be written as:

$$P(r, z, t) = \frac{\partial}{\partial t} \frac{2}{\pi} \left(\frac{1}{\sqrt{t}} * \psi(t) \right) \quad (20)$$

4. A Multi-layered Case

For a multi-layered case, we must consider multiple reflections in addition to refractions. We have the Laplace-transformed pressure:

$$\bar{P}(r, z, s) = -\frac{i}{\pi} \int_{\Gamma} K_0(spr) R(\rho, s) e^{-s\eta_1(z+h)} \frac{\rho}{\eta_1} d\rho, \quad (21)$$

where

$$R(\rho, s) = R_{12}(\rho) + \sum_m (-1)^{m+1} R_{23}^m R_{12}^{m-1} \frac{e^{-2mTh s\eta_2}}{1 - R_{12}^2}$$

Or (21) can be written as:

$$\begin{aligned} \bar{P}(r, z, s) = & -\frac{i}{\pi} \int_{\Gamma} K_0(spr) \frac{\rho}{\eta_1} R_{12}(\rho) e^{-s\eta_1(z+h)} d\rho \\ & - \frac{i}{\pi} \sum_m \int_{\Gamma} K_0(spr) R_{23}^m (-1)^{m+1} R_{12}^{m-1} (1 - R_{12}^2) \frac{\rho}{\eta_1} \times \\ & \times e^{-s\{\eta_1(z+h) + 2mTh\eta_2\}} d\rho. \end{aligned} \quad (22)$$

Further:

$$\bar{P}(r, z, s) = \bar{P}_0(r, z, s) + \sum_m \bar{P}_m(r, z, s), \quad (23)$$

where

$$\bar{P}_m(r, z, s) = -\frac{i}{\pi} \int_{\Gamma} K_0(spr) f_m(\rho) \frac{\rho}{\eta_1} e^{-s g_m(\rho)} d\rho,$$

$$f_m(\rho) = R_{23}^{m+1} R_{12}^{m-1} (1 - R_{12}^2) \cdot (-1)^{m+1},$$

$$g_m(\rho) = \eta_1(z+h) + 2mTh\eta_2.$$

As before, $\bar{P}_m(r, z, s)$ can be transformed back to :

$$\underline{P}_m(r, z, t) = \frac{2}{\pi} \int_m \int_r \frac{p}{\eta_1} \frac{dp}{d\tau} f_m(p) \frac{H(t - \tau_m) d\tau}{\sqrt{(t - \tau_m)(t - \tau_m + 2pr)}} , \quad (24)$$

where

$$\tau_m = pr + \eta_1 \cdot (z+h) + 2Th_m \eta_2 .$$

If layers have different thicknesses and if we change the variables of integration to τ , as before, we get

$$\underline{P}_m(r, z, t) = \frac{2}{\pi} \int_m \int_r \frac{p}{\eta_1} \frac{dp}{d\tau} f_m(p) \frac{H(t - \tau)}{\sqrt{(t - \tau)(t - \tau + 2pr)}} , \quad (25)$$

where

$$\tau = pr + 2 \sum_{j=1}^m \eta_j Th_j ,$$

$$\frac{dp}{d\tau} = \left(r - 2p \sum_{j=1}^m \frac{Th_j}{\eta_j} \right)^{-1} ,$$

m is the last layer that the ray penetrates. Therefore, the refracted wave begins at t_c which corresponds to $p_c = 1/c_{m+1}$ and the reflection occurs at p_0 corresponding to t_0 . As before $1/c_{m+1} < p_0 < 1/c_m$ and as p increases from p_0 , it goes into the complex plane. At this point, we again apply the high frequency approximation (18) to (25) and obtain, for a delta function source:

$$\underline{P}_m(r, z, t) = \frac{2}{\pi} \frac{\partial}{\partial t} \left[\frac{1}{\sqrt{t}} * \psi_m(t) \right] , \quad (26)$$

where

$$\psi_m(t) = \int_m \left\{ f_m(p) \sqrt{\frac{p}{2r}} \frac{1}{\eta_1} \frac{dp}{d\tau} \right\} .$$

The merit of employing the high frequency approximation is, when we add rays (indexed m), from (23),

$$\begin{aligned} P(r, z, t) &= \sum_m P_m(r, z, t) \\ &= \sum_m \frac{2}{\pi} \frac{\partial}{\partial t} \left(\frac{1}{\sqrt{t}} * \psi_m(t) \right). \end{aligned} \quad (27)$$

Since the sum of convolved quantities such as in (27) is the convolved sum, i.e.,

$$P(r, z, t) = \frac{2}{\pi} \frac{\partial}{\partial t} \left(\frac{1}{\sqrt{t}} * \sum_m \psi_m(t) \right). \quad (28)$$

Thus, we need not perform convolution for m times, but only once.

5. Generalized Transmission Coefficient

$f_m(p)$ in (26) is called the generalized transmission coefficient. It can be written as the product of reflection coefficients $R_{ij}(p)$ and transmission coefficients $T_{ij}(p)$.

$R_{ij}(p)$ is the reflection coefficient when the ray is reflected at the boundary of the i th and $i+1=j$ th layers. Its explicit form is:

$$R_{ij}(p) = \frac{A - \eta_2 B}{A' - \eta_2 B'} \quad (29)$$

where

$$\begin{aligned} A &= -a + b, & B &= a + b, \\ A' &= -a' + b', & B' &= a' + b', \end{aligned}$$

$$a = \rho^2 (k_r - \rho^2)^2$$

$$b = \eta_i \eta_i' (k_j - \rho^2)^2 - k_i k_j \eta_i \eta_j'$$

$$a' = \eta_i \eta_i' \eta_j' \rho^2$$

$$b' = \eta_j' (k_i - \rho^2)^2 - \eta_i' k_i k_j$$

$T_{ij}(\rho)$ is the transmission coefficient for the case the ray is refracted from the i th to the $i+1=j$ th layers. Its explicit form is:

$$T_{ij}(\rho) = \frac{2k_i \eta_i \{ \eta_i' (k_i - \rho^2) - \eta_i' (k_j - \rho^2) \}}{D} \quad (30)$$

where

$$D = \rho^2 (k_r - \rho^2)^2 + \eta_i \eta_j \eta_i' \eta_j' \rho^2 + \eta_i \eta_j' (k_j - \rho^2)^2 \\ + \eta_j \eta_i' (k_i - \rho^2)^2 + \eta_j' \eta_i k_i k_j - \eta_i' \eta_j k_i k_j$$

6. First Motion Approximation

As t approaches t_0 , the term dp/dt in (28) goes to infinity, as

$$\frac{dp}{dt} = \left(r - 2\rho \sum_{j=1}^n \frac{T_{hj}}{\eta_j} \right)^{-1}$$

is not defined at $t = t_0$. In order to evaluate $\psi_m(t)$ at $t = t_0$ (which happens to be the most significant point of the ray), we make use of the Simpson's rule.

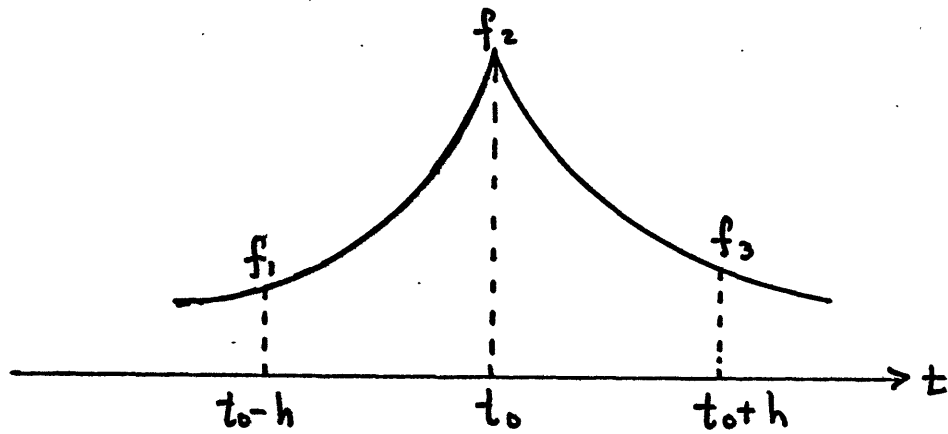


Figure 2.1

Pressure near $t = t_0$

$$\begin{aligned} \int_{t_0-h}^{t_0+h} f(t) dt &= \frac{h}{3} [f(t_0-h) + 4f(t_0) + f(t_0+h)] \\ &= \frac{h}{3} [f_1 + 4f_2 + f_3] \equiv \phi. \end{aligned} \quad (31)$$

From (31) we obtain:

$$f_2 = \frac{1}{4} \{3\phi - (f_1 + f_3)\}, \quad (32)$$

which is what we wish to calculate. ϕ is calculated partly numerically ($t_0 - h < t < t_0 - \delta$, $t_0 + \delta < t < t_0 + h$).

For $t_0 - \delta < t < t_0 + \delta$, we can show that:

$$\int_{t_0-\delta}^{t_0+\delta} f(t) dt = 2f(t_0)\sqrt{\delta}. \quad (33)$$

In order to show (33), we consider the Taylor expansion:

$$t = t_0 + \frac{dt}{dp}(p - p_0) + \frac{d^2t}{dp^2}(p - p_0)^2 \frac{1}{2!} + \dots \quad (34)$$

And since $dt/d\rho \approx 0$ at $t = t_0$, we have:

$$\frac{dt}{d\rho} \approx \sqrt{2(t-t_0) \frac{d^2t}{d\rho^2}} \quad (35)$$

From (25), we obtain by differentiating,

$$\frac{d^2t}{d\rho^2} = -2 \sum_j \frac{Th_j}{\eta_j^3 C_j^2} \quad (36)$$

Substituting (36) into (35) and then into (26), we get:

$$P_m(r, z, t) = \frac{1}{\pi} \frac{\partial}{\partial t} \left[\frac{1}{t} * \frac{1}{t-t_0} \int_m \left\{ \sqrt{\frac{\rho}{r}} f_m(\rho) \frac{1}{\eta_j \sqrt{-\sum_j \frac{Th_j}{\eta_j^3 C_j^2}}} \right\} \right] \quad (37)$$

Now let:

$$\theta \equiv \frac{d^2t}{d^2\rho^2}$$

$$\psi_1(t) \equiv \int_m \left\{ f_m(\rho) \sqrt{\frac{\rho}{r}} \frac{1}{\eta_j \sqrt{\theta}} \right\} \frac{1}{\sqrt{t_0-t}} \quad \text{for } t < t_0,$$

$$\psi_2(t) \equiv \text{Re} \left\{ \int_m \left\{ f_m(\rho) \sqrt{\frac{\rho}{r}} \frac{1}{\eta_j \sqrt{\theta}} \right\} \frac{1}{\sqrt{t_0-t}} \right\} \quad \text{for } t > t_0,$$

$$F_1(t) \equiv \int_m \left\{ f_m(\rho) \sqrt{\frac{\rho}{r}} \frac{1}{\eta_j \sqrt{\theta}} \right\} \quad \text{for } t < t_0,$$

$$F_2(t) \equiv \text{Re} \left\{ \int_m \left\{ f_m(\rho) \sqrt{\frac{\rho}{r}} \frac{1}{\eta_j \sqrt{\theta}} \right\} \right\} \quad \text{for } t > t_0.$$

Consider

$$\int_{t_0-\delta}^{t_0} \psi_1(t) dt = \int_{t_0-\delta}^{t_0} \frac{F_1(t)}{\sqrt{t_0-t}} dt$$

Since $F_1(t)$ varies slowly near $t = t_0$, we get:

$$\approx 2F_1(t_0) \sqrt{\delta} \quad (39)$$

Similarly:

$$\int_{t_0}^{t_0+\delta} \psi_2(t) dt \approx 2F_2(t_0) \sqrt{\delta}.$$

Thus, we have shown for $t_0 - \delta < t < t_0 + \delta$, the part of is

$$2\{F_1(t_0) + F_2(t_0)\} \sqrt{\delta}. \quad (40)$$

For the rest of ϕ , we use the trapezoidal rule to integrate. We have values of $\psi_n(t)$ computed for these outer regions and we divide $t_0 - h$ to $t_0 - \delta$ to five parts (chosen rather arbitrarily), interpolate $\psi_n(t)$ for each p , and do the same for $t_0 + \delta$ to $t_0 + h$. This result and (40) are added to obtain finally ϕ . Then f_2 can be computed from (32).

We now consider the case in which t_c approaches t_0 . We can show that

$$f_n(p) \Rightarrow g(p) \sqrt{z - t_c},$$

$$\frac{df}{dz} \Rightarrow h(p) \frac{1}{\sqrt{t_0 - z}},$$

where $g(p)$ and $h(p)$ are smooth functions of p . Hence, we may delete the pressure from our consideration since it does not vary in any extraordinary way. Consider:

$$\int_{t_c}^{t_0} \frac{\sqrt{z - t_c}}{\sqrt{t_0 - z}} dz = \int_{t_c}^{t_0} \frac{z - t_c}{\sqrt{(z - t_c)(t_0 - z)}} dz. \quad (41)$$

Now let

$$a \equiv -t_c t_0 ,$$

$$b \equiv t_0 + t_c ,$$

$$c \equiv -1 ,$$

$$\Sigma \equiv a + b\tau + c\tau^2 .$$

Thus, $t_0 - t = 2\left(\frac{b}{2} - t\right)$.

Therefore, (41) can be written as:

$$\begin{aligned} \int_{t_c}^{t_0} \frac{\tau - t_c}{\sqrt{\Sigma}} d\tau &= \frac{\sqrt{\Sigma}}{c} \Big|_{t_c}^{t_0} - \frac{b}{2c} \int_{t_c}^{t_0} \frac{d\tau}{\sqrt{\Sigma}} - t_c \int_{t_c}^{t_0} \frac{d\tau}{\sqrt{\Sigma}} \\ &= \frac{\pi}{2} (t_0 - t_c) . \end{aligned}$$

Thus we have shown that when $\psi_m(t)$ is integrated, it behaves linearly with interval $t_0 - t_c$. The justification for integrating $\psi_m(t)$ is that since the source function is very flat and when it is convolved with $\psi_m(t)$, $\psi_m(t)$ is virtually integrated over time. We see now that as $t_0 - t_c$ becomes arbitrarily small, the contribution of $\psi_m(t)$ from this part is essentially negligible.

7. Directivity Function

Instead of solving for pressure in the preceding discussion, we may replace it by the displacement potential $\phi(r, z, t)$ assuming a step function source. And we use the same equations.

However when we measure body wave amplitude on the

surface of the earth, we must be concerned with the conversion of the measured amplitude to the actual amplitude because of the P-SV interaction at the reflecting surface. The conversion factor is given by L. Knopoff, et. al. (1960) as:

For the P-wave,

$$D_p(p) = \frac{-\beta_1^{-2} \eta_p (2p^2 - \beta_1^{-2})^2}{R(p)} ;$$

For the S-wave,

$$D_s(p) = \frac{-4p \eta_p \eta_s \beta_1^{-2}}{R(p)} ;$$

(42)

where β_1 is the shear velocity in the surface layer,

$$\eta_p = \sqrt{\frac{1}{c_1^2} - p^2} \quad ; \quad \eta_s = \sqrt{\frac{1}{s_1^2} - p^2}$$

$$R(p) = (2p^2 - \beta_1^{-2})^2 + 4p^2 \eta_p \eta_s$$

8. Spherical Layer Approximation

The method described above is valid for flat horizontal layers. We know that equations for distance and travel time [Grant and West (1965)]:

$$\Delta = 2p \int_0^h \frac{v(z) dz}{\sqrt{1 - p^2 v^2(z)}} \quad (43)$$

$$t = 2 \int_0^h \frac{dz}{v(z) \sqrt{1 - p^2 v^2(z)}}$$

where $p = \sin(i) / V(z)$ (ray parameter),

h : thickness of the layer,

for horizontal layers. And for spherical layers [Bullen (1965)] :

$$\Delta = 2\gamma \int_{r_p}^{r_0} \frac{dr}{r \sqrt{\eta^2 - p^2}},$$

$$t = 2 \int_{r_p}^{r_0} \frac{\eta^2 dr}{r \sqrt{\eta^2 - p^2}}, \quad (44)$$

where $\eta = r/v$, $p = r \sin(i) / V$, r_0 : radius of the earth, r_p ; radius of the deepest point of penetration. We see immediately that the equations (43) will be equivalent to (44) if the quantities p and V are multiplied by $1/r$.

In our computation, the compressional velocities, the shear velocities, the layer thicknesses and the densities are multiplied by r_0/r , where $r_0 = 6371$ km (the radius of the earth), the justification being the compatibility of the assumption with the equations (43) and (44), and the additional factor of r_0 (a constant) is simply to normalize the quantities to the proper dimensions. Thus,

$$c'_i = c_i Q$$

$$s'_i = s_i Q$$

$$\rho'_i = \rho_i Q$$

$$Th'_i = Th_i Q,$$

where $Q = r_0 / r$.

$$i = 1, 2, 3, \dots \quad (45)$$

The operation above is performed at the very beginning of the computation scheme and hence all the following computation is done with the normalized quantities (45).

9. Transfer Function

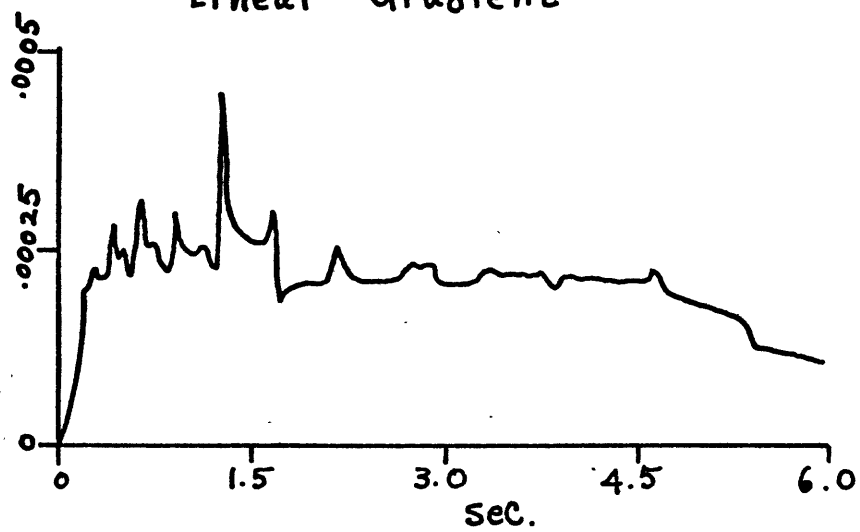
In order to generate synthetic seismograms from theoretical responses, we must devise a system function that takes the theoretical response as the input and generates the synthetic seismogram as the output. Such a transfer function is defined as a convolution of the source function with the instrumentation response. However, we know that at large ranges, 3000 km for example, the earth returns a step function if the input is a step function omitting the Q effects. That is, if we treat the mantle as a simple velocity gradient, then the displacement looks like the input. [See Figure 2.2] Let $R(t)$ be the output at the range 3376 km. Then,

$$R(t) = \frac{\partial}{\partial t} [T(t) * \phi(t)]$$

where $\phi(t)$ is approximately a step function. In such a case $R(t) = T(t)$. $R(t)$ is used as the transfer function throughout this study. In Chapter IV, we will see the actual wave form of the transfer function. A synthetic seismogram is complete when we convolve the pressure (or displacement) [See Eqn. (28)] with the transfer function. In our method using the high frequency approximation, however, we convolve the transfer function with $1/\sqrt{t}$ to obtain the modified transfer function. [See Figures 4.2 and 4.3]

Figure 2.2

Theoretical Response from a Nearly
Linear Gradient



This response was obtained from the Nuttli's model at 3376 km. The peak at 1.4 seconds was caused by a slight decrease in gradient at the depth 850 km.

Since we convolve $1/\sqrt{t}$ with the transfer function which is nearly flat at $t = 0$, we are essentially integrating $1/\sqrt{t}$ in the neighbourhood of $t = 0$. Let $f(t) = 1/\sqrt{t}$. And let h denote some small number. Using the Simpson's rule of integration, we obtain

$$\begin{aligned} \int_0^{2h} \frac{1}{\sqrt{t}} dt &= \int_0^{2h} f(t) dt = \frac{h}{3} [f(0) + 4f(h) + f(2h)] \\ &= \frac{h}{3} \left[f(0) + \frac{4}{\sqrt{h}} + \frac{1}{\sqrt{2h}} \right]. \end{aligned}$$

But analytically, it is equal to $2\sqrt{2h}$. Thus,

$$f(0) = \frac{11\sqrt{2}-4}{2} \frac{1}{\sqrt{h}} \approx \frac{9.56}{\sqrt{h}}$$

In the digital computation, we let h be the digitization interval and thus, $f(0)$ is obtained.

II. METHOD OF COMPUTATION

The procedure for computing the theoretical response to a unit impulse source is described below. The program was originally written for the Control Data 3600 computer at the University of California at San Diego by Dr. Helmberger. It has been converted so that it is compatible with the M.I.T. IBM 360-65/40 computer system in the course of the research for this thesis by Dr. Helmberger and by the author. It will be instructive to refer to Chapter II and the Appendix for the theory and the program listing, as the reader follows this chapter.

In computing the response, we must specify the characteristics of rays we are interested in. We, therefore, specify the layer k to which the ray reaches without reflection and the manner that the ray reflects in the layers beneath k . The number of layers involved in internal reflections can be at most four (neighbouring ones). If more than four layers are involved, the reflection coefficients become exceedingly small and negligible. We name various configurations of internal reflections for the purpose of computation. There are two subroutines that define various constants for each configuration. One (CON) is used for configurations involving only two layers (This is the more usual case than the latter). The other (CONN) is for cases involving four layers. Cases for one and three layers are special cases of two-layer and four-layer cases, respectively. These subroutines define $MT(J)$, the number of transmissions from the J th to the $J+1$ th layers; $LTP(J)$, the number of times

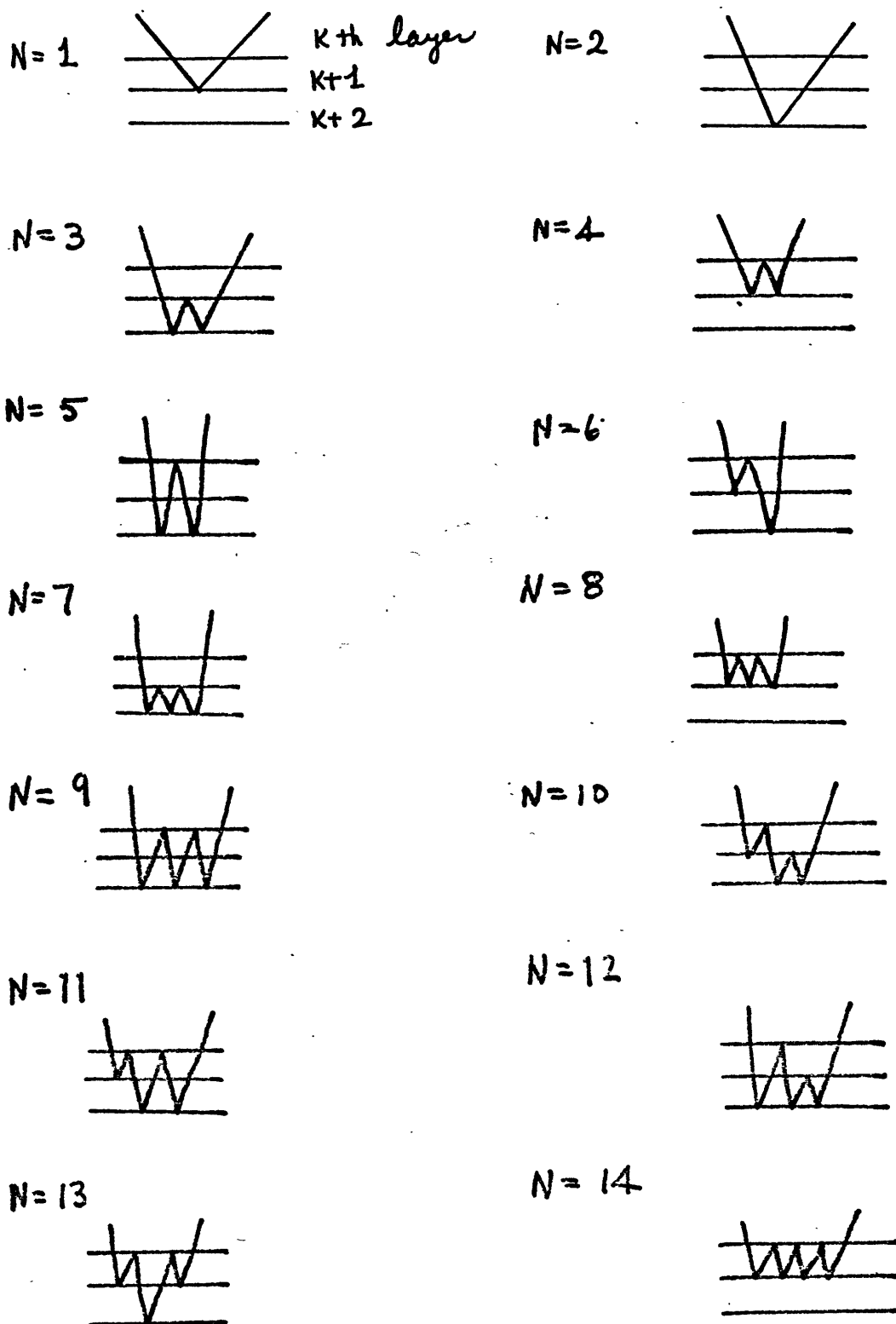
the ray travels through the Jth layer; NN(J), the number of reflections on the J+1th layer from the Jth layer; MM(J), the number of reflections on the J-1th layer from the Jth layer; and NF, the number of possible ways the ray can travel with the same set of constants above. N is used to describe the rays. For CON, the various N's correspond to the following figures [Figures 3.1]. And also for CONN, another set of figures are drawn. Though there are infinitely more configurations, they are not considered here because the intensity of the ray becomes negligible, as the values of the constants go up. The choice of using CON or CONN is made by the parameter MF. That is,

```
MF  1 for CON,
MF  1 for CONN.
```

The program first computes the modified velocities, densities and layer thicknesses according to the spherical layer approximation with SUBROUTINE CURAY [See (43)-(45)]. The MAIN program gives the control to SUBROUTINE SETUP after defining constants and executing CURAY. For each call of SETUP, a response of a particular ray is computed and later all the responses are added. On the argument list of SETUP are:

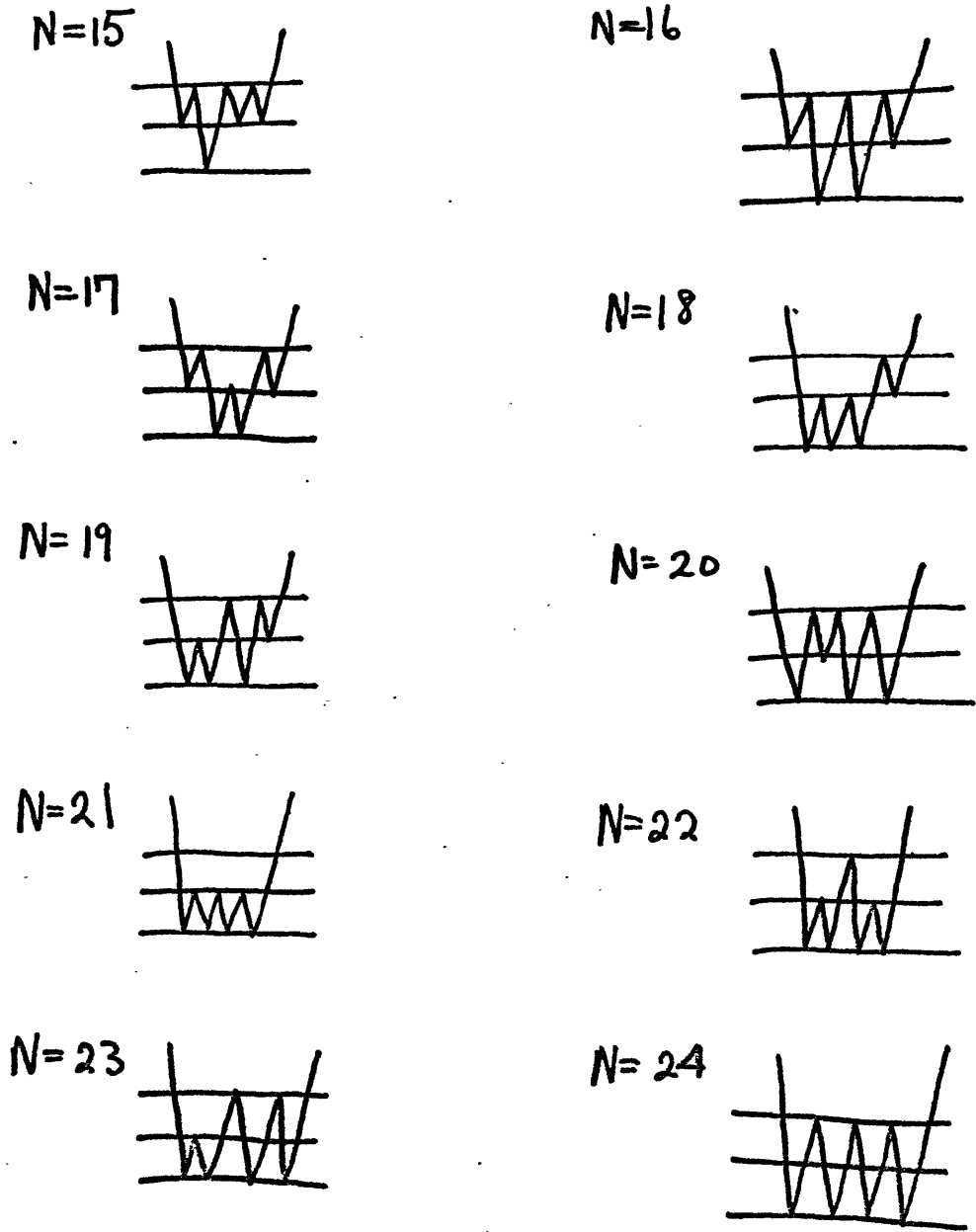
```

K      : First Layer Involved in Internal Reflection
NS     : Starting Ray
NO     : Ending Ray           Range of N
MO     : 0 for Finding the First Arrival Time
        2 for Subsequent Calls
MPLOT  : 0 for No Plot of Theoretical Response
        2 for Plot
```



Figures 3.1 Ray Configurations

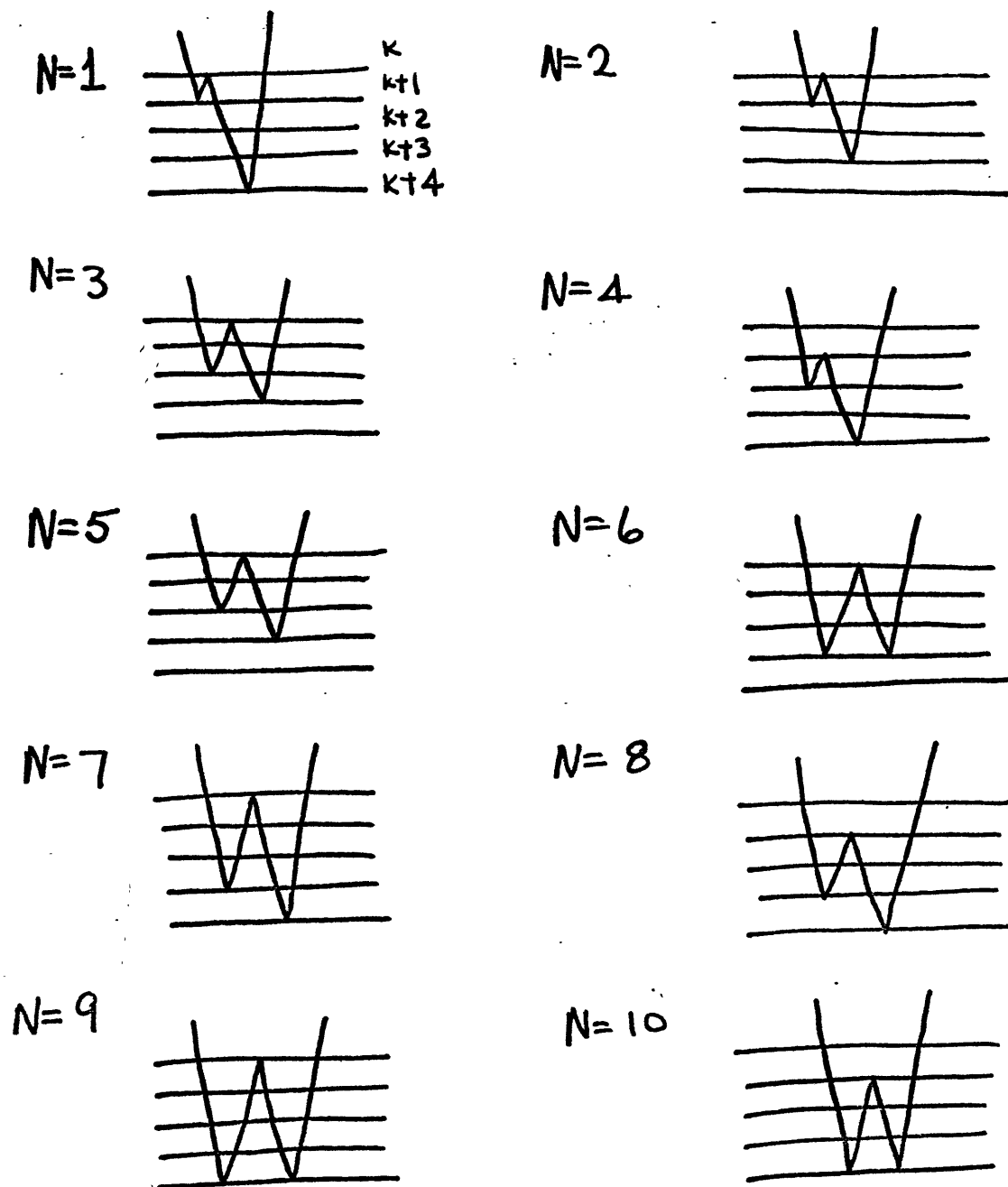
for Two-layered Cases



Figures 3.1 (cont.) Ray Configurations

Using the notation, the generalized transmission coefficient $f_n(p)$ is:

$$\begin{aligned}
 & R_{k_1, k_2}^{MM(k)} \cdot R_{k_1, k_2}^{MM(k+1)} \cdot R_{k_2, k_1}^{MM(k+2)} \cdot R_{k_1, k_2}^{NN(k+2)} \cdot \\
 & \times T_{k_1, k_2}^{MK(k)} \cdot T_{k_1, k_2}^{MK(k+1)}
 \end{aligned}
 \tag{46}$$



Figures 3.2

Ray Configurations for Four-layered Cases

MPUNCH : 0 No Punched Output of Theoretical Response
2 Punch Wanted.

SUBROUTINE SETUP first finds the first arrival of any ray among all the possible rays considered - either reflection or refraction. This is done by FUNCTION TS, which finds the largest c_i 's for $1 \leq i \leq n$, $KST \leq n \leq KEND$. For each n SUBROUTINE FIND2 is called to compute reflection time t_o and corresponding p_o by letting dp/dt go to ∞ or in the actual case, minimizing $|dt/dp|$ [See (25)]. TS also finds the refraction time t_c using FUNCTION PTIM. t_c is simply t that corresponds to $p = \sin \frac{\pi}{2} / c_{n+1} = 1/c_{n+1}$ [See (25)]. t_o and t_c for each n are stored in $T(n)$. TS is set to the minimum of all $T(n)$ and returned to SETUP. Upon returning, $TT(1)$ is set equal to TS, which is the first arrival counting from $t = 0$, when the source explodes. Then, the array TT is defined by incrementing by DEL, which is defined in MAIN. TS is called only once in a series of calls of SETUP.

The reflection and refraction constants described above are defined by calling either CONN, or CONSTN and CON. Then, SUBROUTINE HIGH is called. First, by examining the transmission constant LTP, the deepest layer of penetration is determined and stored in KM. That is, if $LTP(J) = 0$ for some J, then $KM = J - 1$, after LTP(J) have taken non-zero values for all $I < J$. Again FIND2 computes the reflection time t_o for the particular ray. This time,

$$\frac{dt}{dp} = \alpha - p \sum_{j=1}^{KM} \frac{Th_j LTP_j}{\sqrt{\frac{1}{c_j^2} - p^2}},$$

and p_0 is the value of p that makes $dt/dp = 0$ as before. Consequently,

$$t_0 = p_0 \tau + \sum_{j=1}^{KM} Th_j L T p_j \sqrt{\frac{1}{c_j^2} - p_0^2}$$

RG is the difference between t_0 and t_c . SUBROUTINE HELP is then called to find t_c and dp/dt for $p_c = 1/c_{KM+1}$, corresponding to refraction at the $KM+1$ th layer boundary. $TG = t_c - t_0$. To determine how the problem of evaluating $\psi_m(t)$ near t_0 should be dealt with, a series of tests are performed on the magnitude and the sign of TG with four constants defined in MAIN - TN's. If $p_0 < p_c$, then we only evaluate $\psi_m(t)$ for complex p . Also if TG is large, then we do not want to divide the interval $t_c - t_0$ too closely. Thus, SUBROUTINE DELPS is called to set the interval (DELP) so that the divisions are closer as p approaches p_0 and p_c , and wider in the middle. DELPS performs this operation with the trigonometric sine function. NO is the dimension of DELP, or the number of partitions on the real p axis. However, if TG is not very large, then DELP is defined with equal intervals. After the real p 's (DELP) are defined, HIGH calls PLN1 and PLN2 to compute $\psi_m(t)$. [See(14)] PLN1 computes $\psi_m(t)$ for $t_c < t < t_0$, and in this interval p only takes real values. In case of $t_0 \leq t_c$, PLN1 is not called since t_c is fictitious.

The procedure of computing $\psi_m(t)$ as described in (26) is as follows:

- i) Take $p_c = 1/c_{KM+1}$ and increment it by DELP for

each p ; HELP is called to find corresponding time t_c (TT(I)) and dp/dt (DTP).

ii) For each p , call ROC to compute part of $f_m(p)$ [See (46)] using the constants defined in either CON or, CONN and CONSTN. (RPR)

iii) GENCC computes the product of transmission coefficients through layers 1 to K, in which the ray simply travels forth once and back one. (TOT)

iv) CRSTPP computes the transmission coefficient [See(30)];

RET computes the reflection coefficient [See (29)]; and $f_m(p)$ is the product of RPR and TOT above, which is set equal to TQ, and PLN1 stores the imaginary part of TQ in RP.

iv) η_1 (EA) is computed.

v) If the directivity function is desired [See(42)], then NDIRT > 1 and (42) is computed.

vi) $\psi_m(t)$ as described in (19) and (20) are then computed and stored in PHI(I).

vii) Above six steps are repeated for increasing p till DELP(NO) is exhausted, and if the time corresponding to the last p used is reasonably far from t_0 (criterion is DLTP) then the procedure is repeated for p incremented by some small real number till t reaches t_0 .

viii) At the end of PLN1, TT(1) = t_c and PHI(1) = 0 are set. This is to save computation time, since obviously the starting time is the refraction time and $\psi_m(t_c) = 0$ if PLN1 is ever called.

After PLN1 computes $\psi_m(p)$ for $t_c < t < t_0$, PLN2 computes $\psi_m(p)$ for $t_0 < t$ including $\psi_m(p_0)$ [See the first motion approximation]. As PLN1 returns to HIGH, HIGH computes

the complex path of p such that, as in (25), the imaginary part of t is zero. To accomplish it, CONTOR is called. It takes p_0 and increment it by DELP, and for each p , TIME2 is called to find the corresponding imaginary part of p such that $\text{Im}(t) \leq \delta$. If so, complex p and dp/dt and real t are stored in arrays PP, DDPT and TT, respectively, to be used in PLN2. After p reaches the end specified by DELP, CONTOR repeats the operation till t reaches $t_0 + \text{TMX}$ or $t_c + \text{TMX}$ whichever is the smallest. TMX is defined in MAIN. Upon CONTOR's return to HIGH, PLN2 computes $\psi_m(\rho)$. It is very similar to PLN1, but the starting point of PHI(I) is now MO and the ending point is M, both of which are defined in CONTOR. After $\psi_m(\rho)$ is computed for $t_0 < t < t_0 + \text{TMX}$, PLN2 deals with the problem of $\psi_m(\rho)$ as described in the section, the first motion approximation.

FUNCTION SF2 computes Equation (37). To perform the integration by the trapezoidal rule, we utilize the value of $\psi_m(\rho)$ already obtained for $t_0 - h < t < t_0 + h$; SUBROUTINE INTERP is called to obtain $\psi_m(\rho)$ at five points between $t-h$ and $t-\delta$, and $t+\delta$ and $t+h$. In the program $t_0 = \text{TTT}(\text{NO}+1)$, $t_0 - \delta = \text{TTT}(\text{NO})$, $t_0 + \delta = \text{TTT}(\text{MO})$ and $h = \text{DP}$. DELL is the partition. t is increased by DELL starting from $t_0 - h$, $\psi_m(\rho)$ is obtained (interpolated) for each t by INTERP, and finally (39) is used to obtain β . At the very end of PLN2, (31) is applied to get $\psi_m(t)$ at $t = t_0$. As PLN2 returns to HIGH, the maximum indices of the computed time and pressure, TD and PHI in COMMON /EXACT/, are set equal to M, defined in PLN2. When HIGH returns to SETUP, SUBROUTINE ADJUST is called to

locate the index I of the array T in COMMON /THY/ defined in SETUP to be equidistance apart, which corresponds to TD(1) in COMMON /EXACT/. NFIX = I and returned to SETUP. Then, TD is shifted in such a way that t_0 lands on some T. ($\psi_m(t_0)$ is the most important point of all) Since TD is so closely spaced near $t = t_0$ that shifting makes little difference in actual response time. Then, INTERP is used again to interpolate PHI for each T (equispaced) and the values are stored in PP after being multiplied by NF - symmetry constant defined in CONN or in CONSTN and CON. In other words, if there are more than two rays that can be specified by the same values of parameters, then the response must be multiplied by the number of such rays.

After PP is filled, if there are no more rays to consider (that is, if $KO > 1$) then SUBROUTINE SETT is called to perform the last operation [See (27)]. SETT reads the transfer function SS(KO), FUNCTION CONVS convolves SS and PP point by point and the result is stored in CC. Then, the derivative is taken and the result is plotted and printed (P).

This is the end of the program.

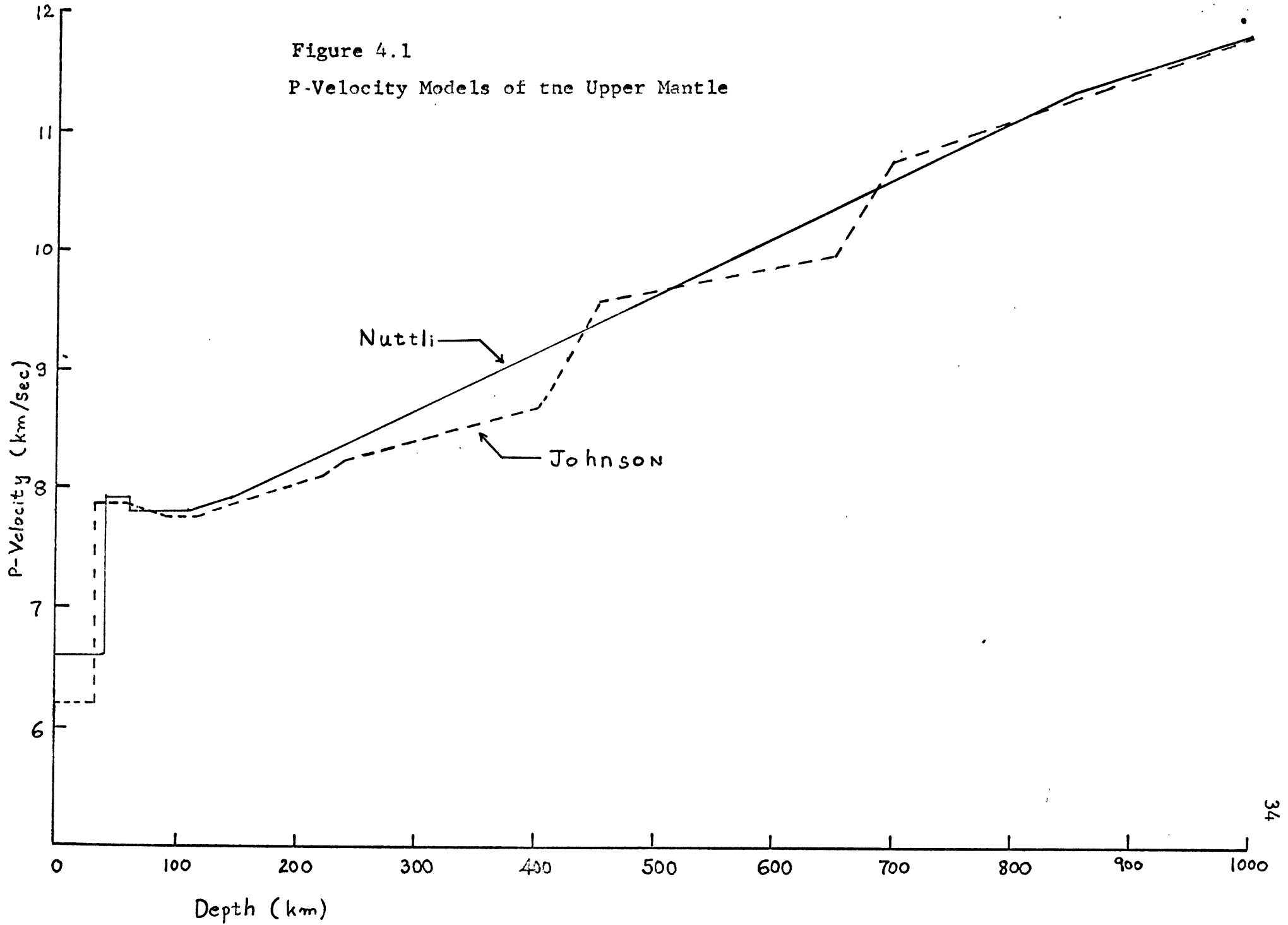
IV. DISCUSSION AND RESULTS

In this chapter some of the results obtained are discussed, the main object being to examine two of the existing models of the upper mantle [Dowling & Nuttli (1964) and Johnson (1967)] and to find a better model for the southern United States using the synthetic seismogram discussed in the previous chapters.

The upper mantle P-models by Nuttli and Johnson are shown on Figure 4.1. Both have a low velocity zone under the Mohorovicic discontinuity, but in the Nuttli's model, the velocity increases almost linearly with depth after the low velocity zone, whereas in the Johnson's model, there are two pronounced changes in the gradient - one at around 450 km and the other at around 700 km. We shall examine synthetic seismograms generated by these models, and compare them with actual records obtained in the Bilby underground explosion (1963).

But, first it may be interesting to look at some sample output of the computer program. [See Figures 4.2-4.7] In Chapter II we referred to the high frequency approximation [See Eqn. (18)]. Another computer program had been written without the approximation. Clearly, this program is more exact, but slower. Figure 4.2 is the transfer function that each response is to be convolved with. Figure 4.3 shows the transfer function convolved with $1/\sqrt{t}$, which we use in our approximate method. Figure 4.4 is the theoretical response to a unit pulse. Figure 4.5 is the response from the approximate method. Note that, in effect, the exact response is the convolution of the approximate response with

Figure 4.1
P-Velocity Models of the Upper Mantle



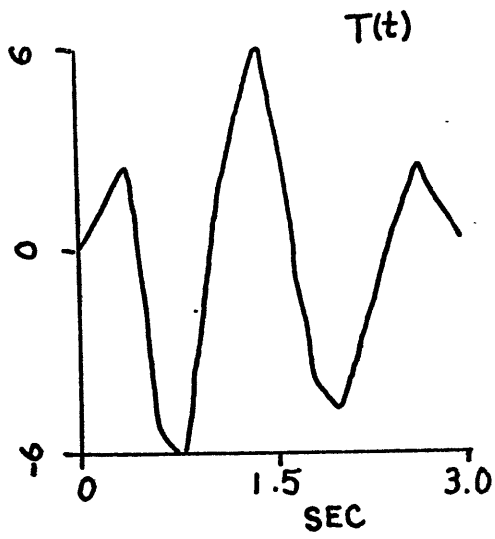


Figure 4.2
Transfer Function

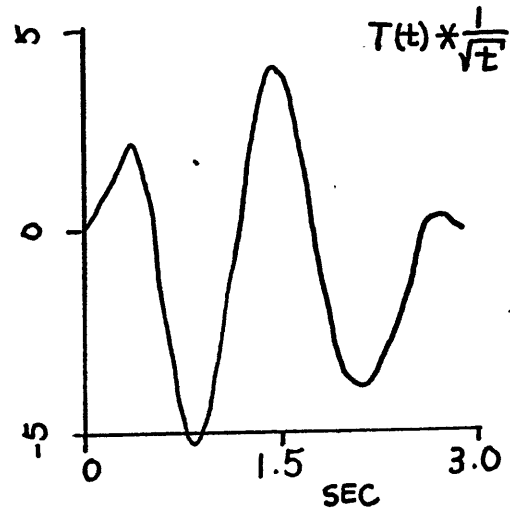


Figure 4.3
Modified Transfer Function

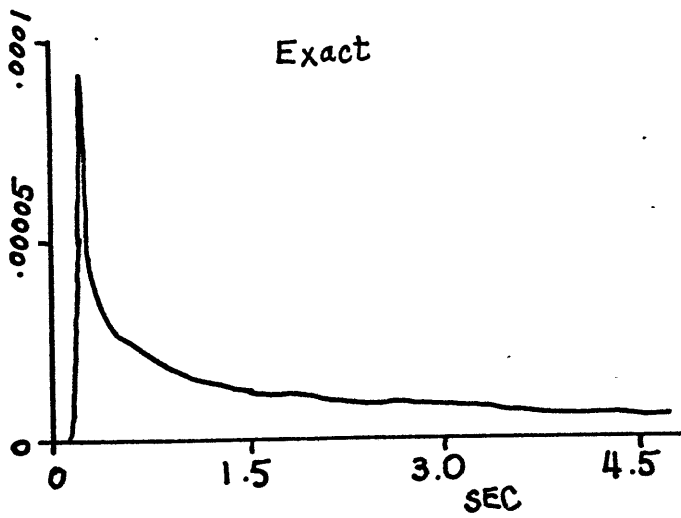


Figure 4.4
Exact Response

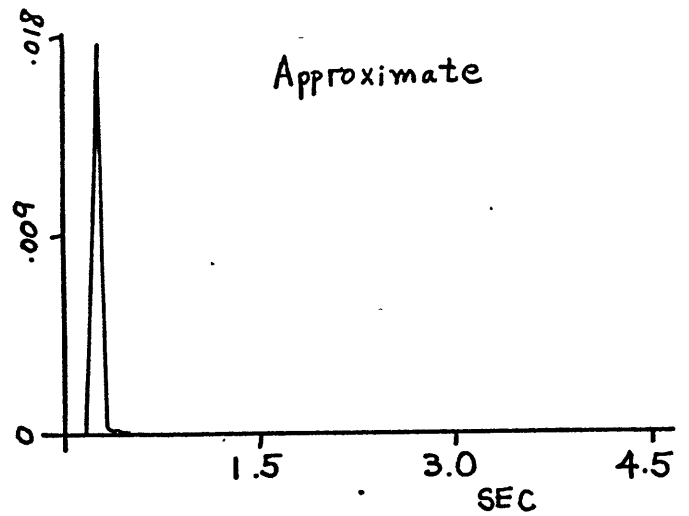


Figure 4.5
Approximate Response

$1/\sqrt{r}$. Figure 4.6 shows the approximate synthetic seismogram, whereas Figure 4.7 shows the exact synthetic seismogram. In terms of amplitude, phase and frequency, the two synthetic seismograms look nearly the same, and provide some evidence to the validity of the approximation.

In the following figures (4.8-4.12), records of the Bilby event are shown. The time scale is the same in all these figures and in all the others that will follow. But the amplitude is not absolute and only significant in one record. The relative amplitudes and the arrival times of these records are tabulated in Table 4.1.

Table 4.1 Bilby Event (1963)

STATION	LATITUDE (° ' ")	LONGITUDE (° ' ")	RANGE (km)	TIME (sec.)	MAGNITUDE (A/T)
Source	37 03 38	116 01 18	--	--	--
Raton N.M.	36 43 46	104 21 37	1039	136.7	11
Shamrock Texas	35 04 58	100 21 50	1426	187.7	165
Durant Okl.	34 02 11	96 13 04	1831	231.8	374
Liddie- ville La.	32 08 10	91 52 30	2274	280.7	915
Orlando Fla.	28 28 01	81 13 17	3376	375.0	265

(all locations are in the Northern and the Western Hemisphere)

Date: 13 Sept. 1963 ; Time: 17:00:00.13 oz

Magnitude: $m=5.8$

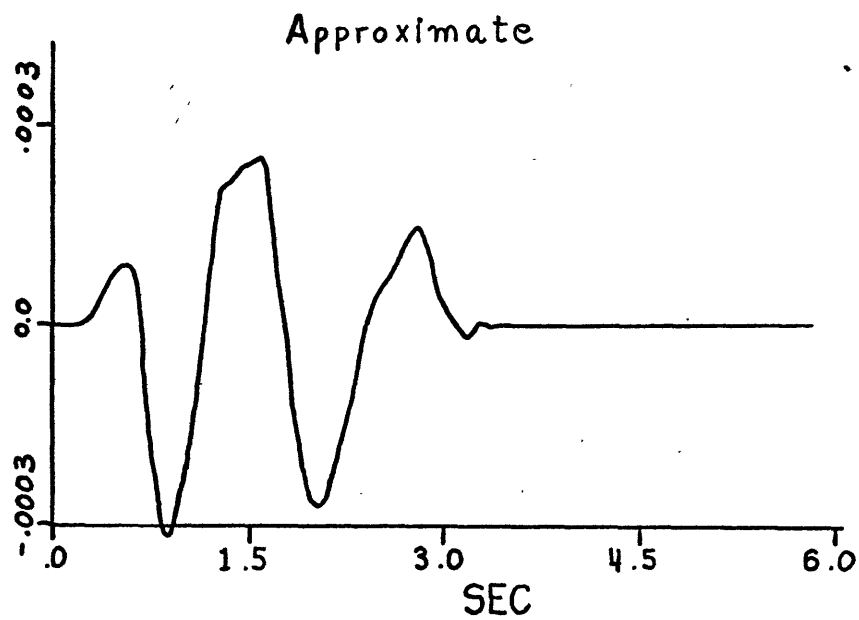


Figure 4.6
Approximate Synthetic Seismogram

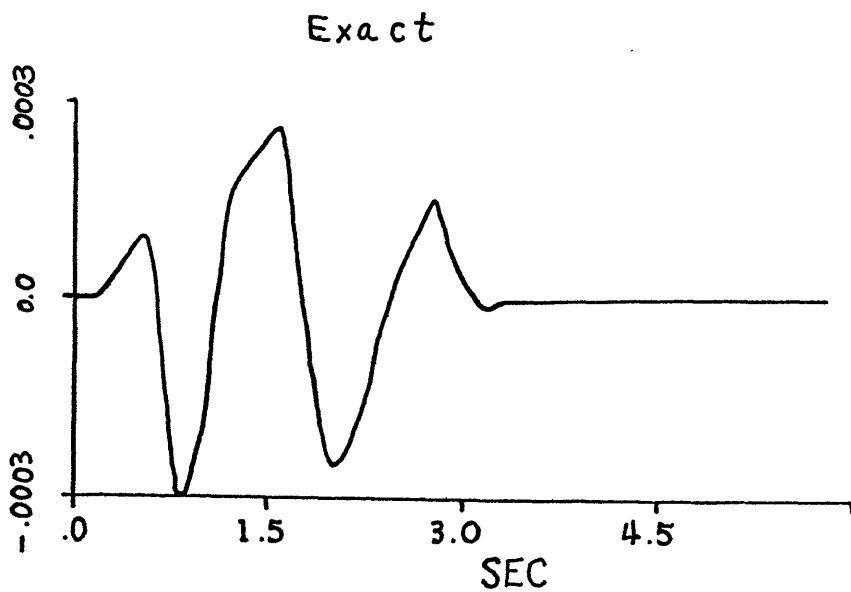
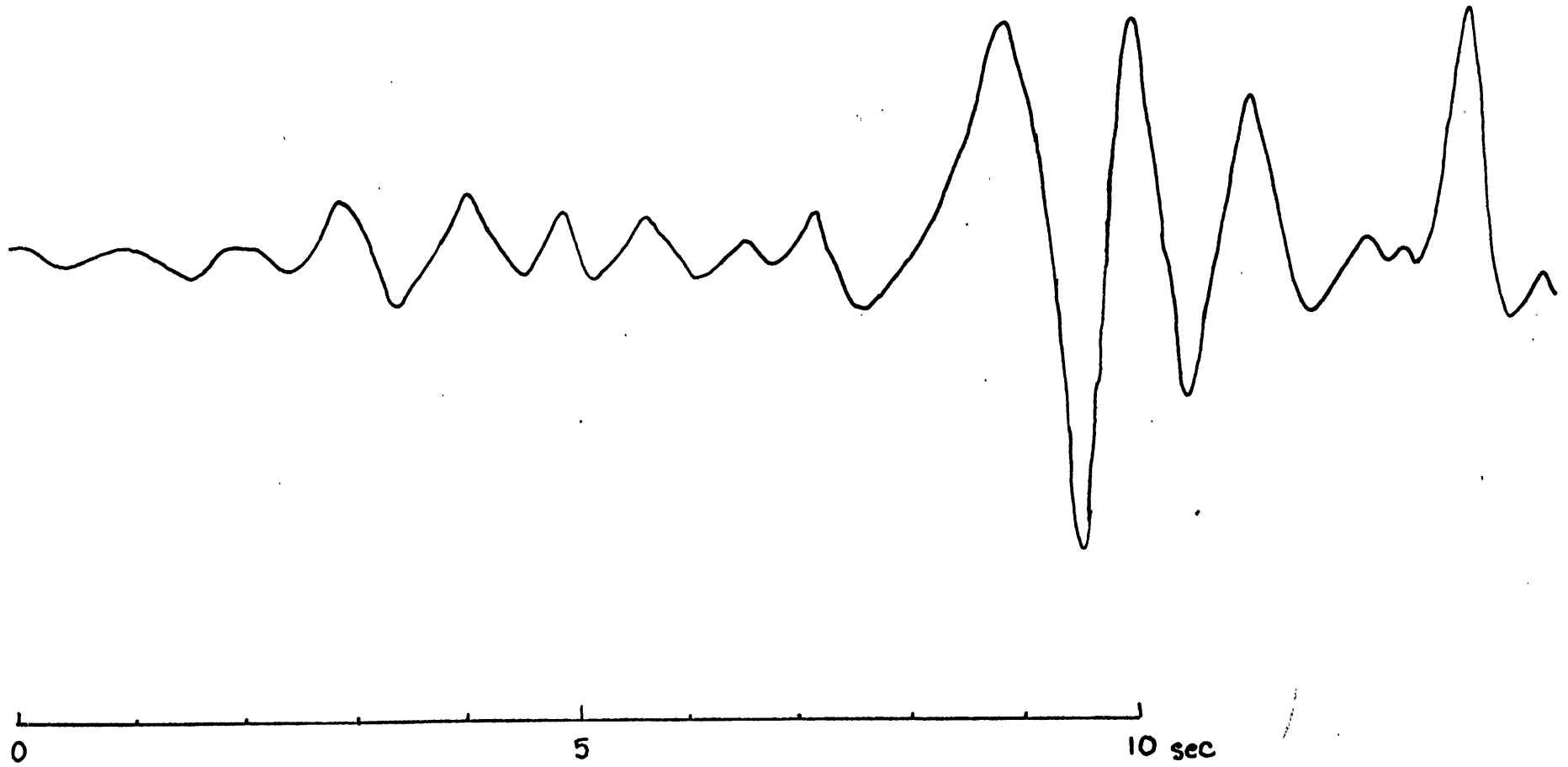


Figure 4.7
Exact Synthetic Seismogram

Range 1039 km

Figure 4.8 Bilby Event



Range 1426 km

Figure 4.9 Bilby Event

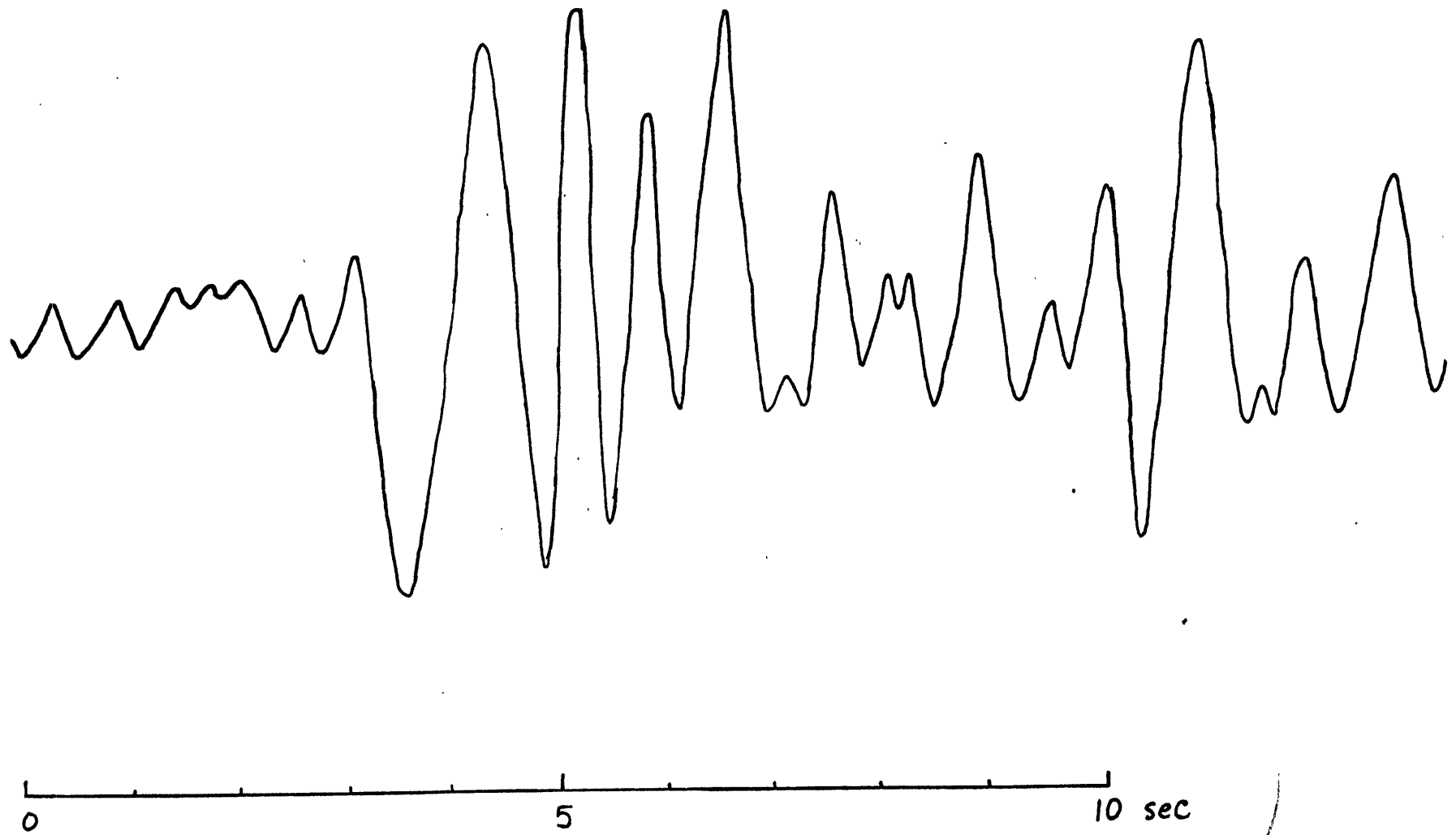
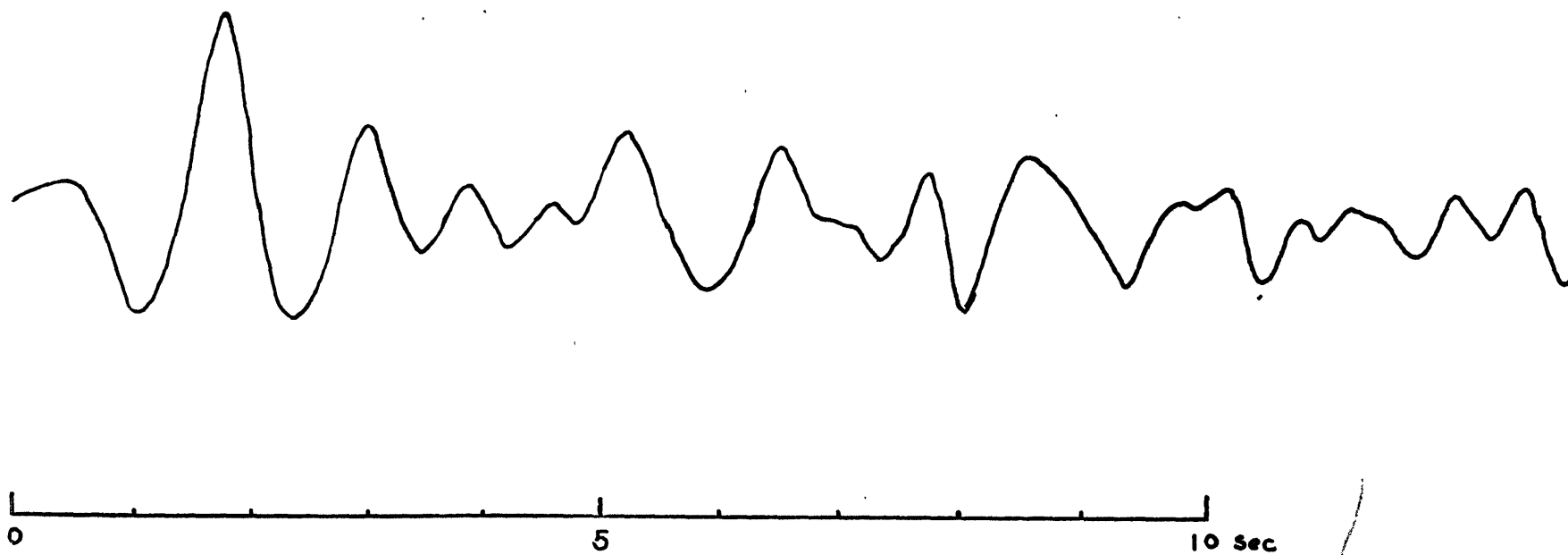


Figure 4.10 Bilby Event

Range 1831 km



Range 2274 km

Figure 4.11 Bilby Event

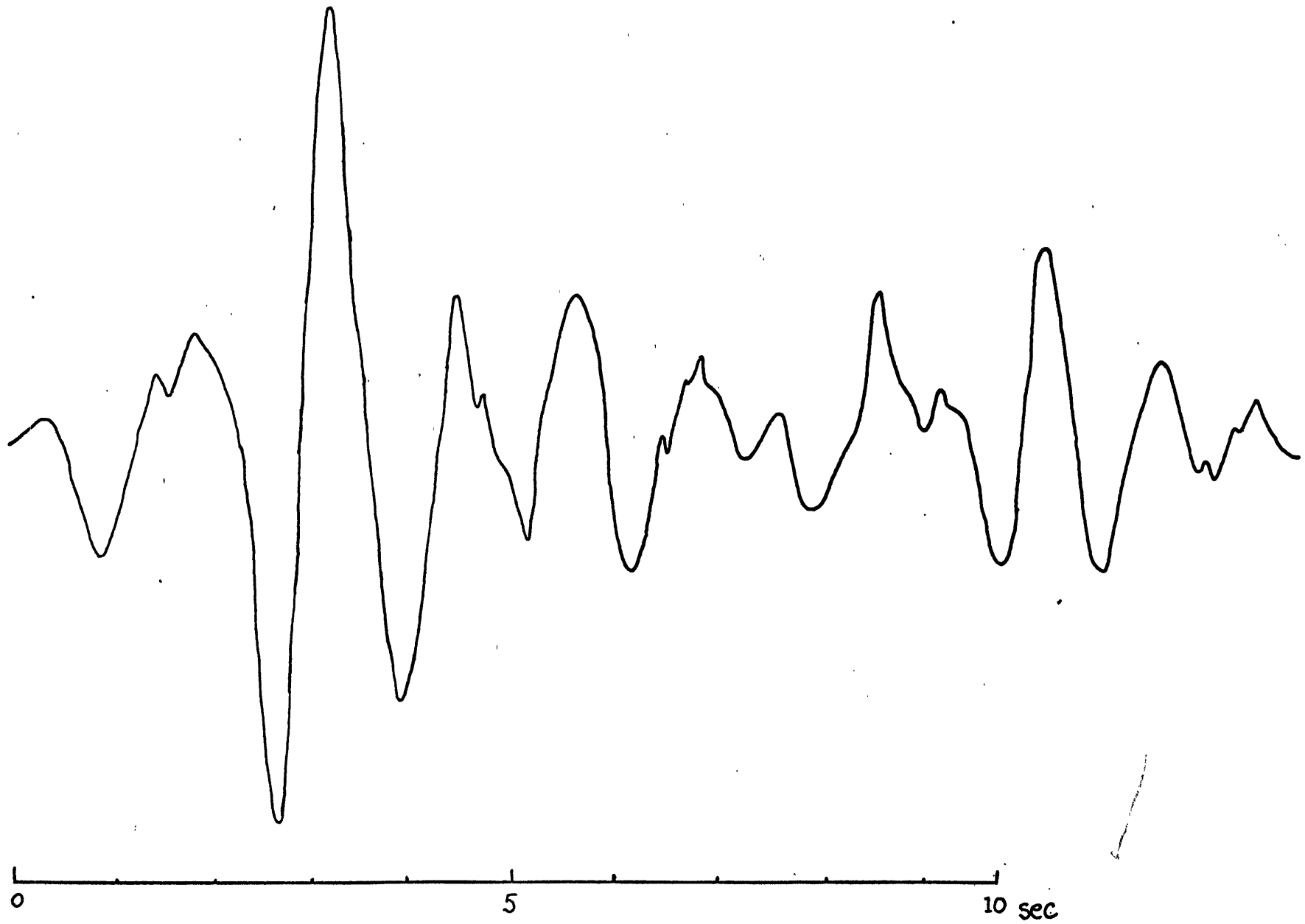
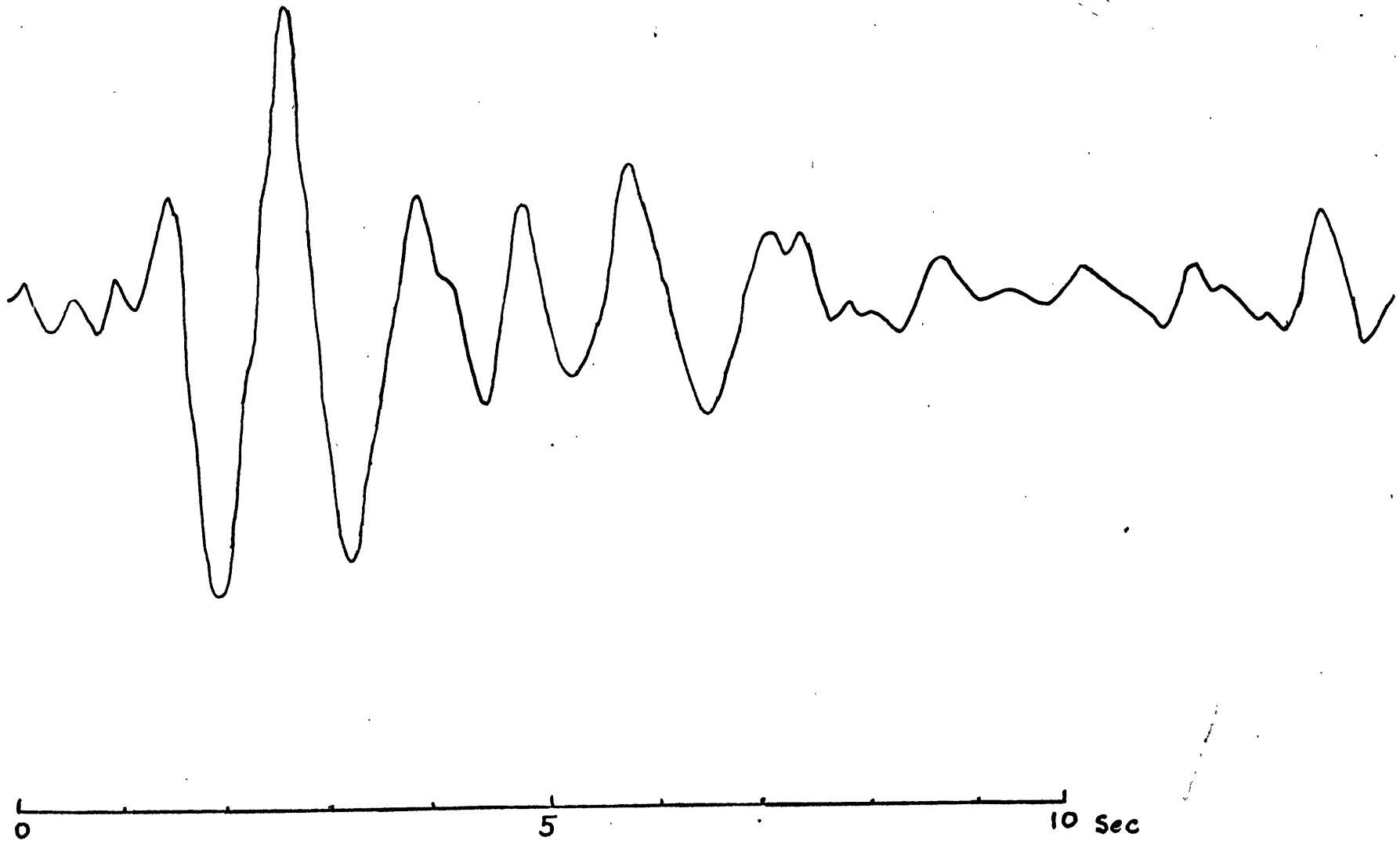


Figure 4.12 Bilby Event

Range 3376 km



Note that these amplitudes are determined for the first arrivals, not the maximum amplitude in general. Thus, in the short ranges - 1039 km and 1426 km - the amplitudes are small because they are of Pn not of P, which arrives later. Notice that the amplitude reaches the maximum at the range of 2274 km. We will be much concerned with this fact when we derive a suitable model.

In examining the models by Nuttli and by Johnson for this region of the North America, the following procedure was used. First we ran a simple program which only computed the arrival times - refraction and reflection - from each layer by the method described in the previous chapters. We found the earliest arrival time at a certain range and found which layer it came from. Then, we examined the arrivals from the surrounding layers, and the responses that came in within so many seconds (usually 6 seconds for the sake of economy) after the first arrival were noted. We, then, ran the synthetic seismogram program to compute the synthetic seismogram considering only those responses found earlier.

We first applied our method to the Nuttli's model. Table 4.2 shows the first arrivals and magnitudes computed by our program. The synthetic response from the first arrival to six seconds later is shown in Figure 4.13. The synthetic seismogram, Figure 4.13 convolved with 4.3, is Figure 4.14. Compare the record (Fig. 4.8) with this figure. The difficulty is that at this range, the ray travels at very shallow depth so that the subsurface structure, which we expect to be extremely non-uniform,

Figure 4.13

Theoretical Response

Nuttli 1039 km

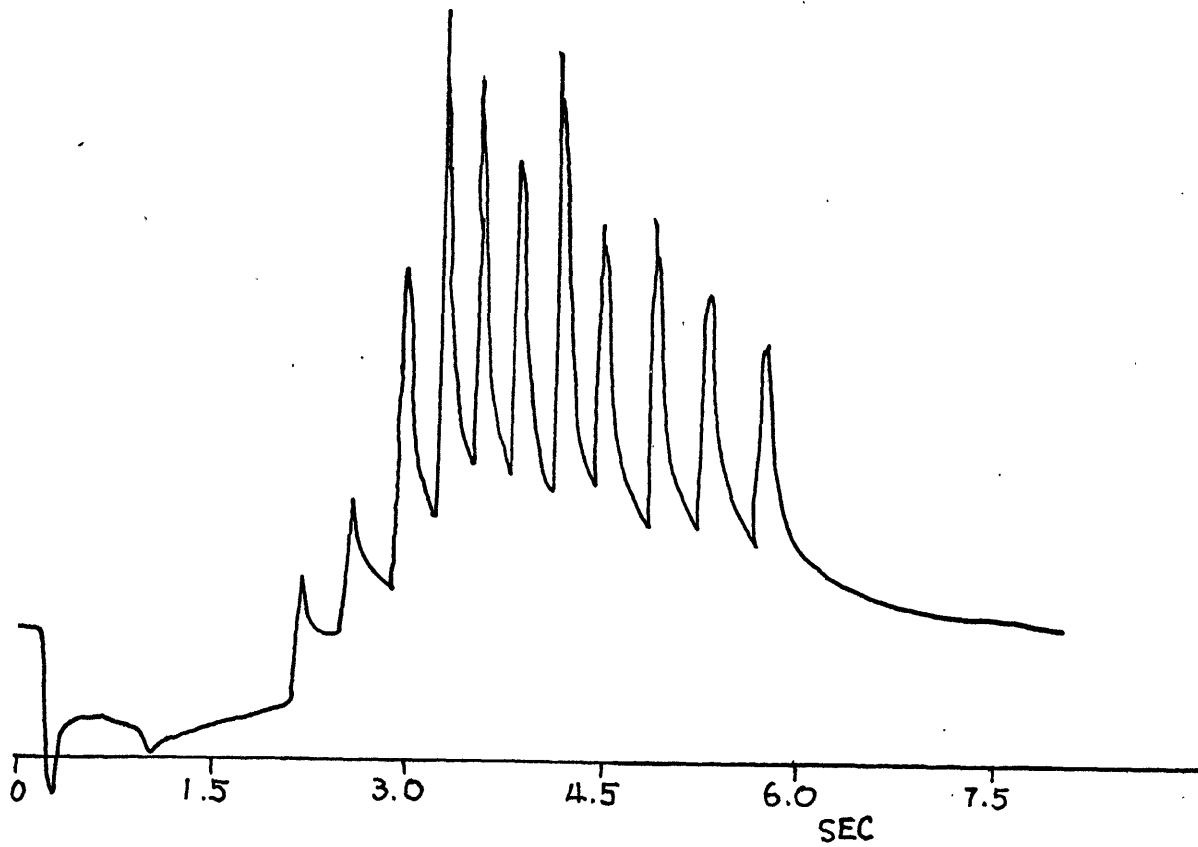


Figure 4.14 Synthetic Response Nuttli 1039 km

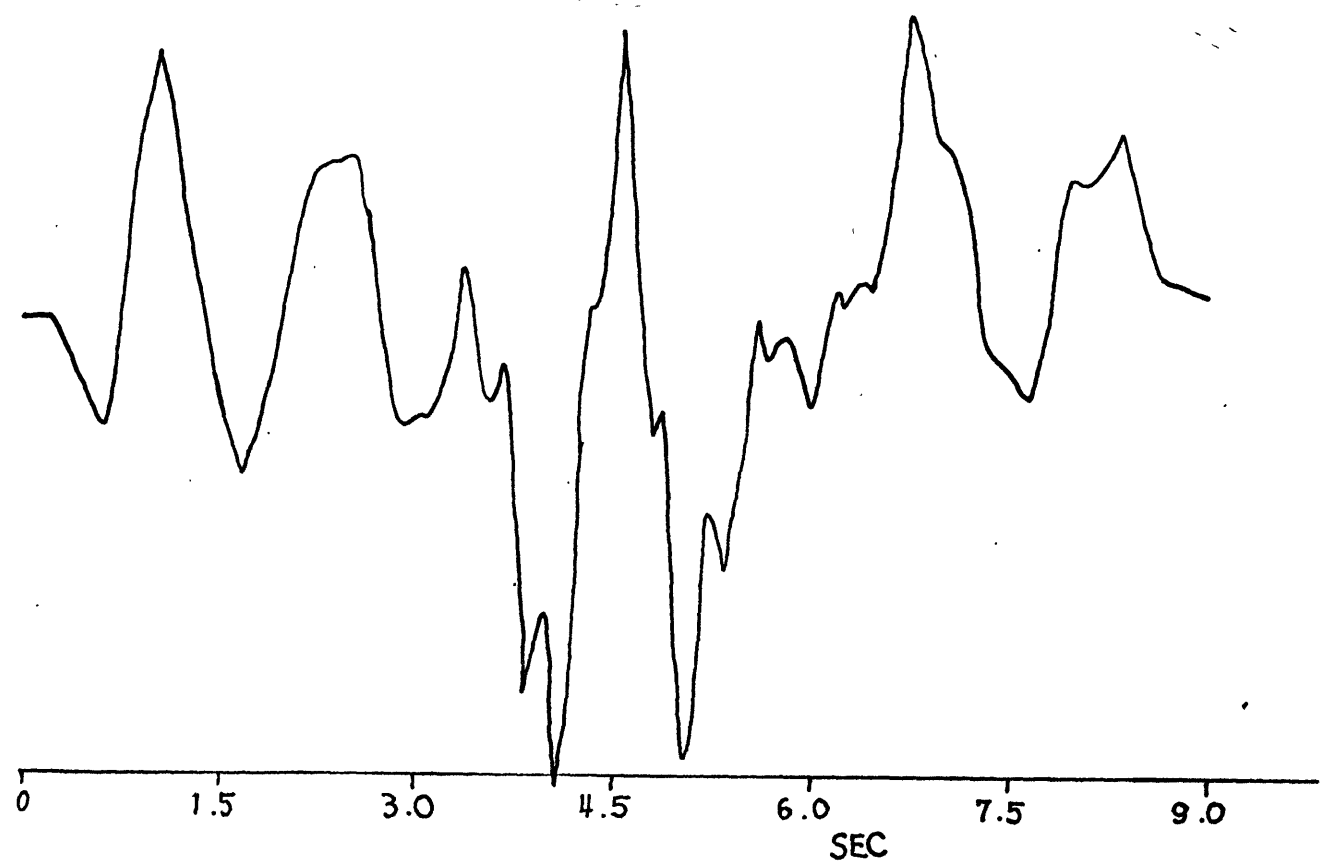


Table 4.2

First Arrival Times and Magnitudes for the Nuttli's Model

Range (km)	Time (sec.)	Magnitude
1039	136.0	15
1426	184.0	---*
1831	232.6	180
2274	278.0	140
3376	373.0	34

(* As shown in Figure 4.15, the magnitude for this range was very small)

greatly affects the ray paths. [See S. W. Smith (1962)] Our assumption is a lateral homogeneity, which may be violated here. Other reasons may be that the model has a negative discontinuity at about 75 km deep which caused the negative peak in the theoretical response and that we neglected all the rays with weak response ($N \geq 5$); if more rays had been added, the response would have been smoother. Similarly, synthetic seismograms were generated for the other ranges (Figures 4.15-4.18). The author reminds the reader that the amplitude between any two seismograms - real or synthetic - may not be compared. We expected a gradual decay in the amplitude with increasing range, since the Nuttli's model has no gradient variations. At the range of 2274 km, therefore, the model does not give a large amplitude and does not give a small first arrival that the record shows. On this ground, we concluded that this model does not fit the actual record in this range, though travel times do fit.

Synthetic Response Nuttli 1426 km

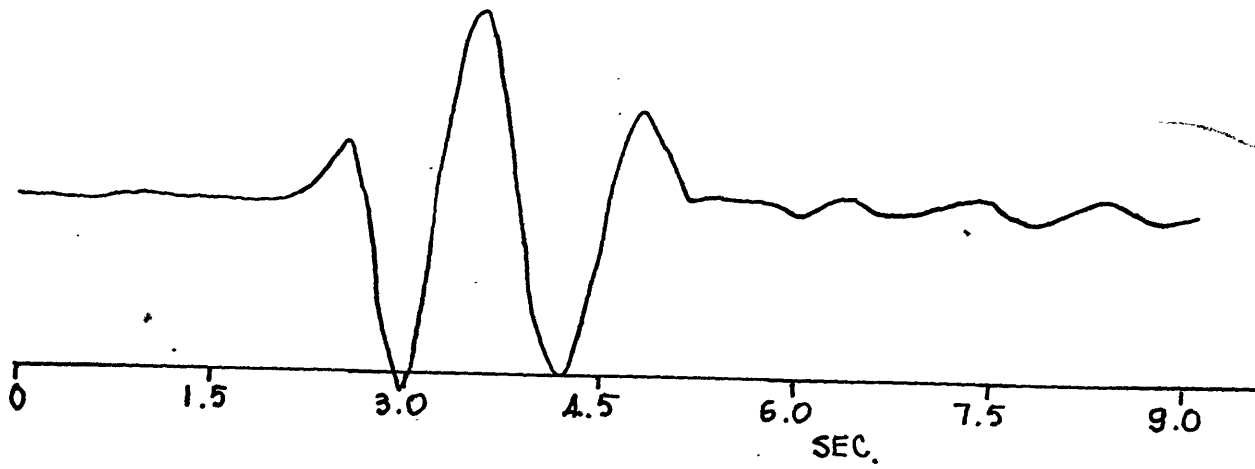


Figure 4.15

Synthetic Response Nuttli 1831 km

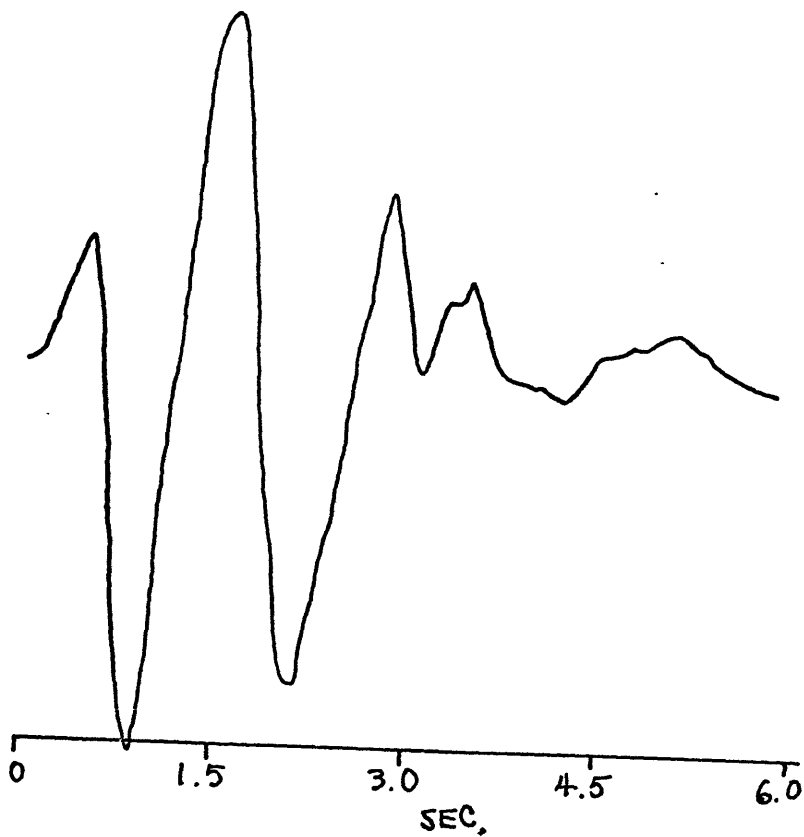


Figure 4.16

Synthetic Response Nuttli 2274 km

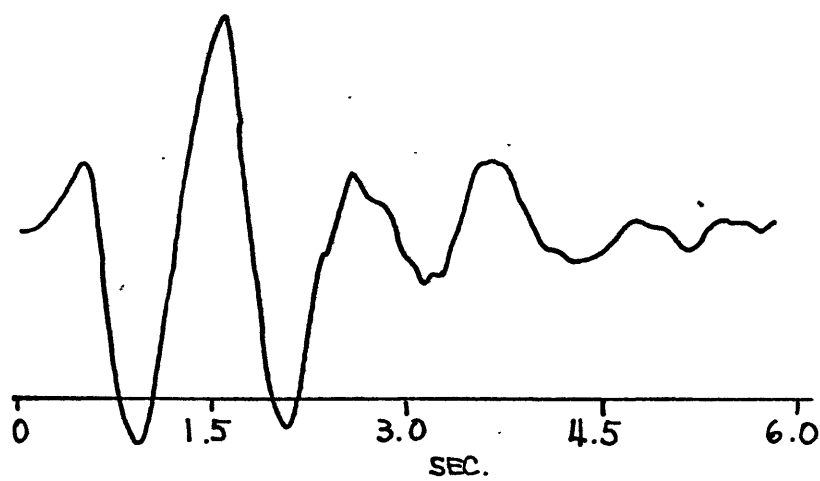


Figure 4.17

Synthetic Response Nuttli 3376 km

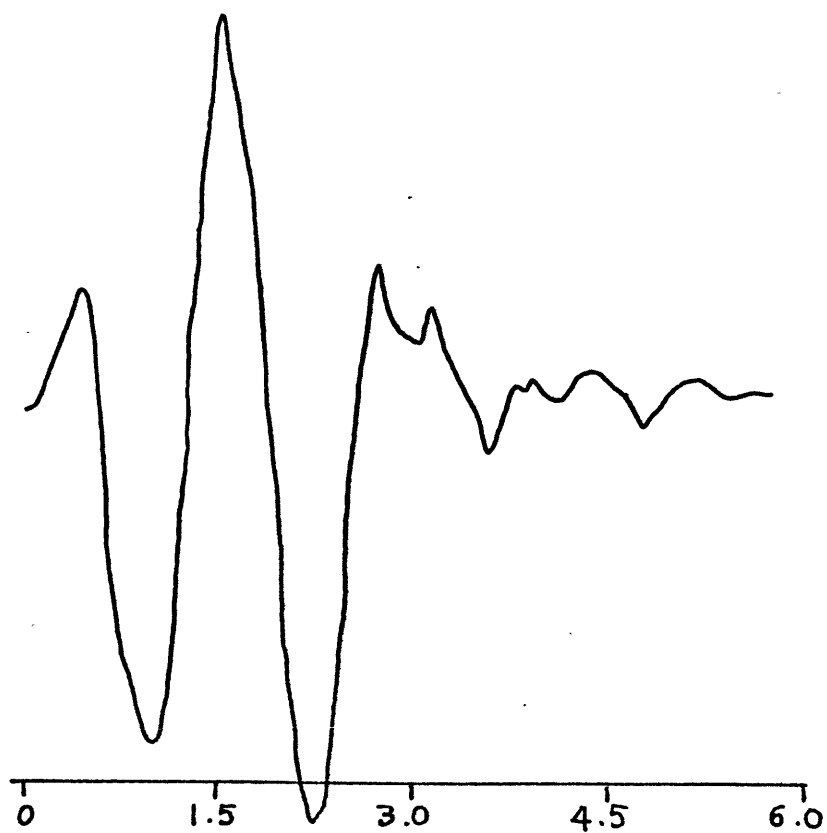


Figure 4.18

Next we examined the Johnson's model [See Table 4.3].

Table 4.3

First Arrivals and Amplitudes for the Johnson's Model

Range (km)	Time (sec.)	Magnitude
1039	137.0	---
1426	186.9	80
2274	279.2	50

Again a difficulty arises at the short ranges. The refracted arrivals are much too early and last too long in the record, perhaps due to destructive interference caused by complex subsurface structure. We ran his model only at three ranges (Figures 4.19-4.21), the most important one being at 2274 km. The Johnson's model generated a small first arrival, but the time between the arrivals of the first ray and the large second ray is much too long, and though the largest amplitude in this synthetic seismogram (Fig. 4.21) is very large, there is little resemblance to the actual record at the range.

We, then, constructed some models with the effort concentrated on the seismogram at 2274 km. The models, along with the Nuttli's, are shown on Figure 4.22. We took the negative discontinuity at 75 km deep. The first model (Model I) has very small change in the slope from the Nuttli's model. The seismogram and the theoretical response at 2274 km are shown on Figures 4.23 and 4.24. Note that the period of the transfer function (Figure 4.3) is 1.15 seconds, and the distribution of

Synthetic Response Johnson 1039 km

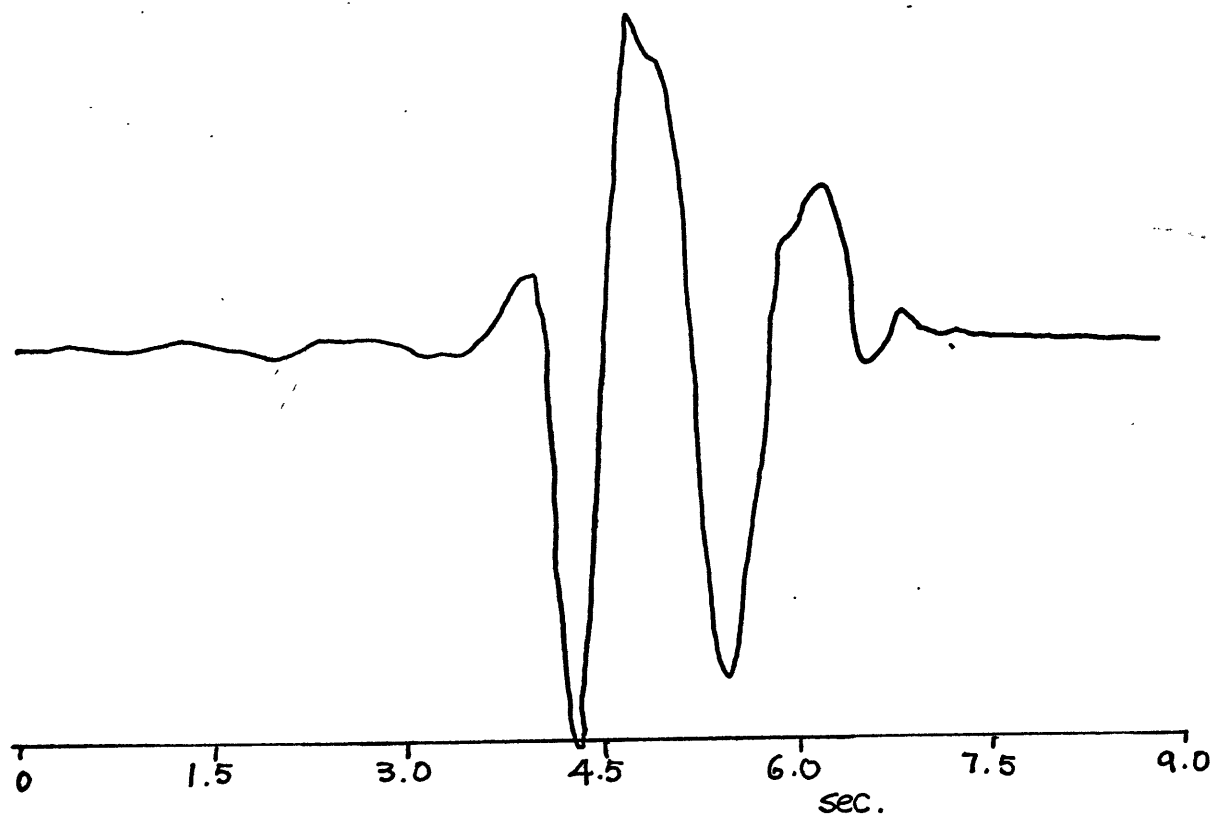


Figure 4.19

Synthetic Response Johnson 1426 km

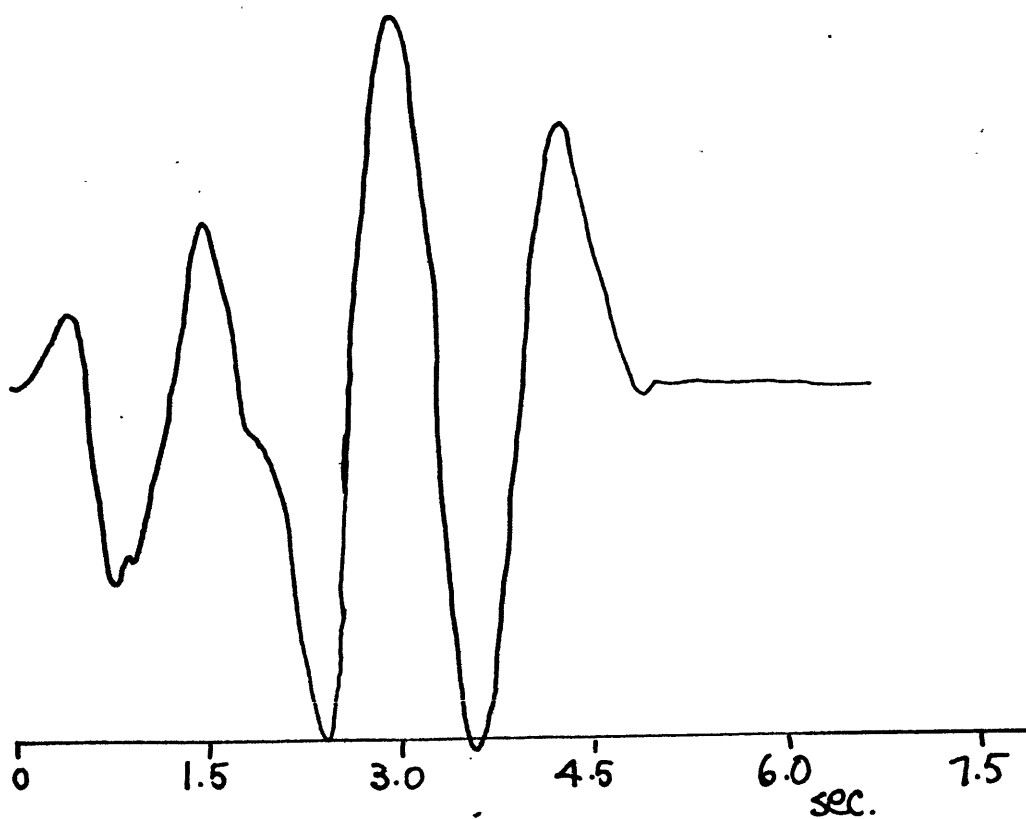


Figure 4.20

Figure 4.21 Synthetic Response Johnson 22.74 km

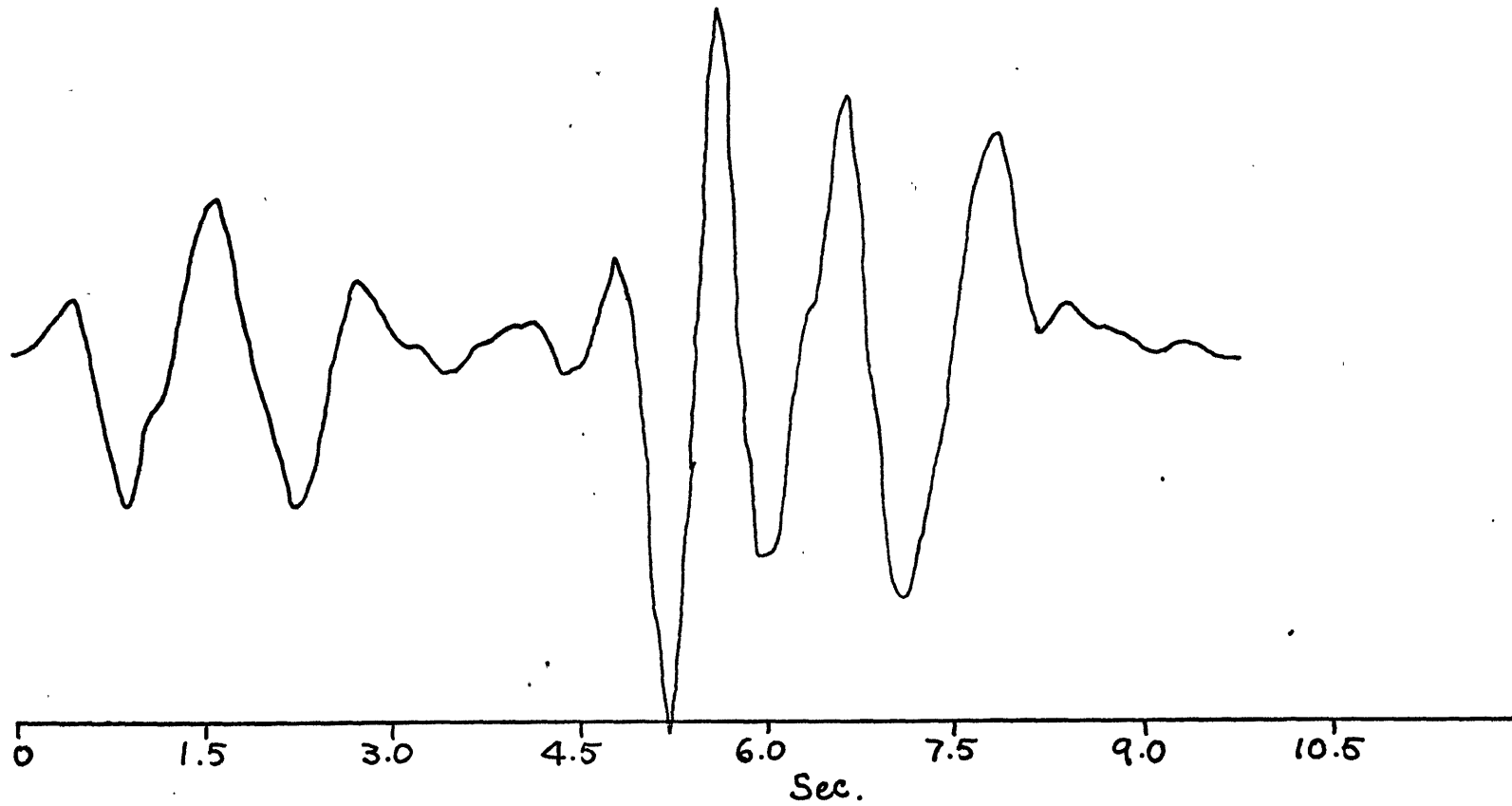
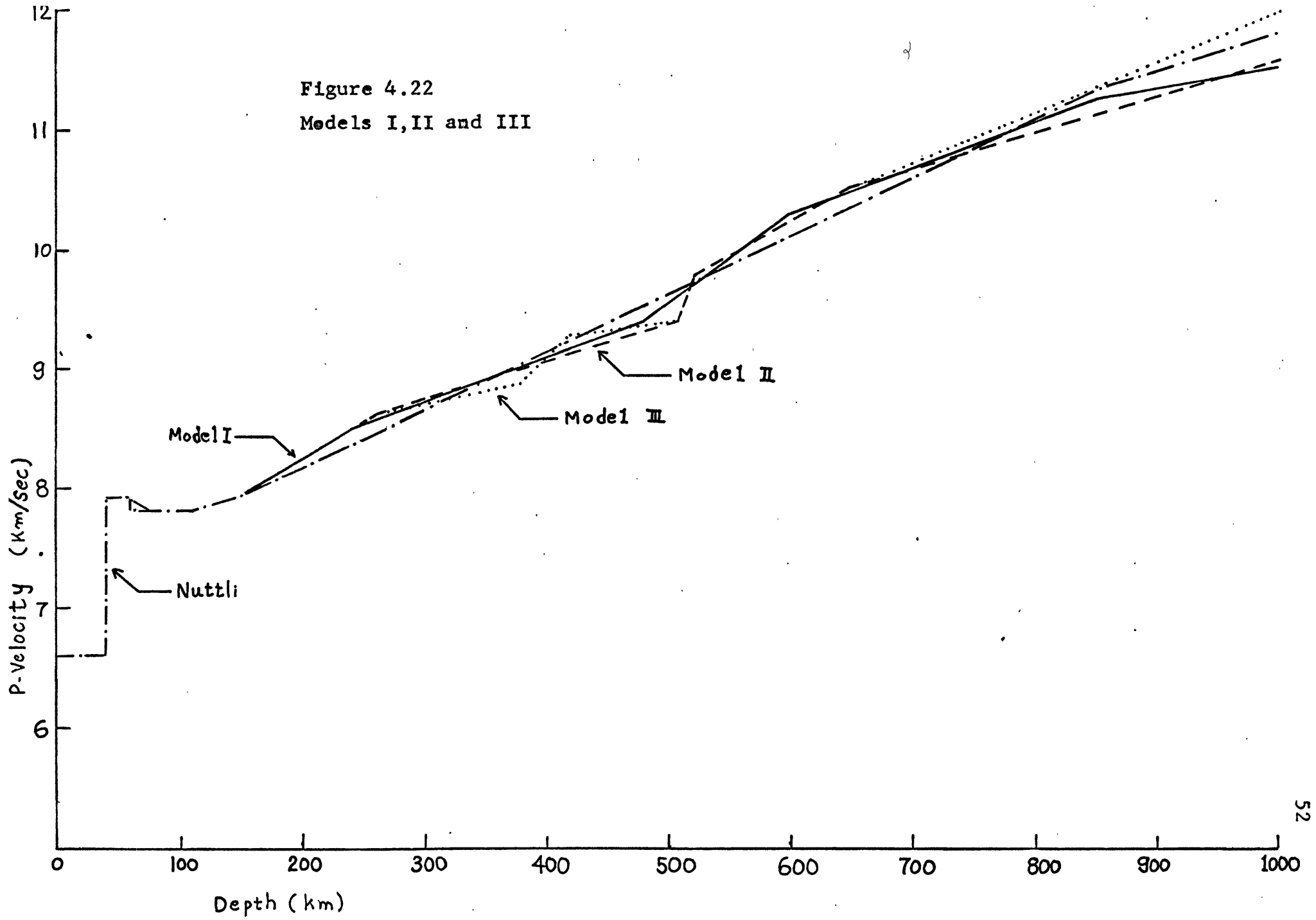


Figure 4.22
Models I, II and III



Synthetic Response Model I 2274 km

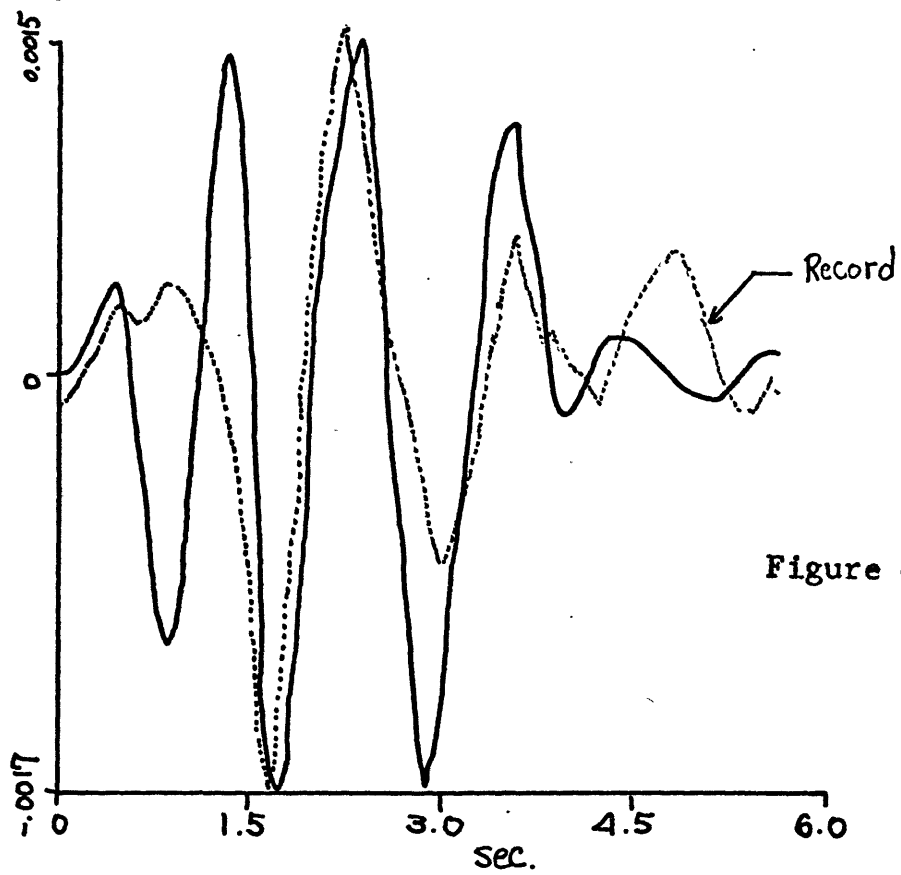


Figure 4.23

Theoretical Response Model I 2274 km

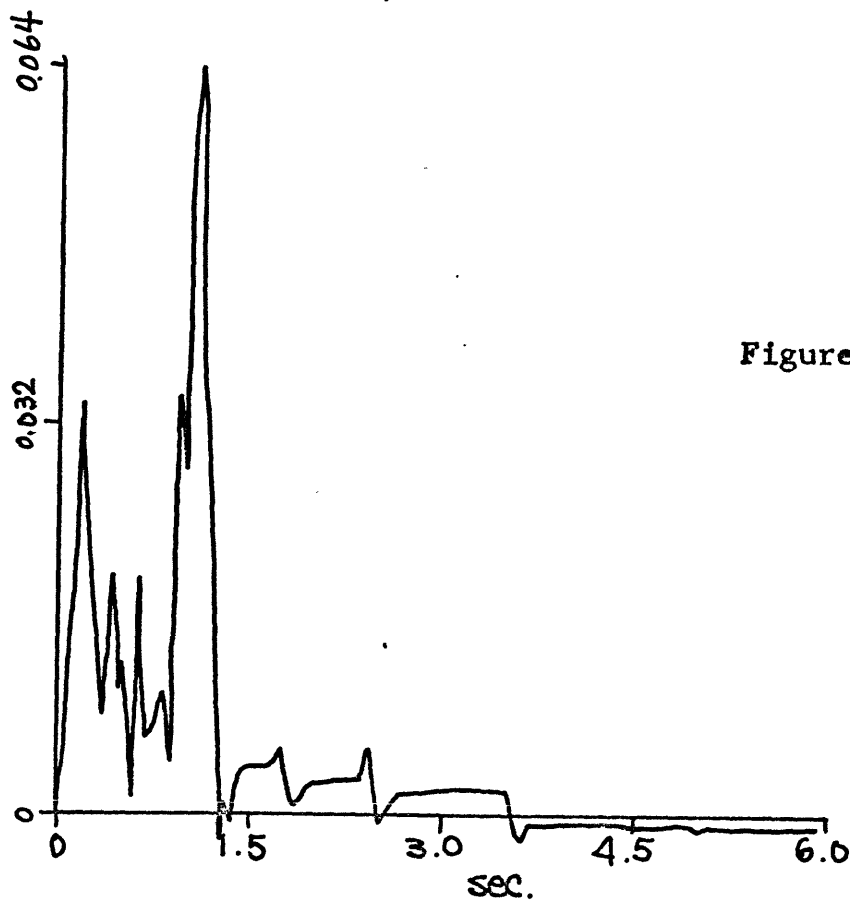


Figure 4.24

the peaks in Figure 4.24 seemed to interfere destructively with each other to generate a poor seismogram. (The synthetic seismograms for all these models are similar to the Nuttli's at other ranges, with the exception of the one at 1039 km without the negative peak. The amplitude at 1831 km is 0.001).

Model II has a more pronounced gradient change at 510 km. This gradient gave a more prominent second arrival starting at 1.1 seconds after the first arrival [See figures 4.25 and 4.26]. Note that the significant factor is the area under the theoretical response, not simply the height of the peaks. In this model the separation of the peaks helped to generate a better synthetic seismogram, but the fit with the record, especially in the first second is not satisfactory.

Model III has another high gradient region at 430 km in addition to the one at 510 km. The first arrival is much smaller and the amplitude in the synthetic seismogram improved [See Figures 4.27 and 4.28]. The wave shape improved as well as the amplitude, somewhat. But a close examination of the actual record indicates that we need a small peak for the first arrival then a much larger peak at 1.5 seconds later. In order to obtain a response like this, Model II is the best of all we have tried, the difficulty being that the first and the second arrivals were too close. To attain a wider separation, further models were studied. Models IV and V are shown on Figure 4.29. The theoretical responses and the synthetic seismograms are on Figures 4.30-4.33. The continued high gradient at 300 km and flat gradient following

Synthetic Response Model II 2274 km

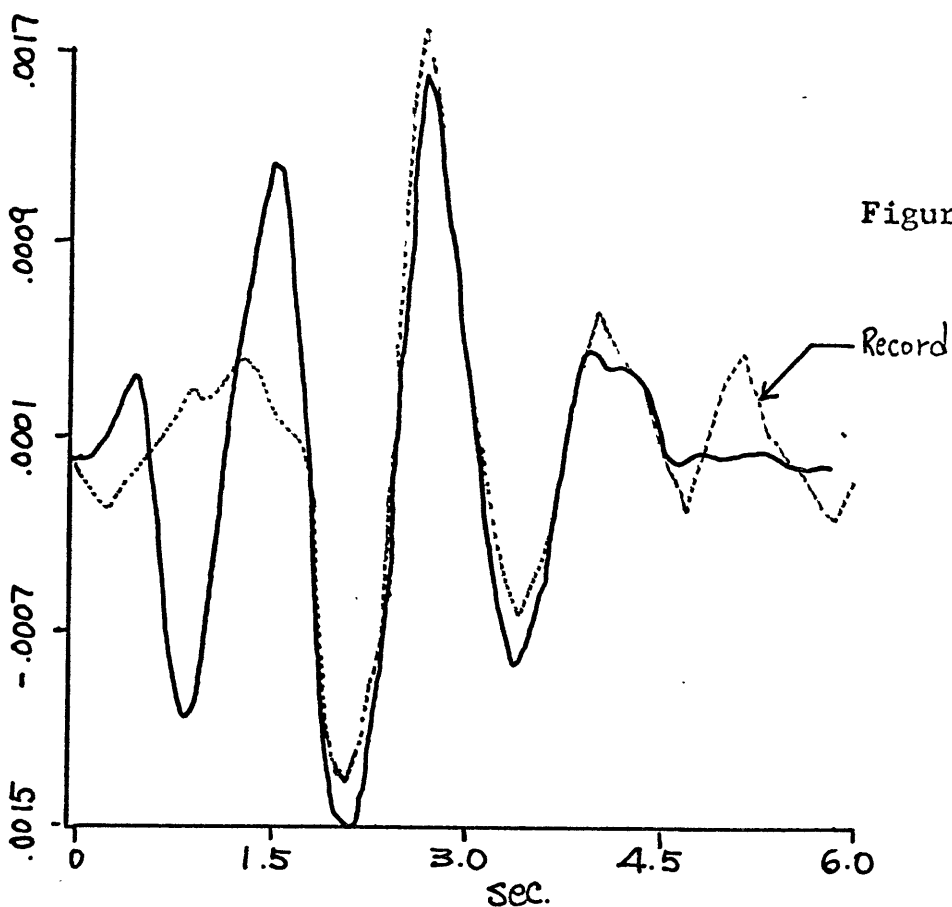


Figure 4.25

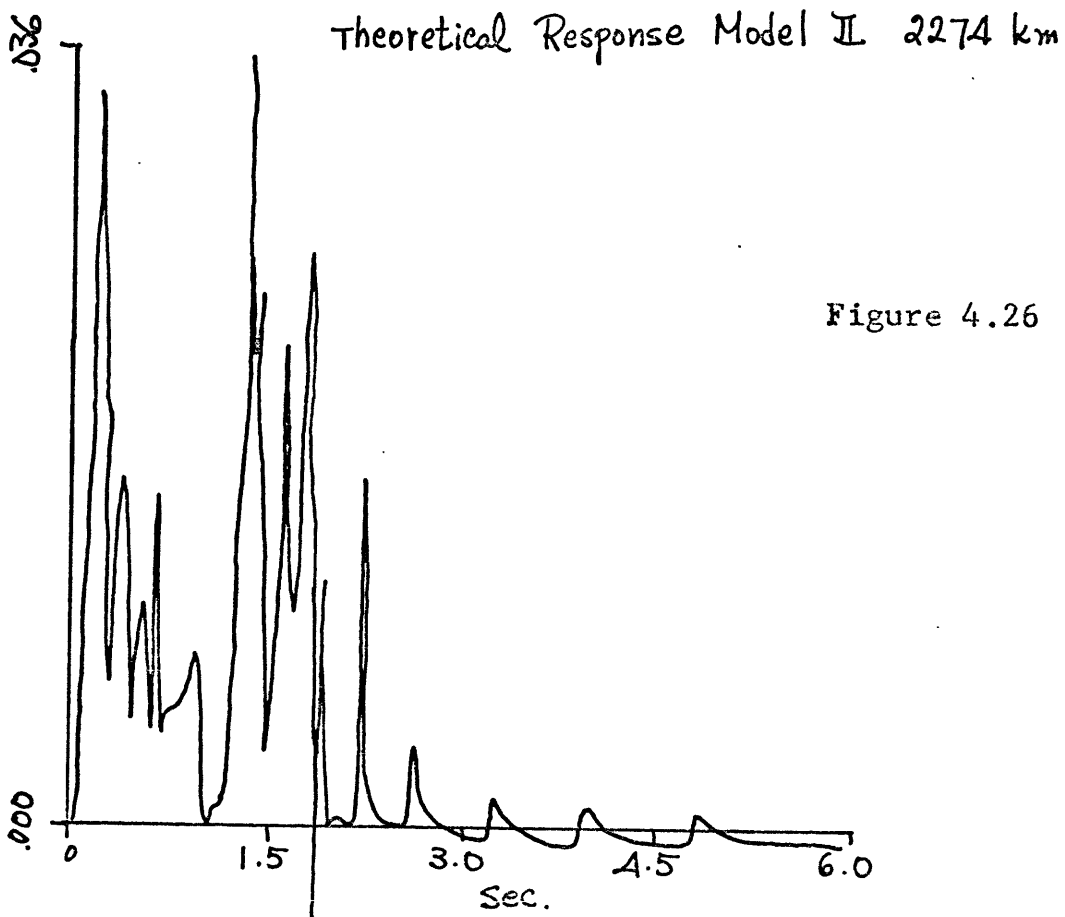
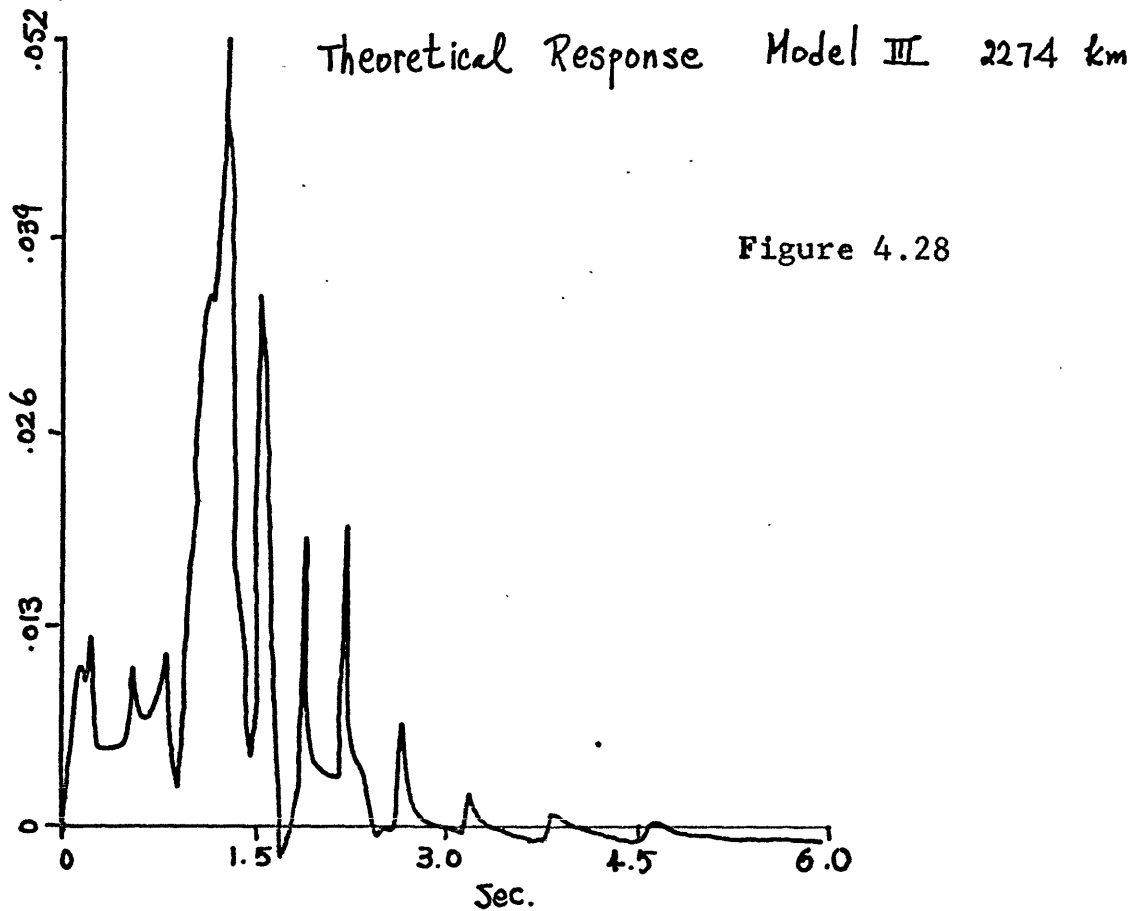
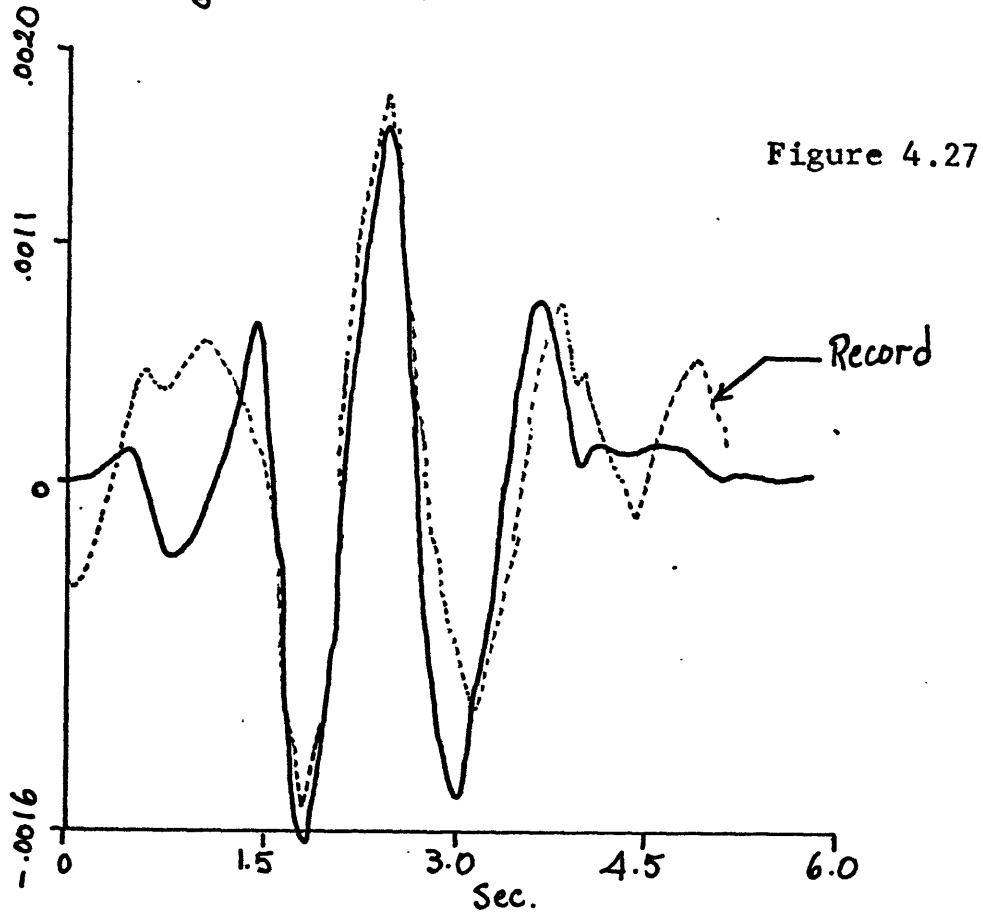


Figure 4.26



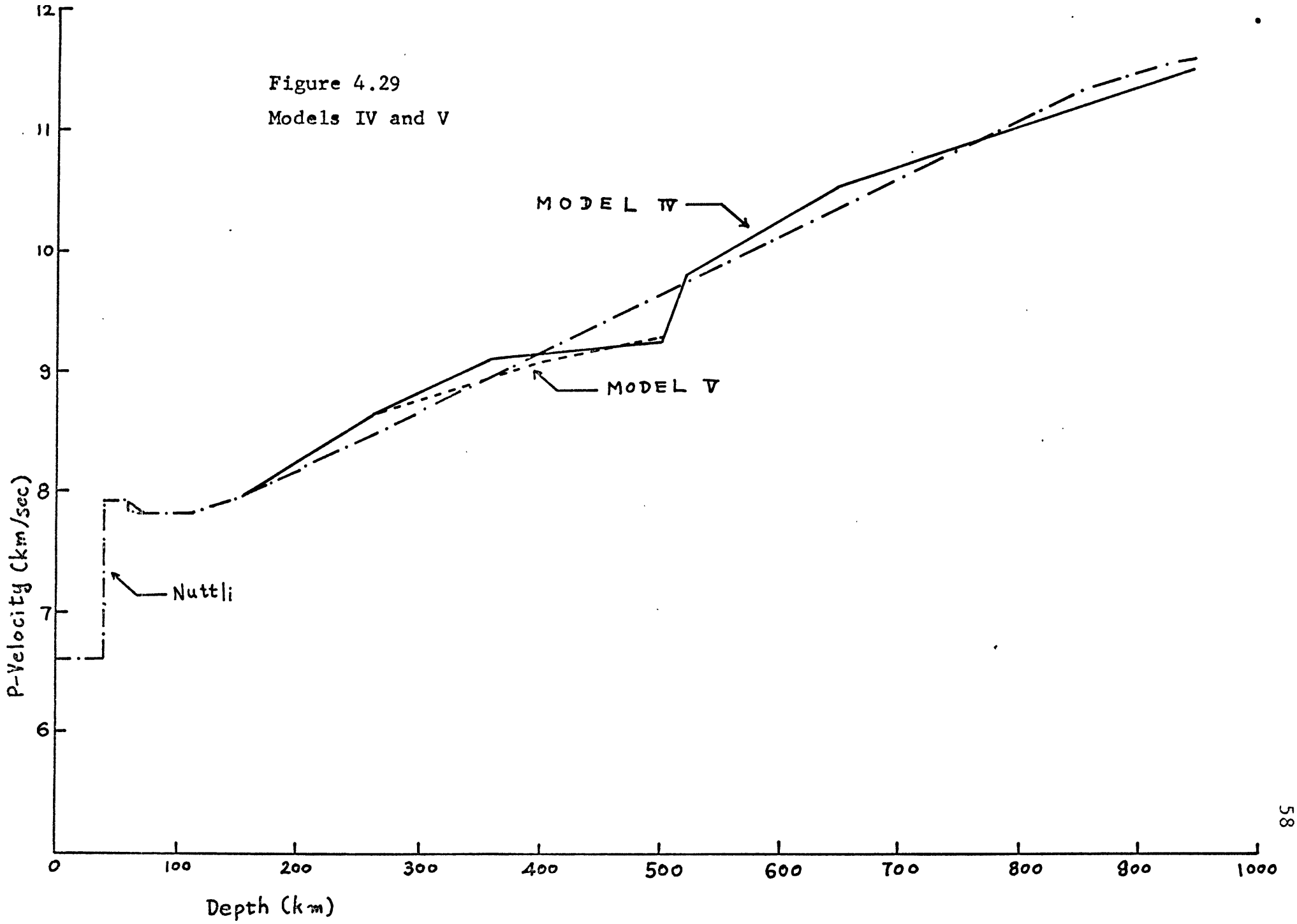
in Model IV gave too late second arrival as shown in Figure 4.31.

On the other hand Model V gave a better fit. For some reason the first arrival in this model is too large, and when experimentally the interfering phases were eliminated - Model V' - [See Figures 4.34-4.35] the synthetic response looks much better.

We conclude that Model V gives the best correlation to the actual record. Perhaps the first arrival can be made smaller by less velocity contrast at around 260 km where the gradient changes. Because of the sensitivity of the program to any minor change, an adjustment of an order of a few thousands of the total velocity made a significant difference in the shape of the synthetic seismogram. The author believed that making adjustments of such an order to achieve a better fit was only tedious and achieved little. Therefore, the author claims that Model V or a model extremely similar to it can generate satisfactory synthetic seismograms. [See Table 4.4 for the P-velocity] Though Model V has been claimed satisfactory, we have yet no way to prove the uniqueness or otherwise. However, beside the conventional method of determining the P-velocity structure using only the travel time information, we now have a much powerful method - synthetic seismogram - to determine more delicate structure variations.

For the completeness of the study, the synthetic seismograms of Model V at ranges 1831 km and 3376 km are shown on Figures 4.37-4.40. As mentioned earlier, since the gradient is nearly flat near the depth where

Figure 4.29
Models IV and V



Synthetic Response Model IV 2274 km

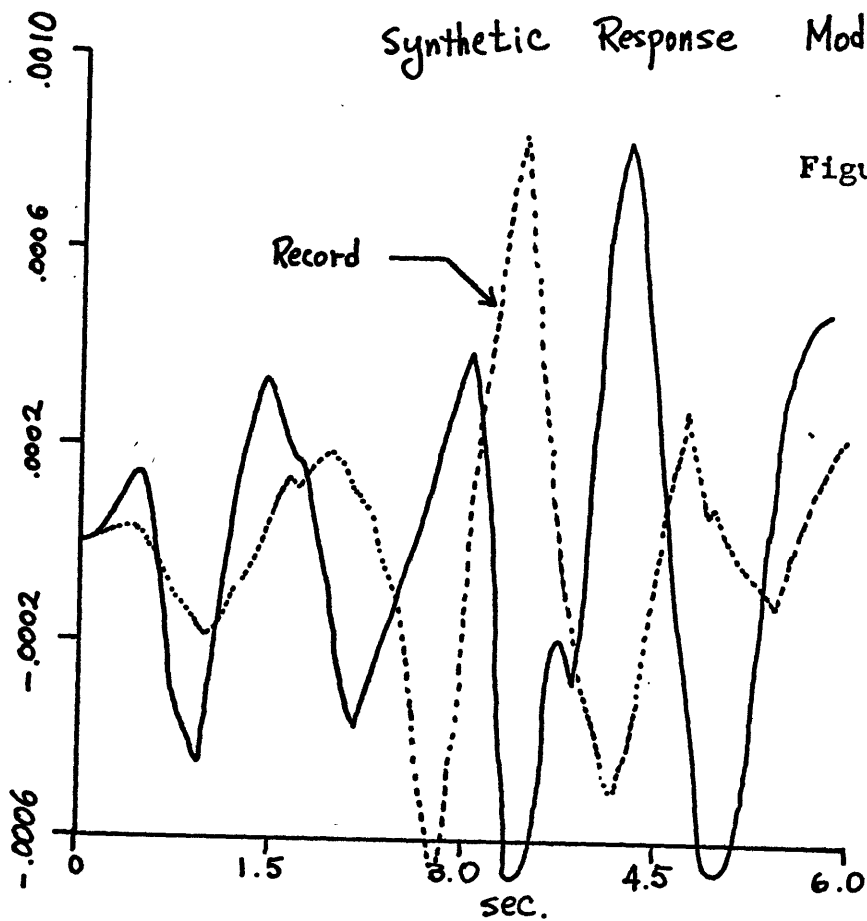


Figure 4.30

Theoretical Response Model IV 2274 km

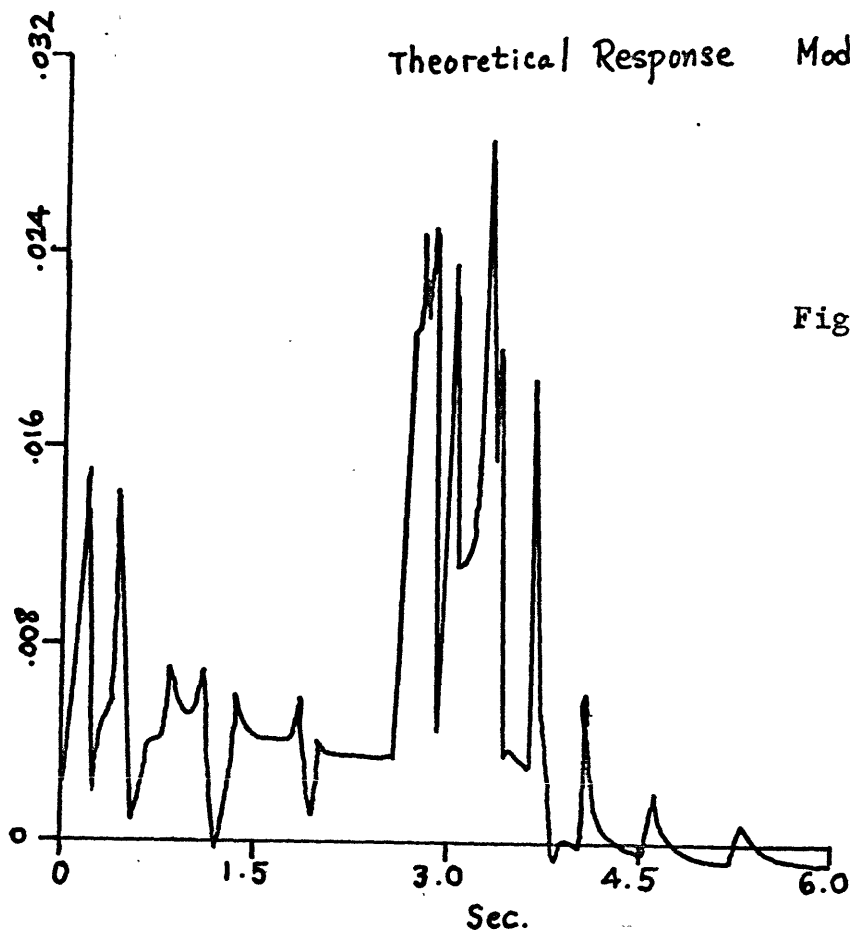
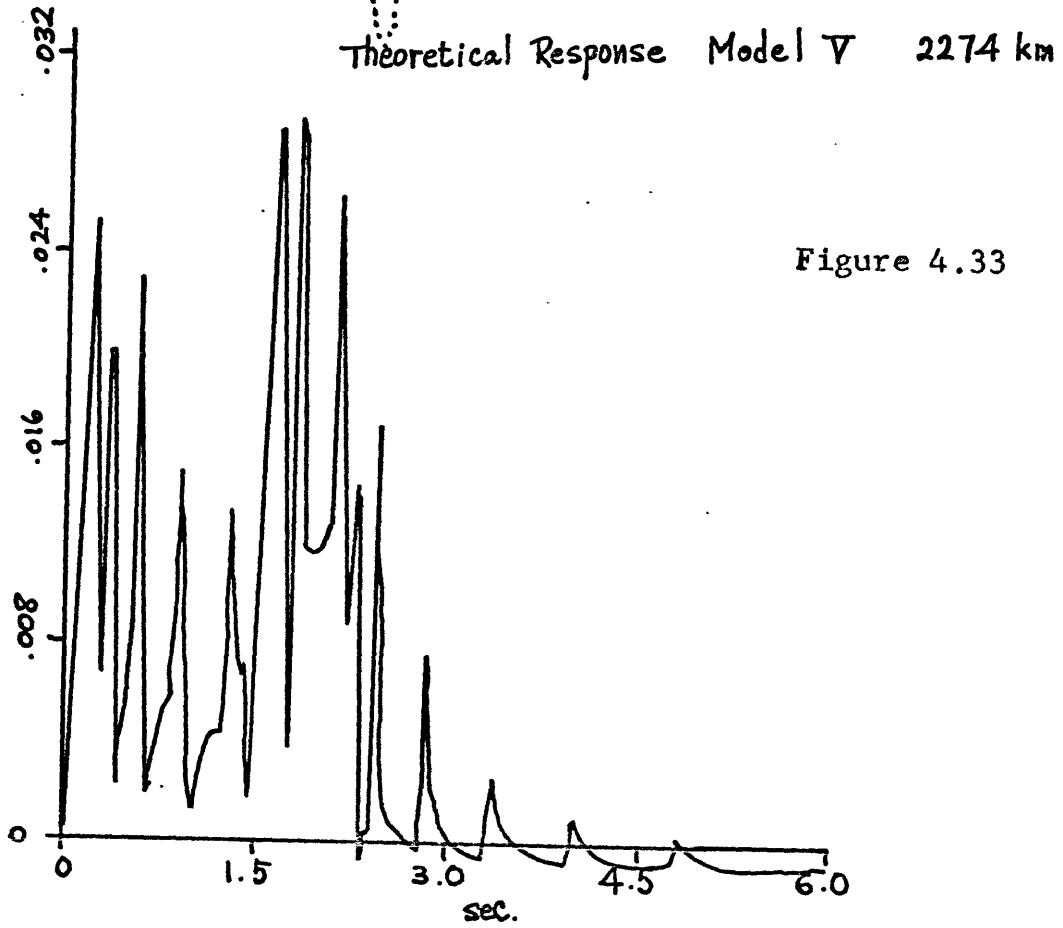
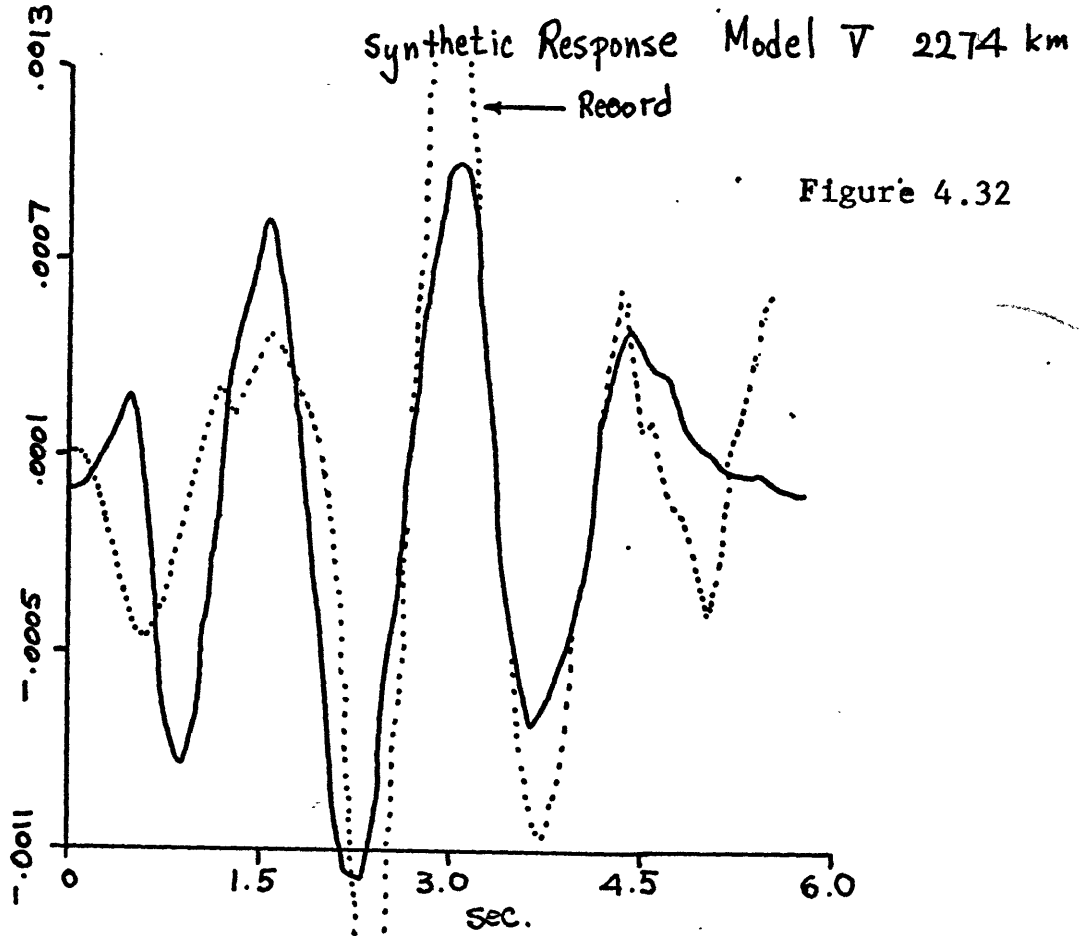


Figure 4.31



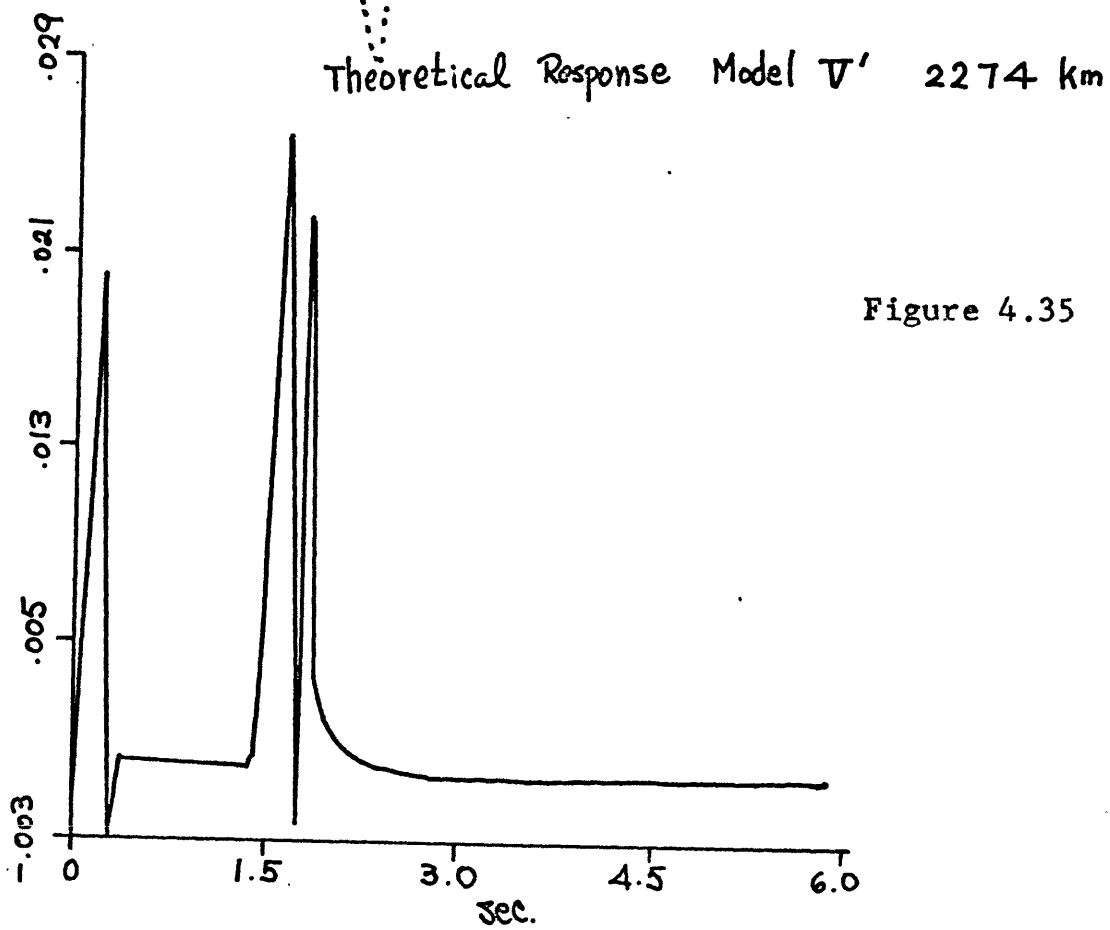
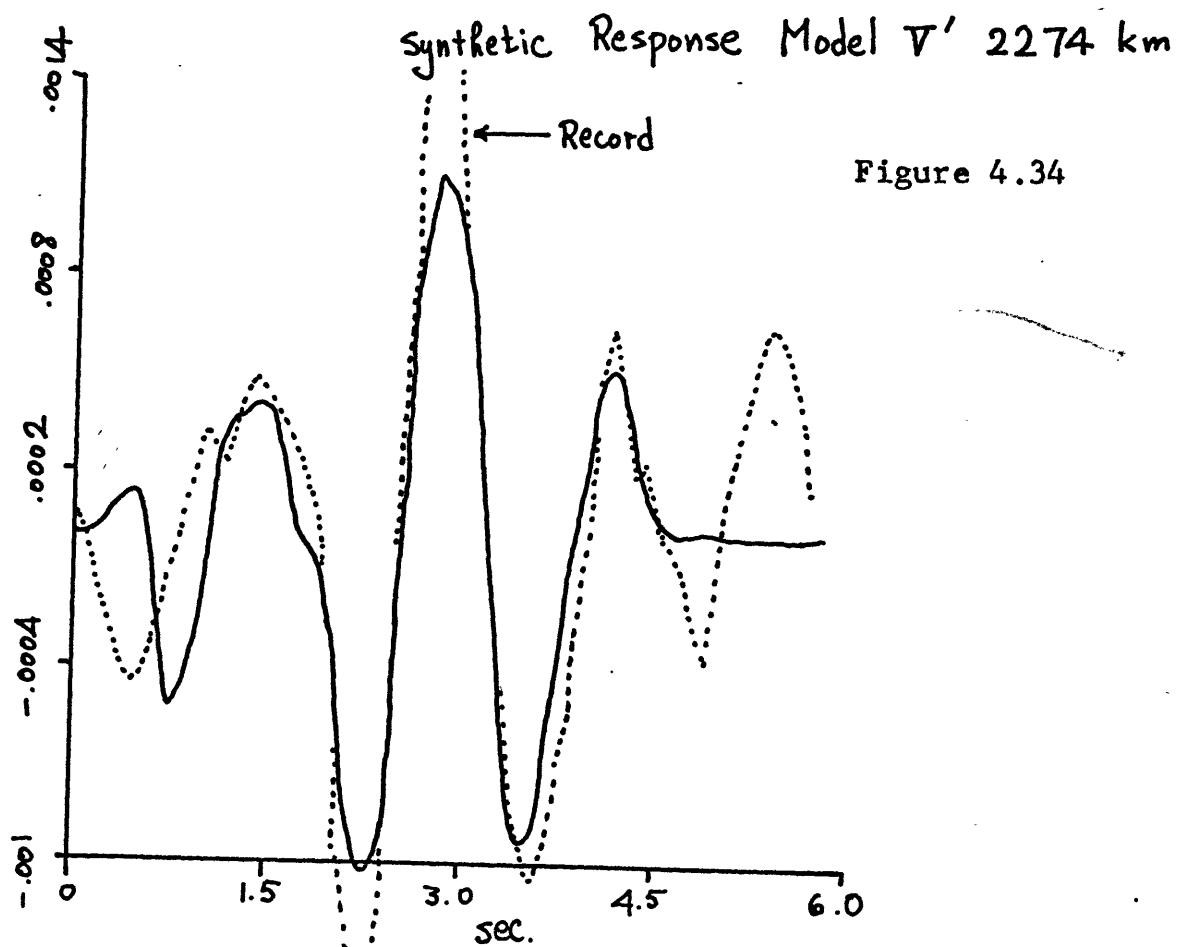
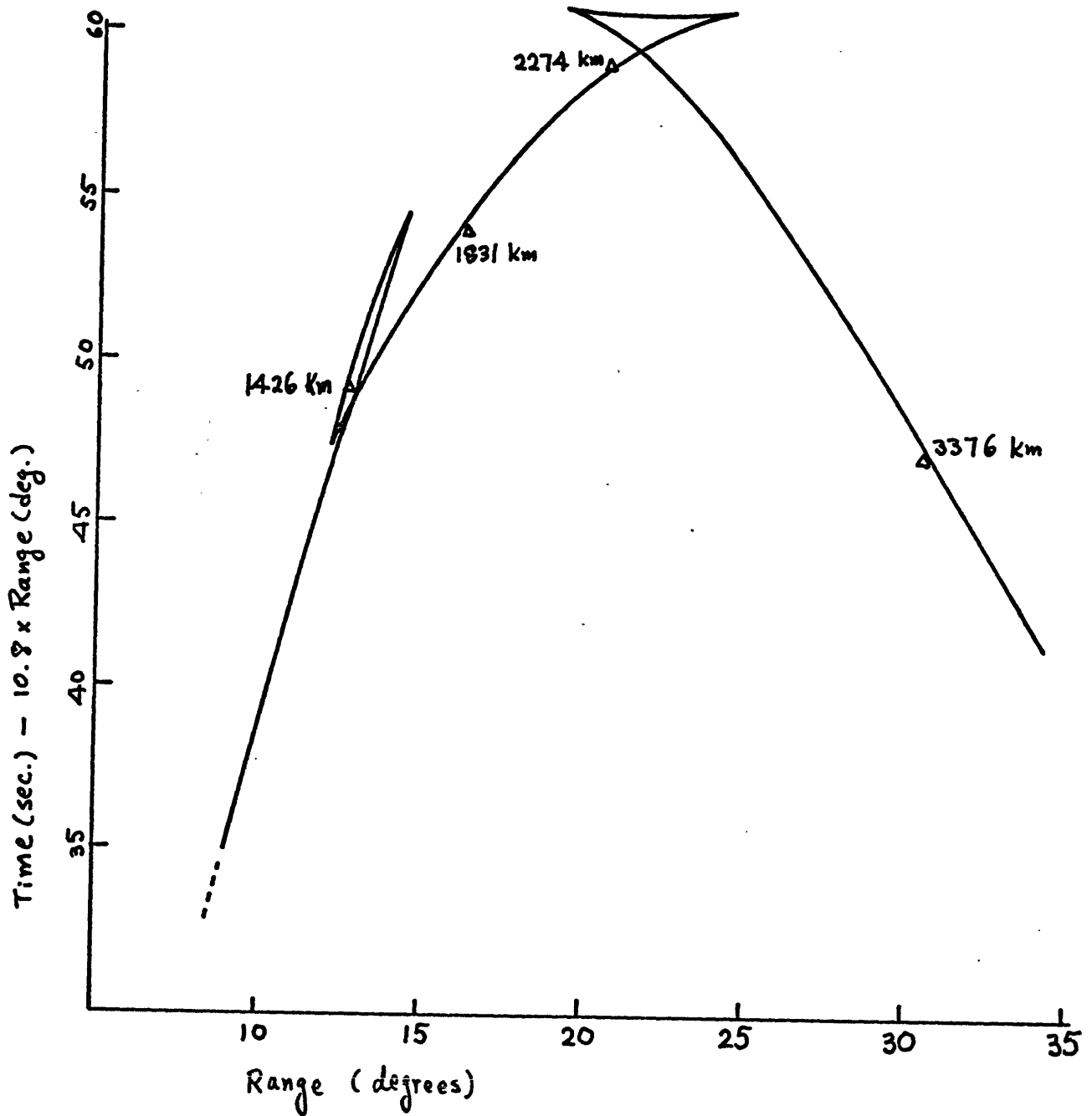


Figure 4.36 Model V
Reduced Time vz. Range



Synthetic Seismogram Model V 1831 km

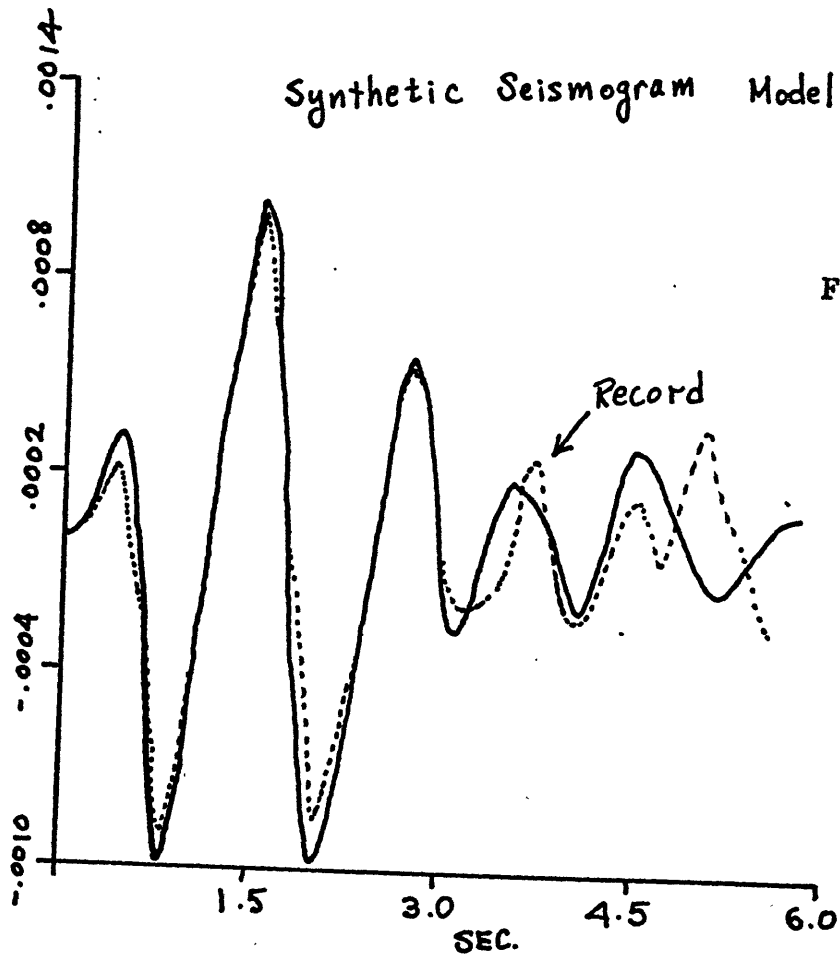


Figure 4.37

Theoretical Response Model V 1831 km

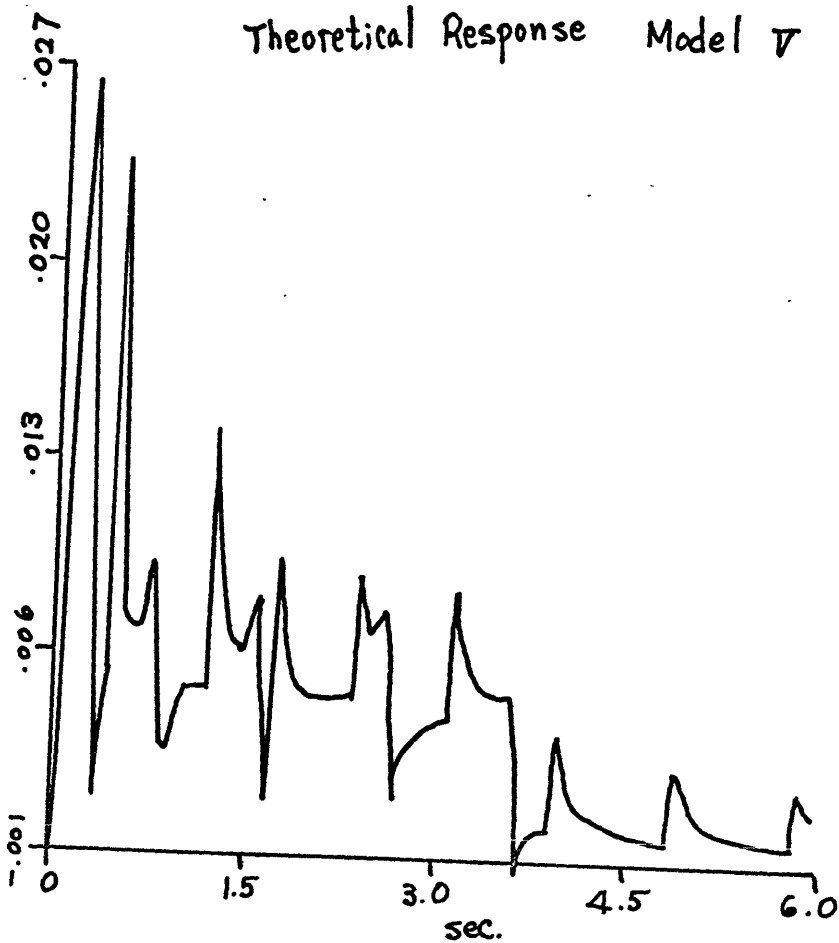


Figure 4.38

Synthetic Seismogram Model V 3376 km

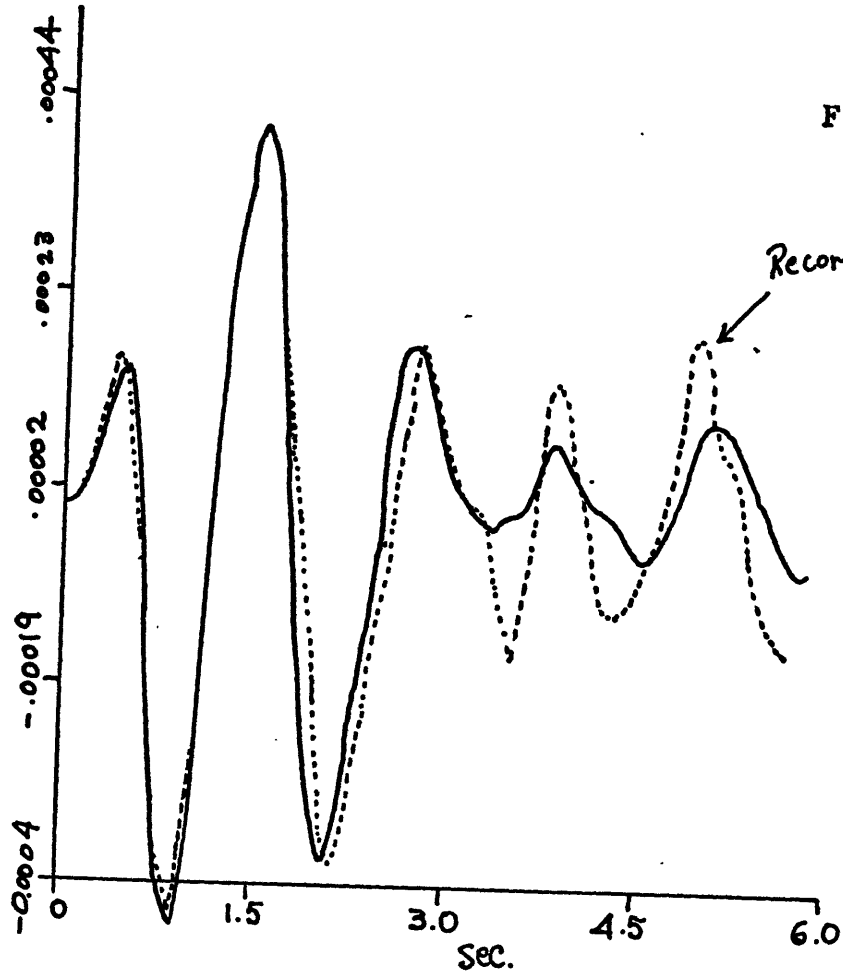


Figure 4.39

Theoretical Response Model V 3376 km

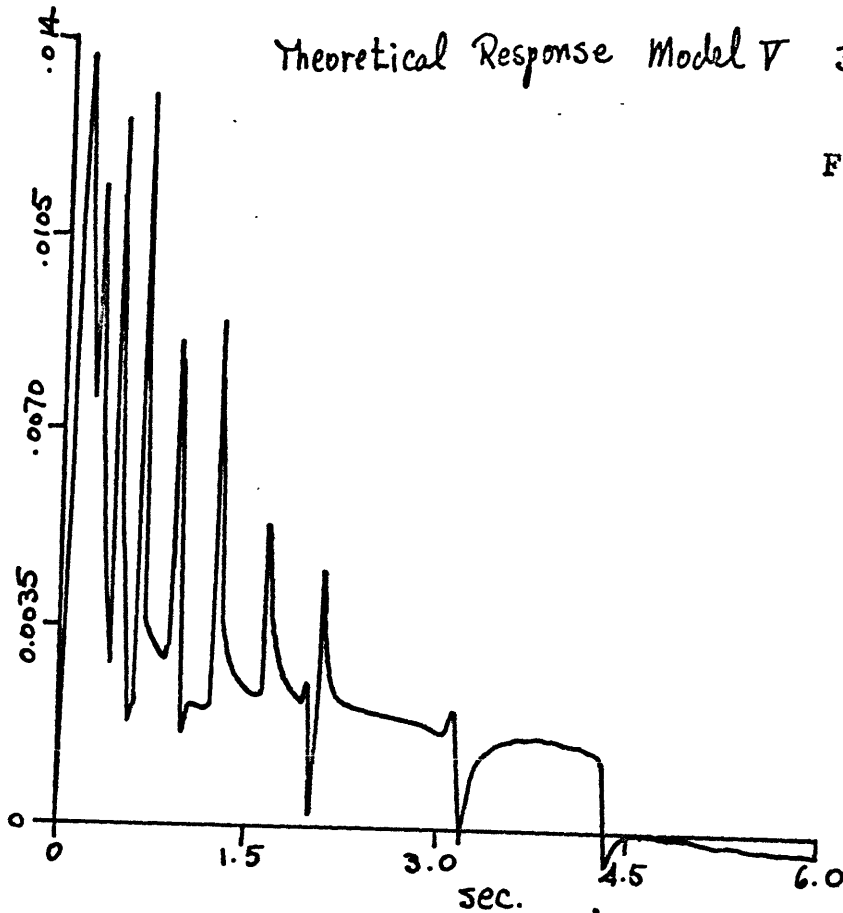


Figure 4.40

Table 4.4 Model V P-Velocity

Depth (km)	Velocity (km/sec)
0	6.59
40	6.61
40	7.93
60	7.93
80	7.80
110	7.80
150	7.93
260	8.64
400	9.10
508	9.41
525	9.80
650	10.55
850	10.98
1000	11.29

[See also Figure 4.36]

the first ray bottoms, the theoretical response take a similar form to a step function, and hence the synthetic seismogram is very similar to the transfer function. The reason why the record does not resemble the corresponding synthetic seismogram after a few seconds may be that there is a complex interaction due to the Moho or due to very shallow structure of the earth.

V. CONCLUSION

In this thesis, we attempted to investigate the P-velocity structure in the upper mantle of the earth in the southern part of the United States, using a newly developed technique of synthetic seismograms, instead of the conventional Wiechert-Herglotz method.

Although the validity of this new method is yet to be proven for the case of spherical layers, the method is known to give correct travel times. The method computes synthetic seismograms which can contain all the compressional response from all the depths - not only the travel times and $d^2t/d\Delta^2$, which were the only information obtained from the conventional method. Due to the increased amount of information, we were able to examine models more accurately with added criteria such as amplitude as functions of time and of range, or the period and the phase of seismograms, which had seldom been considered before in the study of velocity structures.

Among two existing models we examined, the model by Dowling and Nuttli (1964) reached from the same data [BILBY Report (1963)] as we used, did not give satisfactory results. Due to the linear increase of the P-velocity with depth, the seismogram generated by this model were decreasing in amplitude with range. On the other hand the record from the Bilby event showed clearly that, at the range of 2274 km, there was a small first arrival about 1.5 seconds before a very large major P-arrival. The other model we tested was the Johnson's (1967) calculated from the data obtained at the Tonto

Forest Seismological Observatory in Arisona. Due to its two prominent steps in velocity, the synthetic seismogram at the range 2274 km showed a small first arrival followed too late by a major P-arrival. Therefore, it showed little resemblance to the record at this range. We then constructed some models with the correct arrival times, and tested them, with the main emphasis on the range 2274 km. Among the five models tested, one showed a satisfactory fit to the record. This model, Model V, has a pronounced step in velocity at the depth of 500 km and gives a strong arrival at the range 2274 km from this step.

Though there are more improvements to be made and approximations to be shown valid rigorously, we believe that this method of computing synthetic seismograms is extremely useful and convincing because of the remarkable resemblance between the synthetic seismograms and the records, which we demonstrated in this thesis, at least for the upper mantle where the curvature is small.

The uniqueness of the solution cannot be proven at this stage, and therefore, the structure proposed as Model V in this thesis may not be the only representation of the upper mantle. There may be other models that give similarly good seismograms. Nonetheless, by adding more criteria to these provided by the conventional method of computing velocity as a function of depth, we may be able to limit the possibilities.

References

- BILBY Report, Scientific report prepared for the Air Force Technical Applications Center by United Electrodynamics Corp., Nov. 8, 1963.
- Bullen, K. E., An Introduction to the Theory of Seismology, Third Edition, Cambridge University Press, Cambridge, England, 1965.
- Dix, C. H., The Method of Cagniard in Seismic Pulse Problem, Geophysics, Vol. 19, pp. 722-738, 1953.
- Dowling, John & O. Nuttli, Travel-time Curves for a Low-Velocity Channel in the Upper Mantle, Bulletin of the Seismological Society of America, Vol. 54, No. 6, Part A, pp. 1981-1996, 1964.
- Grant, F. S. & G. F. West, Interpretation Theory in Applied Geophysics, McGraw Hill Book Co., New York, 1965.
- HelMBERGER, Donald V., The Relationship between Point & Line Seismic Sources, Doctoral Oral Examination Paper at the University of California at San Diego, 1965.
- HelMBERGER, Donald V., Head Waves from the Oceanic Mohorovicic Discontinuity, Ph.D. Thesis at the University of California at San Diego, 1967.
- de Hoop, A. T., A Modification of Cagniard Method for Solving Seismic Pulse Problem, Applied Scientific Research, Sec. B, Vol. 8, pp. 349, 356, 1960.
- Johnson, Lane R., Array Measurements of P Velocities in the Upper Mantle, Journal of Geophysical Research, Vol. 72, No. 24, pp. 6309-6325, 1967.
- Julian, Bruce & D. Anderson, Travel Times, Apparent Velocities and Amplitudes of Body Waves, Bulletin of the Seismological Society of America, Vol. 58, No. 1, pp. 339-366, 1968.

Knopoff, L., F. Gilbert & W. L. Pilant, Wave Propagation in a Simple Layer, Journal of Geophysical Research, Vol. 65, No. 1, pp. 265-278, 1960.

Smith, S. W., A Reinterpretation of Phase Velocity Data Based on the Gnome Travel Time Curves, Bulletin of the Seismological Society of America, Vol. 52, No. 5, pp. 1031-1036, 1962.

Strick, E., Propagation of Elastic Wave Motion from an Impulsive Source Along a Fluid/Solid Interface, II. Theoretical Pressure Pulse, Royal Society Philosophical Transactions (London), Series A, Vol. 251, pp. 465-523, 1959.

APPENDIX

On the following pages, the computer program discussed in the thesis in Chapter III is listed.

```
C ... MAIN PROGRAM
COMMON/TINP/DELTM,DLTM,MTD,DLTP,JO,NDIRT
COMMON/STUFF/C(100),S(100),D(100),TH(100),X
COMMON/TFIX/TN1,TN2,TN3,TN4,JN1,JN2,JN3,JN4
COMMON/CONFIX/DEL,NN,NDP,TMX,XDIM,YDIM,DP,KO
COMMON/THY/TT(8000),PP(8000)
COMMON/SYTH/XD11,YD11,XD22,YD22,XD33,YD33
COMMON/FOURCT/MF,NMF,KMF,KNMF
COMMON/PLOTG/CON,NNF,NPT
COMMON/LPRINT/PRNT,PRNTS,KST,KEND
LOGICAL PRNT,PRNTS
PRNT = .FALSE.
PRNTS = .TRUE.
JN1=12
JN2=10
JN3=8
JN4=100
TN1=.8
TN2=.2
TN3=.1
TN4=.01
NDIRT=0
NNF=1
NPI=2
X = 2274.0
CO=(2./X)**.5/(3.1416)
CON=CO
MTD=3
DLTM=.5
DELTM=1.E-6
JO = 45
CALL CURAY(JO)
DLTP=.04
XD11=2.
YD11=2.
XD22 = 4.0
XD33 = 4.0
XDIM = 4.0
YD22 = 4.0
YD33 = 4.0
YDIM=2.
DP=.04
DEL=DP
NDP=15
TMX = 6.0
NN = 150
MF=0
CALL NEWPLT ('M5207','6267','WHITE ','BLACK')
KC = 0
KST = 17
KEND = 20
CALL CLOK1
CALL SETUP (18,0,1,2,0,2,0)
CALL CLOK2
CALL CLOK1
CALL SETUP (24,0,1,1,2,2,0)
1 CALL CLOK2
CALL SETUP (27,0,1,2,2,2,0)
KO = 75
CALL CLOK1
CALL SETUP (29,0,1,2,2,0,2)
CALL CLOK2
CALL ENDPLT
```


CALL EXIT
END

A-3

* Subroutines CLOK1 and CLOK2 are to find the time spent between the two calls; they are not listed in the Appendix.

BLJCK DATA

A-4

C..... TEST NO.5

COMMON/STUFF/C(100),S(100),D(100),TH(100),X

DATA TH/0.0,40.0,20.0,2*10.0,30.0,20*20.0,2*10.0,22*20.0/

DATA C/0.0001,6.2,7.93,7.88,7.84,7.8,7.84,7.88,8.00,8.13,

A8.25,8.38,8.505,8.61,8.677,8.743,8.81,8.877,8.943,9.01,

B9.06,9.12,9.17,9.23,9.28,9.37,9.58,9.79,9.9,10.02,

C10.14,10.25,10.37,10.49,10.58,10.63,10.68,10.72,10.77,10.82,

D10.87,10.92,10.96,11.01,11.06,11.11,11.16,11.2,11.25,11.3/

DATA S/0.0001,3.7,4.49,4.42,4.36,4.3,4.36,4.42,4.46,4.5,

A4.55,4.59,4.64,4.69,4.74,4.8,4.85,4.9,4.95,5.0,

B5.04,5.09,5.13,5.18,5.22,5.31,5.42,5.53,5.64,5.73,

C5.83,5.92,6.02,6.11,6.16,6.2,6.24,6.28,6.33,6.37,

D6.41,6.45,6.49,6.53,6.57,6.61,6.66,6.7,6.74,6.78/

DATA D/0.0001,2.84,3.44,3.442,3.444,3.45,3.445,3.475,3.495,3.52,

A3.54,3.57,3.59,3.6,3.62,3.63,3.65,3.66,3.68,3.7,

B3.71,3.72,3.74,3.75,3.76,3.78,3.82,3.86,3.89,3.92,

C3.95,3.98,4.01,4.04,4.05,4.06,4.07,4.08,4.09,4.1,

D4.11,4.12,4.13,4.14,4.15,4.16,4.17,4.18,4.19,4.2/

END

```
• SUBROUTINE ADJUST(NFIX)
COMMON/THY/T(8000),PH(8000),FF(600)
COMMON/EXACT/PHI(500),TD(500),NEND,NM
M=NM&1
TR=TD(M)
I=0
80  I=I&1
    IF(T(I).GT.TR) GO TO 81
    GO TO 80
81  DNE=TR-T(I-1)
    DPL=T(I)-TR
    IF(ABS(DNE).GT.ABS(DPL)) GO TO 83
    DELTA=-DNE
    NFIX=I-1
    GO TO 85
83  DELTA=DPL
    NFIX=I
85  DO 84 J=1,NEND
    TD(J)=TD(J)&DELTA
84  CONTINUE
END
```

```
SUBROUTINE CON(N,K1,K2)
COMMON/CFIX/NT,KT,M ,N ,LT,LTP(100),NF
COMMON/CN/NNT(100),MMT(100),MMB(100),NNB(100),LU(100),LB(100),
2LL(100),NNF(100)
DO 5 J=1,100
5 LTP(J) = 0.0
NT=NNT(N)
KT=MMT(N)
MB=MMB(N)
NB=NNB(N)
LT=LL(N)
LTP(K1)=LU(N)
LTP(K2)=LB(N)
NF=NNF(N)
RETURN
END
```

```

SUBROUTINE CONN(N,K,KN)
COMMON/CFIX/NT,KT,MB,NB,LT,LTP(100),NF
COMMON/NFIX/MM(100),NN(100),MT(100)

```

```

DO 25 J=1,100

```

```

MM(J)=0

```

```

NN(J)=0

```

```

MT(J)=0

```

```

LTP(J)=0

```

```

25  CONTINUE

```

```

K1=K&1

```

```

K2=K&2

```

```

K3=K&3

```

```

K4=K&4

```

```

MT(K1)=1

```

```

GO TO (1,2,3,4,5,6,7,8,9,10) ,N

```

```

1  MM(K1)=1

```

```

MM(K4)=1

```

```

NN(K1)=1

```

```

LTP(K1)=4

```

```

LTP(K2)=2

```

```

LTP(K3)=2

```

```

LTP(K4)=2

```

```

NF=2

```

```

MT(K2)=1

```

```

MT(K3)=1

```

```

MT(K4)=1

```

```

GO TO 30

```

```

2  MM(K1)=1

```

```

MM(K3)=1

```

```

NN(K1)=1

```

```

LTP(K1)=4

```

```

LTP(K2)=2

```

```

LTP(K3)=2

```

```

NF=2

```

```

MT(K2)=1

```

```

MT(K3)=1

```

```

GO TO 30

```

```

3  MM(K2)=1

```

```

MM(K4)=1

```

```

NN(K1)=1

```

```

LTP(K1)=4

```

```

LTP(K2)=4

```

```

LTP(K3)=2

```

```

LTP(K4)=2

```

```

NF=2

```

```

MT(K2)=2

```

```

MT(K3)=1

```

```

MT(K4)=1

```

```

GO TO 30

```

```

4  MM(K2)=1

```

```

MM(K4)=1

```

```

NN(K2)=1

```

```

LTP(K1)=2

```

```

LTP(K2)=4

```

```

LTP(K3)=2

```

```

LTP(K4)=2

```

```

NF=2

```

```
MT(K2)=1
MT(K3)=1
MT(K4)=1
5 GO TO 30
MM(K2)=1
MM(K3)=1
NN(K1)=1
LTP(K1)=4
LTP(K2)=4
LTP(K3)=2
NF=2
MT(K2)=2
MT(K3)=1
6 GO TO 30
MM(K3)=2
NN(K1)=1
LTP(K1)=4
LTP(K2)=4
LTP(K3)=4
NF=1
MT(K2)=2
MT(K3)=2
7 GO TO 30
MM(K3)=1
MM(K4)=1
NN(K1)=1
LTP(K1)=4
LTP(K2)=4
LTP(K3)=4
LTP(K4)=2
NF=2
MT(K2)=2
MT(K3)=2
MT(K4)=1
8 GO TO 30
MM(K3)=1
MM(K4)=1
NN(K2)=1
LTP(K1)=2
LTP(K2)=4
LTP(K3)=4
LTP(K4)=2
NF=2
MT(K2)=1
MT(K3)=2
MT(K4)=1
9 GO TO 30
MM(K4)=2
NN(K1)=1
LTP(K1)=4
LTP(K2)=4
LTP(K3)=4
LTP(K4)=4
NF=1
MT(K2)=2
MT(K3)=2
MT(K4)=2
```

```
10  GO TO 30  
    MM(K4)=2  
    NN(K2)=1  
    LTP(K1)=2  
    LTP(K2)=4  
    LTP(K3)=4  
    LTP(K4)=4  
    NF=1  
    MT(K2)=1  
    MT(K3)=2  
    MT(K4)=2  
30  CONTINUE  
    END
```

```

SUBROUTINE CONSTN(NO)
COMMON/CN/NNT(100),MMT(100),MMB(100),NNB(100),LU(100),LB(100),
ILL(100),NNF(100)
DO 5 J=1,NO
NNT(J)=0
MMT(J)=0
MMB(J)=0
NNB(J)=0
LU(J)=0
LB(J)=0
NNF(J)=1
LL(J)=0
5   CONTINUE
N=1
MMT(N)=1
LU(N)=2
N=2
NNB(N)=1
LU(N)=2
LB(N)=2
LL(N)=1
N=3
MMT(N)=2
NNT(N)=1
LU(N)=4
N=4
NNB(N)=2
MMB(N)=1
LU(N)=2
LB(N)=4
LL(N)=1
N=5
NNB(N)=2
NNT(N)=1
LU(N)=4
LB(N)=4
LL(N)=2
N=6
NNB(N)=1
MMT(N)=1
NNT(N)=1
LU(N)=4
LB(N)=2
NNF(N)=2
LL(N)=1
N=7
NNB(N)=3
MMB(N)=2
LU(N)=2
LB(N)=6
LL(N)=1
N=8
MMT(N)=3
NNT(N)=2
LU(N)=6
N=9
NNB(N)=3
NNT(N)=2
LU(N)=6
LB(N)=6
LL(N)=3
N=10
NNB(N)=2

```


MMT(N)=1
LL(N)=1
MMB(N)=1
NNT(N)=1
LU(N)=4
LB(N)=4
NNF(N)=2
N=11
NNB(N)=2
MMT(N)=1
LL(N)=2
NNT(N)=2
LU(N)=6
LB(N)=4
NNF(N)=3
N=12
NNB(N)=3
MMB(N)=1
NNT(N)=1
LU(N)=4
LB(N)=6
NNF(N)=2
LL(N)=2
N=13
NNB(N)=1
MMT(N)=2
NNT(N)=2
LU(N)=6
LB(N)=2
NNF(N)=3
LL(N)=1
N=14
MMT(N)=4
NNT(N)=3
LU(N)=8
N=15
MMT(N)=3
NNB(N)=1
NNT(N)=3
LU(N)=8
LB(N)=2
LL(N)=1
NNF(N)=4
N=16
NNB(N)=2
MMT(N)=2
NNT(N)=3
LU(N)=8
LB(N)=4
NNF(N)=6
LL(N)=2
N=17
MMB(N)=1
NNT(N)=2
NNB(N)=2
MMT(N)=2
LU(N)=6
LB(N)=4
NNF(N)=3
LL(N)=1
N=18
MMT(N)=1
NNB(N)=3

MMB(N)=2
NNT(N)=1
LU(N)=4
LB(N)=6
NNF(N)=2
LL(N)=1
N=19
MMT(N)=1
NNB(N)=3
LL(N)=2
MMB(N)=1
NNT(N)=2
LU(N)=6
LB(N)=6
NNF(N)=8
N=20
MMT(N)=1
NNB(N)=3
NNT(N)=3
LL(N)=3
LU(N)=8
LB(N)=6
NNF(N)=4
N=21
NNB(N)=4
MMB(N)=3
LU(N)=2
LB(N)=8
LL(N)=1
N=22
NNB(N)=4
MMB(N)=2
NNT(N)=1
LL(N)=2
LU(N)=4
LB(N)=8
NNF(N)=3
N=23
NNB(N)=4
MMB(N)=1
NNT(N)=2
LL(N)=3
LU(N)=6
LB(N)=8
NNF(N)=3
N=24
NNB(N)=4
NNT(N)=3
LL(N)=4
LU(N)=8
LB(N)=8
END

```
FUNCTION CCNVS(FA,FP,DEL,NF,N)
DIMENSION FP(1),FA(1)
COMPUTES CONVOLUTION OF FP AND FA T=DEL*2N
NF MUST BE ODD
NN=N
DN=DEL
IF(NN.LT.1) GO TO 2
NDO=MINO(NN,(NF-1)/2)
IP=2
NP=2*NN
EVEN=FP(IP)*FA(NP)
ODD=0
IF(NDO.LT.2) GO TO 11
DO 10 I=2,NDO
IP=IP&1
NP=NP-1
ODD=ODD&FP(IP)*FA(NP)
IP=IP&1
NP=NP-1
EVEN=EVEN&FP(IP)*FA(NP)
10 CONTINUE
11 CONTINUE
ENDS=FP(1)*FA(2*NN&1)&FP(IP&1)*FA(NP-1)
CONVS=DN*(ENDS&4.*EVEN&2.*ODD)/3.
RETURN
2 CONVS=0.
END
```

```
COMPLEX FUNCTION CR(P,C)
```

```
COMPLEX P,CZ
```

```
CZ=1./C**2-P*P
```

```
U=REAL(CZ)
```

```
X=AIMAG(CZ)
```

```
R=SQRT(X*X&U*U)
```

```
W1=ABS(R&U)/2.
```

```
W2=ABS(R-U)/2.
```

```
R1=SQRT(W1)
```

```
R2=SQRT(W2)
```

```
CR=R1-R2*(0.,1.)
```

```
END
```

```
COMPLEX FUNCTION CRSTPP(P,V1,S1,RHO1,V2,S2,RHO2)
  COMPLEX CR,P,E1P,E2P
  COMPLEX E1,E2,C1,C2,C3,C4,C5,C6,T
  COMPLEX A,B,AP,BP
  REAL K1,K2,K3,K4
  K4=RHO2*S2**2/(RHO1*S1**2)
  B1=.5/(1-K4)
  B2=.5*K4/(K4-1)
  K1=B1/S1**2
  K2=B2/S2**2
  K3=K1+K2
  E1=CR(P,V1)
  E2=CR(P,V2)
  E2P=CR(P,S2)
  E1P=CR(P,S1)
  C1=(P**2)*(K3-P**2)**2
  C2=P**2*E1*E1P*E2P
  C3=(E1*E1P)*(K2-P**2)**2
  C4=E2P*(K1-P**2)**2
  C5=K1*K2*E1*E2P
  C6=K1*K2*E1P
  AP=C1+C3-C5
  BP=C2+C4-C6
  T=2.*K1*E1*(E2P*(K1-P**2)-E1P*(K2-P**2))
  B=AP+E2*BP
  CRSTPP=T/B
  RETURN
  END
```

```
• SUBROUTINE CURAY(JC)
COMMON/STUFF/C(100),S(100),D(100),TH(100),X,RCSQ(100),RSSQ(100)
COMMON /SENSE/ DRCSQ(100)
DIMENSION DEPTH(100)
REAL*8 DRCSQ
PRINT 2, X
2 FORMAT (1H1,10X'CURAY'/11X'RANGE'F10.0/16X'THICKNESS'9X'DEPH'5X'P
&-VELOCITY'5X'S-VELOCITY'8X'DENSITY')
DEPTH(1) = TH(1) / 2.0
DO 10 J = 2,JO
10 DEPTH(J) = DEPTH(J-1) & (TH(J)&TH(J-1))/2.0
DO 5 J = 1,JO
Q = 6371.0 / (6371.0-DEPTH(J))
C(J) = C(J) * Q
S(J) = S(J) * Q
D(J) = D(J) * Q
TH(J) = TH(J) * Q
DRCSQ(J) = 1.0 / DBLE(C(J))**2
RCSQ(J) = DRCSQ(J)
5 RSSQ(J) = 1.0 / S(J) ** 2
PRINT 1, (J,TH(J),DEPTH(J),C(J),S(J),D(J),J=1,JO)
1 FORMAT (15,5X,5G15.4)
RETURN
END
```

```
SUBROUTINE FIND2 (Q,K,DEL,DET,PQ,TQ,KN,N)
COMMON/STUFF/C(100),S(100),D(100),TH(100),X
COMMON /SENSE/ RCSQ(100)
COMMON/CFIX/NT,KT,MB,NB,LT,LTP(100),NF
COMMON / LPRINT/ PRNT,PRNTS
LOGICAL PRNT,PRNTS
REAL*8 E(100),BLTEM,TOTEM,PG,TO,BL,P,PSQ,RCSQ
KOUNT = 0
TDE = DEL
J1=K&1
J2=J1&KN
8 P = Q
KCUNT = KOUNT & 1
5 P=P&DEL
PSQ = P ** 2
BLTEM = 0.0
DO 10 J = 1,K
E(J) = DSQRT(DABS(RCSQ(J)-PSQ))
10 BLTEM = BLTEM - TH(J) / E(J)
BLTEM = 2.0 * BLTEM
DO 30 J = J1,J2
E(J) = DSQRT(DABS(RCSQ(J)-PSQ))
30 BLTEM = BLTEM-TH(J)*LTP(J)/E(J)
BL = X & BLTEM*P
IF (ABS (DEL).LE.1.E-18) GO TO 1
6 IF (DABS(BL).LE.X/DET) GO TO 1
2 IF (BL)3,1,4
3 DEL=-ABS (DEL*.5)
GO TO 5
4 DEL=ABS(DEL*.5)
GO TO 5
1 IF (DABS(BL).LT.0.0) GO TO 7
IF (KOUNT.GE.5) GO TO 7
Q = Q/10.0
DEL = TDE
GO TO 8
7 PG = P
TOTEM = 0.0
DO 11 J = 1,K
11 TOTEM = TOTEM & E(J) * TH(J)
TOTEM = TOTEM * 2.0
DO 31 J=J1,J2
31 TOTEM = TOTEM & E(J)*TH(J)*LTP(J)
TO = P*X & TOTEM
PQ = PG
TQ = TO
IF (DABS(BL).LT.1.0E-6) RETURN
IF (.NOT.PRNT) RETURN
PRINT 17, PG, TO, BL
17 FORMAT (1H0,4X'PG = 'G18.6,10X'TO = 'G18.6,10X'BL = 'G18.6)
RETURN
END
```

```
SUBROUTINE DELPS (NNN, RG, NN, N)
DIMENSION PP(50)
COMMON/SPE/DELP(400), DD1, DD2, DD3, DD4, NO
RG=RG-1.E-08
PI=3.141593
AN=PI/(NNN*2.)
J=NN
A=AN
DELP(J)=RG*(SIN (A)**N)
TO=DELP(J)
A=A&AN
PP(1)=DELP(1)
1  J=J&1
PP(J)=RG*SIN(A)**N
DELP(J)=PP(J)-PP(J-1)
DELP(J)=ABS (DELP(J))
TO=TO&DELP(J)
A=A&AN
IF(TO.LT.RG) GO TO 1
2  NO=J-1
END
```



```
• COMPLEX FUNCTION GENCC(P,N)
  COMPLEX P,CRSTPP,GCD,GCU,TO
  DIMENSION GCD(100),GCU(100)
  COMMON/STUFF/C(100),S(100),D(100),TH(100),X
  KK=N-1
  IF(KK.LT.2) GO TO 40
  DO 34 J=2,KK
  VV1=C(J)
  SS1=S(J)
  RR1=D(J)
  VV2=C(J&1)
  SS2=S(J&1)
  RR2=D(J&1)
  GCD(J)=CRSTPP(P,VV1,SS1,RR1,VV2,SS2,RR2)
  GCU(J)=CRSTPP(P,VV2,SS2,RR2,VV1,SS1,RR1)
34  CONTINUE
40  TO=1.
  IF(KK.LT.2) GO TO 36
  DO 35 J=2,KK
  TO =TO*GCD(J)*GCU(J)
35  CONTINUE
36  GENCC=TO
  END
```

```
• SUBROUTINE HELP(K,N,P,TTP,DTP,KN)
COMMON/STUFF/C(100),S(100),D(100),TH(100),X,RCSQ(100),RSSQ(100)
COMMON/CFIX/NT,KT,MB,NB,LT,LTP(100),NF
J1=K&1
J2=J1&KN
PSQ = P**2
BLTEM = 0.0
TOTEM = 0.0
DO 11 J = 1,K
E = SQRT(ABS(RCSQ(J)-PSQ))
TOTEM = TOTEM & E*TH(J)
11 LTEM = LTEM-TH(J)/E
TOTEM = TOTEM * 2.0
BLTEM = BLTEM * 2.0
DO 31 J = J1,J2
E = SQRT(ABS(RCSQ(J)-PSQ))
BLTEM = BLTEM - TH(J)*LTP(J)/E
31 TOTEM = TOTEM & E * TH(J)*LTP(J)
BL = X & P*BLTEM
TO = P*X & TOTEM
DTP=1./BL
TTP=TO
RETURN
END
```

```

SUBROUTINE HIGH(NDP, TMX, K, KI, N)
COMMON/TFIX/TN1, TN2, TN3, TN4, JN1, JN2, JN3, JN4
COMMON/CFIX/NT, KT, MB, NB, LT, LTP(100), NF
COMMON/STUFF/C(100), S(100), D(100), TH(100), X
COMMON/EXACT/PHI(500), TD(500), NEND, NM
COMMON/MAGIC/PP(300), DDPT(300), TT(300)
COMMON/SPE/DELP(400), DD1, DD2, DD3, DD4, NO
COMMON/PATHC/PO, TO, KK
COMMON/TINP/DELT, DLT, MTD, DLTP, JO, NDIRT
COMMON / LPRINT/ PRNT, PRNTS
LOGICAL PRNT, PRNTS
DIMENSION E(100)
COMPLEX PP, CDPT
KK=K
KM=K
J=K

```

```

17   J=J&1
      IF(LTP(J).LT.1) GO TO 16
      KM=J
      GO TO 17
16   CONTINUE
333  FORMAT(6I10)
      IF(.NOT.PRNT) GO TO 4
      PRINT 1
1   FORMAT (5X'(LTP(J),J=1,KM)')
      WRITE(6,333) (LTP(J),J=1,KM)
      PRINT 3
3   FORMAT (9X'K'9X'N'8X'KM')
      WRITE (6,333) K,N,KM
4   V2=C(KM&1)
      XM=0.
      DO 98 J=1,KM
      XM=AMAX1(XM,C(J))
98   CONTINUE
      DEL=1./XM
81   P=-1.E-9
      DET=1.E&12
      KN=KM-K
      KP=KN-1
      CALL FIND2 (P, KK, DEL, DET, PO, TO, KP, N)
      RG=A S(PO-1./V2)
      NK=2
      ANN=NDP
      KP=KN-1
      P=1./V2
      CALL HELP(K, N, P, TTP, DTP, KP)
      TC=TTP
      TG=TO-TTP
      IF(PO.LE.1./V2) GO TO 6
      IF(TG.GT.TN1) GO TO 6
      JN=JN1
      IF(TG.GT.TN2) GO TO 8
      JN=JN2
      IF(TG.GT.TN3) GO TO 8
      JN=JN3
8   QZ = RG/(JN&1)
      DO 15 J = 1, JN

```

```
DEL P(J) = QZ
15 CONTINUE
NO=JN
IF(TG.LT.TN4) GO TO 2
GO TO 19
6 CALL DELPS(NNN, RG, 1, NK)
IF (.NOT.PRNT) GO TO 19
PRINT 7, V2, XM, PO, RG, TC, TO, (DEL P(J), J=1, NO)
7 FORMAT (1H0, 4X'V2 = 'G13.6, 5X'XM = 'G13.6, 5X'PO = 'G13.6/5X'RG = '
&G13.6, 5X'TC = 'G13.6, 5X'TO = 'G13.6/5X'DEL P'/(G15.6))
19 IF(PO.LE.1./V2) GO TO 2
CALL PLN1(PO, TO, K, N, TC, KN, V2)
2 MO=NO&2
IF(TG.LT.TN4) MO=2
IF(PO.LT.1./V2) MO=2
CALL CONTOR(TMX, M, KN, N, MO)
IF (.NOT.PRNT) GO TO 620
PRINT 5
5 FORMAT (1H0, 13X'PP'27X'DDPT'24X'TT')
JJ=MO
WRITE(6, 200) (PP(J), DDPT(J), TT(J), J=JJ, M)
200 FORMAT(5E15.4)
620 CALL PLN2(PC, TO, K, MO, M, KN)
NEND=M
NM=NO
IF(PO.LT.1./V2) NM=0
IF(TG.LT.TN4) NM=0
IF(PRNTS) PRINT 9, (TD(LLM), PHI(LLM), LLM=1, NEND)
9 FORMAT (1H0, 14X'TD'23X'PHI'/(2G25.7))
RETURN
END
```

```
• SUBROUTINE INTERP(XP,YP,N,X,Y)
  DIMENSION XP(N),YP(N)
  REAL DIF1,CIF2,CIFY,DR
  1 IF (X .GT. XP(N))GO TO 6
  IF (X .LT. XP(1)) GO TO 6
  2 DO 10 I=1,N
  IF (XP(I) -X) 10,102,3
  10 CONTINUE
  3 K= I-1
  DIF1=XP(I) -XP(K)
  DIF2=XP(I) -X
  RATIO = DIF2/DIF1
  DIFY = ABS (YP(I) - YP(K))
  DR = DIFY*RATIO
  IF (YP(I) .GT. YP(K)) GO TO 4
  5 Y = YP(I) & DR
  RETURN
  4 Y= YP(I) - DR
  RETURN
  102 Y=YP(I)
  RETURN
  6 Y = 0.
  RETURN
  END
```

```

SUBROUTINE PLN1(PO,TO,K,N,TC,KN,V2)
COMMON/TINP/DELM,DLTM,MTD,DLTP,JO,NDIRT
COMMON/SPE/DELP(400),DD1,DD2,DD3,DD4,NO
COMMON/STUFF/C(100),S(100),D(100),TH(100),X
COMMON/EXACT/PHI(500),TT(500),NEND,NM
COMMON / LPRINT/ PRNT,PRNTS
LOGICAL PRNT,PRNTS
COMPLEX RPR,ROC,Q,TOT,GENCC,TQ
K1=K&1
K2=K1&1
KP=KN-1
P=1./V2
DO 80 I=2,NC
J=I-1
P=P&DELP(J)
Q=P&0.*(0.,1.)
CALL HELP(K,N,P,TTP,DTP,KP)
TT(I)=TTP
RPR=ROC(Q,K,KN)
TOT=GENCC(Q,K)
TQ=TOT*RPR
RP=AIMAG(TQ)
EA=(1./C(2)**2-P*P)**.5
IF(NDIRT.GT.1) GO TO 1
R3=1./EA
GO TO 2
1 EB=(1./S(2)**2-P*P)**.5
R1=EB**2-P*P
R2=R1**2&4.*P*P*EA*EB
R3=R1/(R2*S(2)**2)
IF (PRNT) PRINT 10, EA, EB, R1, R2
10 FORMAT (1H0,'EA ='G13.6,5X'EB ='G13.6,5X'R1 ='G13.6,5X'R2 ='G13.6)
2 PHI(I)=(RP*DTP*R3*P**.5)
IF (PRNT) PRINT 9,P,DELP(I),TTP,DTP,TOT,RPR,R3,PHI(I),RP
9 FORMAT (1H0,'P ='G15.6,5X'DELP ='G15.6,5X'TTP ='G15.6,5X'DTP ='G
&15.6/' TOT ='2G20.6,5X'RPR = '2G20.6/' R3 ='G15.6,5X'PHI ='G15.6
&,5X'RP ='G15.6)
80 CONTINUE
4 IF(TO-TTP.LT.DLTP) GO TO 3
PP = PO - P
P = P & PP/2.0
I = NO & 1
NO = I
Q = P
CALL HELP(K,N,P,TTP,DTP,KP)
TT(I)=TTP
RPR=ROC(Q,K,KN)
TOT=GENCC(Q,K)
TQ=TOT*RPR
RP=AIMAG(TQ)
EA=(1./C(2)**2-P*P)**.5
IF(NDIRT.GT.1) GO TO 5
R3=1./EA
GO TO 6
5 EB=(1./S(2)**2-P*P)**.5
R1=EB**2-P*P
R2=R1**2&4.*P*P*EA*EB

```

```
R3=R1/(R2*S(2)**2)
• IF (PRNT) PRINT 10, EA, E , R1, R2
6 PHI(I)=(RP*DTP*R3*P**.5)
  IF (PRNT) PRINT 9,P,DELP(I),TTP,DTP,TOT,RPR,R3,PHI(I),RP
  GO TO 4
3 TT(1)=TC
  PHI(1)=0.
  RETURN
  END
```

```

SUBROUTINE PLN2(PO,TO,K,MO,M,KN)
COMMON/TINP/DELTM,DLTM,MTD,DLTP,JO,NDIRT
COMMON/MAGIC/PP(300),DDPT(300),TT(300)
COMMON/EXACT/PHR(500),TTT(500),NEND,NM
COMMON/STUFF/C(100),S(100),D(100),TH(100),X
DIMENSION FF(50)
COMMON / LPRINT/ PRNT,PRNTS
LOGICAL PRNT,PRNTS
      COMPLEX P,ROC ,FM,E1
      COMPLEX PP,BT,DDPT,RP,RPP,GC
      COMPLEX RBT,TL,CR,RD,GENCC
COMPLEX EA,EB,R1,R2,R3,PH
KP=KN-1
      K1=K+1
      K2=K1+1
      DC 5 I=MO,M
      TTT(I)=TT(I)
      P=PP(I)
      RP=ROC(P,K,KN)
      GC =GENCC(P,K)
      EA=CR(P,C(2))
      IF(NDIRT.GT.1) GO TO 32
      R3=1./EA
      GO TO 38
32  EB=CR(P,S(2))
      R1=EB**2-P*P
      R2=R1**2+4.*P*P*EA*EB
      R3=R1/(R2*S(2)**2)
38  BT=CSQRT(P)
      PH=R3*DDPT(I)*GC*RP*BT
      PHR(I)=AIMAG(PH)
      IF(PRNT) PRINT 9, P, GC, RP, R1, R2, R3,EA, EB, PH
9  FORMAT (1H0,4X'P = '2G18.6/5X'GC = '2G18.6/5X'RP = '2G18.6/
+5X'R1 = '2G18.6/5X'R2 = '2G18.6/5X'R3 = '2G18.6/5X'EA = '2G18.6/
+5X'EB = '2G18.6/5X'PH = '2G18.6)
5  CONTINUE
      P=PO*(1.,0.)+0.*(0.,1.)
      I=MO-1
      Q=PO
      SF=SF2(Q,K,KP,N)
      TTT(I)=TO
      GC=GENCC(P,K)
      RP=ROC(P,K,KN)
      RPP=SF*GC*RP*(X/2.)**.5
      IF(NDIRT.LT.1) GO TO 2
      EA=CR(P,C(2))
      EB=CR(P,S(2))
      R1=EB**2-P*P
      R2=R1**2+4.*P*P*EA*EB
      R3=(R1*EA)/(R2*S(2)**2)
      RPP=RPP*R3
2  PRE=REAL(RPP)
      PIM=AIMAG(RPP)
      IF(.NOT.PRNT) GO TO 3
      PRINT 1, Q, SF, PRE, PIM
          PRINT 9, P, GC, RP, R1, R2, R3,EA, EB, PH
1  FCRMAT (5X'Q = 'G18.6,10X'SF = 'G18.6/
+5X'PRE = 'G18.6,10X'PIM = 'G18.6)
3  NC=MO-2
      DP=DLTP
      F1=0.
      SUM=0.
      IF(MO.LE.3) GO TO 46

```



```
FUNCTION FTIMP,N)
COMMON/STUFF/CT(100),ST(100),DT(100),TH(100),X,RCSQ(100),RCSQ(100)
PSQ = P ** 2
RR = 0.0
DO 5 J = 1,N
E = SORT(ABS(DTCSQ(J)) - P)
5 RR = RR + IN(J) * E
FTIME = P * X + RR * Z.0
RETURN
END
```

```
COMPLEX FUNCTION RET(P,V1,S1,D1,V2,S2,D2)
  COMPLEX E1P,P,A,B,AP,BP,BT,CR
  COMPLEX E1,E2,E2P,C1,C2,C3,C4,C5,C6
  REAL K1,K2,K3,K4
D=D1/D2
K4=S2**2/(S1**2*D)
B1=.5/(1-K4)
B2=.5*K4/(K4-1)
K1=B1/S1**2
K2=B2/S2**2
K3=K1+K2
E1=CR(P,V1)
E2=CR(P,V2)
E2P=CR(P,S2)
E1P=CR(P,S1)
C1=(P**2)*(K3-P**2)**2
C2=P**2*E1*E1P*E2P
C3=(E1*E1P)*(K2-P**2)**2
C4=E2P*(K1-P*P)**2
C5=K1*K2*E1*E2P
C6=K1*K2*E1P
AP=C1+C3-C5
BP=C2+C4-C6
A=-C1+C3-C5
B=-C2+C4-C6
BT=AP+BP*E2
RET=(A-B*E2)/BT
  RETURN
  END
```

```

COMPLEX FUNCTION ROC(P,K,KN)
COMMON/STUFF/C(100),S(100),D(100),TH(100),X
COMMON/CFIX/NT,KT,MB,NB,LT,LTP(100),NF
COMMON/NFIX/MM(100),NN(100),MT(100)
      COMPLEX Q,RF,RNT,RMT,RNB,TD,TU,T1,T2,TDU,RET,P,RMB,CRSTPP
Q=(1.,0.)&C.*(0.,1.)
IF(KN.GT.2) GO TO 90
K1=K&1
K2=K&2
V1=C(K1-1)
S1=S(K1-1)
D1=D(K1-1)
V2=C(K1)
S2=S(K1)
D2=D(K1)
V3=C(K2)
S3=S(K2)
D3=D(K2)
V4=C(K2&1)
S4=S(K2&1)
D4=D(K2&1)
IF(K.LT.2) GO TO 51
T1=CR STPP(P,V1,S1,D1,V2,S2,D2)
T2=CR STPP(P,V2,S2,D2,V1,S1,D1)
GO TO 52
51  T1=Q
    T2=Q
52  CONTINUE
    TDU=T1*T2
    IF(NT.GT.0) GO TO 1
    2  RNT=Q
    GO TO 10
    1  RNT=RET(P,V2,S2,D2,V1,S1,D1)
    10 RMT=RET(P,V2,S2,D2,V3,S3,D3)
    IF(LT.LT.1) GO TO 4
    3  TD=CR STPP(P,V2,S2,D2,V3,S3,D3)
    TU=CR STPP(P,V3,S3,D3,V2,S2,D2)
    IF(MB.GT.0) GO TO 5
    6  RMB=Q
    GO TO 20
    5  RMB=RET(P,V3,S3,D3,V2,S2,D2)
    20 RNB=RET(P,V3,S3,D3,V4,S4,D4)
    GO TO 30
    4  TC=Q
    TU=Q
    RMB=Q
    RN =Q
    ROC=RNT**NT*RMT**KT
    GO TO 40
    30 CONTINUE
    ROC=RNT**NT*RMB**MB* RMT**KT*RNB**NB*(TD*TU)**LT
    40 ROC=ROC*TDU
    GO TO 91
    90 TDU=Q
    RNT=Q
    RMT=Q
    J2=K&KN

```

```
J1=K&1
DO 63 J=J1,J2
N=J
M=J&1
IF(MM(J).GT.0) GO TO 61
GO TO 62
61 T1=RET(P,C(N),S(N),D(N),C(M),S(M),D(M))
RMT=RMT*T1**MM(J)
62 CONTINUE
63 CONTINUE
DO 73 J=J1,J2
N=J-1
M=J
IF(NN(J).GT.0) GO TO 71
GO TO 72
71 T1=RET(P,C(M),S(M),D(M),C(N),S(N),D(N))
RNT=RNT*T1**NN(J)
72 CONTINUE
73 CONTINUE
DO 83 J=J1,J2
N=J-1
M=J
IF(N.EQ.1) MT(J)=0
IF(MT(J).GT.0) GO TO 81
GO TO 82
81 TD=CRSTPP(P,C(N),S(N),D(N),C(M),S(M),D(M))
TU=CRSTPP(P,C(M),S(M),D(M),C(N),S(N),D(N))
T1=(TD*TU)**MT(J)
TDU=TDU*T1
82 CONTINUE
83 CONTINUE
ROC=RMT*RNT*TDU
91 END
```

```
SUBROUTINE SETT(KO,DP,LN)
COMMON/SYTH/XD11,YD11,XD22,YD22,XD33,YD33
COMMON/THY/T(8000),PP(8000),RP(600)
DIMENSION P(1000)
COMMON/PLOT/CON,NNF,NPT
COMMON / LPRINT/ PRNT,PRNTS
LOGICAL PRNT,PRNTS
DIMENSION SS(200),TT(200)
DIMENSION C(1000),TD(1000)
DIMENSION XL(2),YL1(4),YL2(4),YL3(4)
DATA XL/'TIME SEC'/
DATA YL2/' THEORETICAL PO '/
DATA YL3/' SYTHETIC RESP '/
DATA YL1/' TRANSFER FTN '/
300  FORMAT(2E15.4)
      READ(5,300) (SS(J),J=1,KO)
      IF (PRNT) PRINT 1, (SS(J),J=1,KO)
1  FORMAT (1H0,'SOURCE FUNCTION'/(2G15.4))
      TT(1)=0.
      DO 16 J=2,KO
      TT(J)=TT(J-1)&DP
16  CONTINUE
      IF(NPT.LT.1) GO TO 31
      LS1=0
      CALL PICTUR(XD11,YD11,XL,-8,YL1,-16,
2  TT,SS,KO,0.,LS1)
31  CONTINUE
      T(1)=0.
      DO 10 J=2,LN
      T(J)=T(J-1)&DP
10  CONTINUE
      CALL PICTUR(XD22,YD22,XL,-8,YL2,-16,
2  T,PP,LN,0.,LS1)
      L=0
      NK=LN/2-1
      DO 20 N=1,NK,NNF
      L=L&1
      C(L)=CONVS(PP,SS,DP,KO,N-1)
      TD(L)=2.*DP*(N-1)
20  CONTINUE
      DO 30 J=2,L
      P(J)=(C(J)-C(J-1))/(DP*2.)
      P(J)=P(J)*CCN
30  CONTINUE
      P(1)=0.
      CALL PICTUR(XD33,YD33,XL,-8,YL3,-16,
2  TD,P,L,0.,LS1)
      IF(PRNTS) PRINT 2, (TD(J),P(J),J=1,L)
2  FORMAT (1H0,10X'TIME'10X'PRESSURE'/(2G18.4))
      END
```

```
SUBROUTINE SETUP(K,MM,NS,NO,MO,MPL0T,MPUNCH)
COMMON/CONFIX/DEL,NN,NDP,TMX,XDIM,YDIM,DP,KO
COMMON/CFIX/NT,KT,MB,NB,LT,LTP(100),NF
COMMON/FOURCT/MF,NMF,KMF,KNMF
COMMON/THY/TT(8000),PP(8000),FF(600)
COMMON/EXACT/PHI(500),TD(500),NEND,NM
COMMON/LPRINT/PRNT,PRNTS
LOGICAL PRNT,PRNTS
DIMENSION XL(2),YL1(4),YL2(4),YL3(4)
DATA YL2/' THEORETICAL PO '/
DATA XL/'TIME SEC'/
IF(MO.GT.1) GO TO 11
I=K
TT(1)=TS(I)
PP(1)=0.
DO 10 J=2,NN
TT(J)=TT(J-1) &DEL
PP(J)=0.
10 CONTINUE
11 CONTINUE
IF(MF.LT.1) GO TO 30
CALL CONN(NMF,KMF,KNMF)
CALL HIGH(NDP,TMX,KMF,KNMF,NMF)
CALL ADJUST(NFIX)
M=NM&1
N2=NFIX&1
N1=NFIX-1
IF(N1.LE.2) GO TO 41
DO 35 J=1,N1
CALL INTERP(TD,PHI,NEND,TT(J),Y)
PP(J)=PP(J)&Y*NF
35 CONTINUE
41 CONTINUE
PP(NFIX)=PP(NFIX) &NF*PHI(M)
DO 36 J=N2,NN
CALL INTERP(TD,PHI,NEND,TT(J),Y)
PP(J)=PP(J)&Y*NF
36 CONTINUE
GO TO 7
30 CONTINUE
CALL CONSTN(NO)
K1=K&1
K2=K&2
DO 32 N=NS,NO
CALL CON(N,K1,K2)
CALL HIGH(NCP,TMX,K,KI,N)
CALL ADJUST(NFIX)
M=NM&1
N2=NFIX&1
N1=NFIX-1
IF(N1.LE.2) GO TO 42
DO 31 J=1,N1
CALL INTERP(TD,PHI,NEND,TT(J),Y)
PP(J)=PP(J)&Y*NF
31 CONTINUE
42 CONTINUE
PP(NFIX)=PP(NFIX) &NF*PHI(M)
```

```
      DO 33 J=N2,NN
      CALL INTERP(TD,PHI,NEND,TT(J),Y)
      PP(J)=PP(J)&Y*NF
33     CONTINUE
32     CONTINUE
      7 IF(.NOT.PRNT) GO TO 12
      PRINT 13, (TD(J),PHI(J),J=1,NEND)
      13 FORMAT (1H0,15X'TD'15X'PHI'/(2G18.6))
      PRINT 14,(TT(J),PP(J),J=1,NN)
      14 FORMAT (1H0,15X'TT'15X'PP'/(2G18.6))
      12 IF(MPLOT.LT.1) GO TO 1
      CALL PICTUR(XDIM,YDIM,XL,-8,YL2,-16,
      2 TT,PP,NN,0.,0)
1     CONTINUE
      IF(MPUNCH.LT.1) GO TO 2
      LN=NN
      NK=LN
      DEL=DP
      WRITE(7,100) TT(1),DP,DEL
      WRITE(7,200) NN,LN,NK
      WRITE(7,100) (PP(J),J=1,LN)
200   FORMAT(3I10)
      100 FORMAT (5E15.6)
      2 IF(KO.LT.1) RETURN
      CALL SETT (KO,DP,NN)
      RETURN
      END
```



```
FUNCTION SF2(P,K,KN,N)
COMMON/CFIX/NT,KT,M,N,LT,LTP(100),NF
COMMON/STUFF/C(100),S(100),D(100),TH(100),X,RCSQ(100),RSSQ(100)
PSQ = P ** 2
TE = 0.0
DO 5 J = 1,K
ESQ = ABS(RCSQ(J)-PSQ)
E = SQRT(ESQ)
5 TE = TE & TH(J) * RCSQ(J) / (ESQ*E)
TE = TE * 2.0
J1 = K & 1
J2 = J1 & KN
DO 10 J = J1,J2
ESQ = ABS(RCSQ(J)-PSQ)
E = SQRT(ESQ)
10 TE = TE & TH(J) * LTP(J) * RCSQ(J) / (ESQ*E)
SF2 = SQRT(P/(X*TE*ABS(RCSQ(2)-PSQ)))
RETURN
END
```

```
SUBROUTINE TIME2(P,PC,DPT,T,KN,N)
```

```
COMMON/PATHC/PO,TO,K
```

```
COMPLEX E,P,T,PC,CR,BL,DPT ,F
```

```
DIMENSION E(100),F(100)
```

```
COMMON/STUFF/C(100),S(100),D(100),TH(100),X
```

```
COMMON/CFIX/NT,KT,MB,NB,LT,LTP(100),NF
```

```
COMMON / LPRINT/ PRNT,PRNTS
```

```
LOGICAL PRNT,PRNTS
```

```
DL=PO*.5
```

```
KO=K
```

```
DET = 1.0E-10
```

```
K1=KO&1
```

```
K2=KO&KN
```

```
6 P=P&DL*(0.,1.)
```

```
T=P*X
```

```
DO 1 J=1,KO
```

```
E(J)=CR(P,C(J))
```

```
T=T&2.*TH(J)*E(J)
```

```
1 CONTINUE
```

```
DO 11 J=K1,K2
```

```
E(J)=CR(P,C(J))
```

```
T=T&TH(J)*(E(J)*LTP(J))
```

```
11 CONTINUE
```

```
CT=AIMAG(T)
```

```
IF (ABS(DL).LE.1.0E-9) GO TO 2
```

```
7 IF(ABS(CT).LE.DET) GO TO 2
```

```
3 IF(CT) 4,2,5
```

```
4 DL=ABS(DL)*.5
```

```
GO TO 6
```

```
5 DL=-ABS(DL)*.5
```

```
GO TO 6
```

```
2 CONTINUE
```

```
PC=P
```

```
L=X
```

```
DO 10 J=1,KO
```

```
BL=BL-2.*P*TH(J)/E(J)
```

```
10 CCONTINUE
```

```
DO 12 J=K1,K2
```

```
BL=BL- P*TH(J)*(LTP(J)/E(J))
```

```
12 CONTINUE
```

```
DPT=1./BL
```

```
IF (CT.LT.1.0E-5) RETURN
```

```
IF (.NOT.PRNT) RETURN
```

```
PRINT 110, P, E(1), T, DPT
```

```
110 FORMAT (1H0,4X'P = '2G18.6/5X'E(1) ='2G17.6/5X'T = '2G18.6/  
&5X'DPT ='2G18.6)
```

```
9 END
```

```
FUNCTION TS(K)
COMMON/CFIX/NT,KT,MB,NB,LT,LTP(100),NF
COMMON/STUFF/C(100),S(100),D(100),TH(100),X,RCSQ(100),RSSQ(100)
COMMON/LPRINT/PRNT,PRNTS,KST,KEND
LOGICAL PRNT,PRNTS
DIMENSION T(200)
DET=1.E&12
N=0
X1=0.
DO 98 M = 1,KST
X1=AMAX1(X1,C(M))
98  CONTINUE
DO 102 J=KST,KEND
X1 = AMAX1(X1,C(J))
P=-1.E-9
DEL=1./X1
LTP(J)=2
M=J-1
CALL FIND2(P,M,DEL,DET,PO,TO,0,1)
N=N&1
T(N)=TO
102  CONTINUE
DO 103 J=KST,KEND
N=N&1
PX=1./C(J&1)
TX=PTIM(PX,J)
T(N)=TX
103  CONTINUE
TS=1.E&6
DO 106 J=1,N
TS=AMINI(T(J),TS)
106  CONTINUE
IF (PRNT) PRINT 1, (T(J),J=1,N)
1  FORMAT (5X'T(J),J=1,N'/(4G18.4))
RETURN
END
```

0.0	0.1876E 00
0.3446E 00	0.5343E 00
0.7517E 00	0.9965E 00
0.1268E 01	0.1562E 01
0.1878E 01	0.2150E 01
0.2117E 01	0.1619E 01
0.8531E 00	-0.1217E 00
-0.1227E 01	-0.2247E 01
-0.3050E 01	-0.3771E 01
-0.4445E 01	-0.5041E 01
-0.5364E 01	-0.5299E 01
-0.5003E 01	-0.4526E 01
-0.3913E 01	-0.3260E 01
-0.2629E 01	-0.1970E 01
-0.1274E 01	-0.5426E 00
0.2053E 00	0.9577E 00
0.1729E 01	0.2522E 01
0.3290E 01	0.3835E 01
0.4036E 01	0.4042E 01
0.3901E 01	0.3627E 01
0.3193E 01	0.2587E 01
0.1849E 01	0.9941E 00
0.6724E-01	-0.7881E 00
-0.1483E 01	-0.2114E 01
-0.2708E 01	-0.3255E 01
-0.3658E 01	-0.3860E 01
-0.3944E 01	-0.3933E 01
-0.3847E 01	-0.3706E 01
-0.3524E 01	-0.3298E 01
-0.3029E 01	-0.2720E 01
-0.2367E 01	-0.1968E 01
-0.1529E 01	-0.1053E 01
-0.5685E 00	-0.1882E 00
0.1828E-01	0.1340E 00
0.1832E 00	0.1820E 00
0.1525E 00	0.1088E 00
0.4464E-01	-0.3975E-01
-0.1481E 00	

(Transfer Function)